



การศึกษาคุณสมบัติของยีน Translationally controlled tumor protein (TCTP)
ของกุ้งก้ามกรามและการศึกษาทรานสคริปโตมของกุ้งก้ามกรามระยะโพสต์ลาร์วา
ในการตอบสนองต่อเชื้อ *M. rosenbergii* nodavirus (*MrNV*)

CHARACTERIZATION OF A TRANSLATIONALLY CONTROLLED TUMOR PROTEIN
(TCTP) GENE FROM *Macrobrachium rosenbergii* AND TRANSCRIPTOMIC ANALYSIS
OF *M. rosenbergii* POST-LARVAE IN RESPONSE TO *M. rosenbergii* NODAVIRUS
(*MrNV*)

PHONGTHANA PASOOKHUSH

การศึกษาคุณสมบัติของยีน Translationally controlled tumor protein (TCTP)
ของกิ้งก่ามกราคมและการศึกษาทรานสคริปโตมของกิ้งก่ามกราคมระยะโพสต์ลาวา
ในการตอบสนองต่อเชื้อ *M. rosenbergii* nodavirus (MrNV)



ปริญญานิพนธ์นี้เป็นส่วนหนึ่งของการศึกษาตามหลักสูตร
ปรัชญาดุษฎีบัณฑิต สาขาวิชาเทคโนโลยีชีวภาพ
คณะวิทยาศาสตร์ มหาวิทยาลัยศรีนครินทรวิโรฒ
ปีการศึกษา 2562
ลิขสิทธิ์ของมหาวิทยาลัยศรีนครินทรวิโรฒ

CHARACTERIZATION OF A TRANSLATIONALLY CONTROLLED TUMOR
PROTEIN (TCTP) GENE FROM *Macrobrachium rosenbergii* AND
TRANSCRIPTOMIC ANALYSIS OF *M. rosenbergii* POST-LARVAE IN
RESPONSE TO *M. rosenbergii* NODAVIRUS (*MrNV*)



A Dissertation Submitted in partial Fulfillment of Requirements
for DOCTOR OF PHILOSOPHY (Biotechnology)
Faculty of Science Srinakharinwirot University

2019

Copyright of Srinakharinwirot University

THE DISSERTATION TITLED

CHARACTERIZATION OF A TRANSLATIONALLY CONTROLLED TUMOR PROTEIN
(TCTP) GENE FROM *MACROBRACHIUM ROSENBERGII* AND TRANSCRIPTOMIC
ANALYSIS OF *M. ROSENBERGII* POST-LARVAE IN RESPONSE TO *M. ROSENBERGII*
NODAVIRUS (MRNV)

BY

PHONGTHANA PASOOKHUSH

HAS BEEN APPROVED BY THE GRADUATE SCHOOL IN PARTIAL FULFILLMENT OF
THE REQUIREMENTS FOR THE DOCTOR OF PHILOSOPHY IN BIOTECHNOLOGY
AT SRINAKHARINWIROT UNIVERSITY

..... Dean of Graduate School

(Assoc. Prof. Dr. Chatchai Ekpanyaskul, MD.)

ORAL DEFENSE COMMITTEE

..... Major-advisor

(Assoc. Prof. Parin Chaivisuthangkura, Ph.D.)

..... Chair

(Saengchan Senapin, Ph.D.)

..... Co-advisor

(Assoc. Prof. Siwaporn Longyant, Ph.D.)

..... Committee

(Prof. Paisarn Sitthigorngul, Ph.D.)

Title	CHARACTERIZATION OF A TRANSLATIONALLY CONTROLLED TUMOR PROTEIN (TCTP) GENE FROM <i>Macrobrachium rosenbergii</i> AND TRANSCRIPTOMIC ANALYSIS OF <i>M. rosenbergii</i> POST-LARVAE IN RESPONSE TO <i>M. rosenbergii</i> NODAVIRUS (<i>MrNV</i>)
Author	PHONGTHANA PASOOKHUSH
Degree	DOCTOR OF PHILOSOPHY
Academic Year	2019
Thesis Advisor	Associate Professor Parin Chaivisuthangkura , Ph.D.

The translationally controlled tumor protein (TCTP) is involved in many biological processes including anti-apoptosis, which is connected to anti-viral mechanisms. This study reported full-length cDNA of *M. rosenbergii* TCTP (*MrTCTP*) which consisted of a 783 bp encoding a 18.94 kDa polypeptide. *MrTCTP* demonstrated all major characteristics of TCTP. The expression analysis showed that *MrTCTP* was expressed in every tissue sample examined, preferentially in the hepatopancreas and muscle. The up-regulations of *MrTCTP* in muscle from one to four days after the infection with *MrNV* were reported. Additionally, *MrTCTP*-knockdown prawn using RNAi exhibited higher mortality rates after being challenged with *MrNV*. The transcriptomic data on how *M. rosenbergii* post-larvae response to infection with *MrNV* is not yet available. Therefore, this study reported highly complete transcriptome for *M. rosenbergii* post-larvae, as well as list of candidate genes involved in the infection. The assembled transcriptome consisted of 96,362 unigenes. The assembled transcriptome demonstrated high completeness and was annotated against various public databases. EdgeR software showed 2,413 up-regulated and 3,125 down-regulated genes during the infection of *MrNV*. These differentially expressed genes that involved in antiviral immunity were categorized into thirteen functional groups. More significantly, the expression of nine genes from nine functional groups in separate biological samples was validated by qRT-PCR.

Keyword : *Macrobrachium rosenbergii*, *M. rosenbergii* nodavirus, crustacean immunity, Translationally controlled tumor protein, RNA interference, RNAseq, de novo transcriptome assembly

ACKNOWLEDGEMENTS

Foremost, I would like to express my sincere gratitude toward my advisor Assoc. Prof. Dr. Parin Chaivisuthangkura for his support, encouragement, guidance, and great patience throughout my Ph.D. He always respect my opinions and guided me throughout my Ph.D. I gratefully acknowledge Assoc. Prof. Dr. Siwaporn Longyant, my co-advisor, and Prof. Dr. Paisarn Sitthigorngul for their advices, and encouragements. I would like to thank dissertation chair, Dr. Saengchan Senapin, for valuable comments. I also would like to thank my proposal committee: Asst. Prof. Dr. Siriruk Sarawaneeyaruk, and Dr. Thanawan Tejangrura.

My sincere gratitude goes to Prof. Dr. William G. Bendena, my mentor, from Department of Biology, Queen's university and his wife Hollis Mitchell for their kind hospitalities and supports throughout my year in Kingston, Canada. Not only Dr. Bendena supported and guided me through my year of research in Canada, he is also being a great friend. Working with him was a great honor and one of the best decision I've ever made. I would like to thank Prof. Dr. Ian Chin-Sang and members of Chin-Sang/Bendena Lab including volunteer and lab technicians and BIOL537 2018 students. I also would like to thank Dr. Charles Hindmarch from Queen's Cardiopulmonary Unit (QCPU), Queen's university.

I thank my fellow lab members: Dr. Akapon Vaniksampanna and Orapan Manajit for our friendship and I thank all the members of 1103/1113 SWUBiotech Lab. The adult and post-larvae prawn supplies from Kanokpon Shrimp Farm is acknowledged.

I thank my partner, Tantamas Suklorm, for her love and support, her empathetic ear, and for always be there for me. I thank you for playing a huge part of this journey. I could not imagine my successful Ph.D. without her. I thank my dogs: Seur (Tiger), Singha (Lion), Bayah, B1, and B2. Last but not least, I'm grateful for my parents: Panawas (Jethawan) Pasookhush and Thamon (Aruwan) Eiamchamroonlarp, my aunt: Suganda Pasookhush, and my brother: Akthanatt Pasookhush for being the greatest family I've ever had.

Partial of this work regarding transcriptomic analysis has been published in BMC genomics (ISSN 1471-2164), volume 20, article number 762, entitled “Transcriptomic analysis of *Macrobrachium rosenbergii* (giant fresh water prawn) post-larvae in response to *M. rosenbergii* nodavirus (MrNV) infection: de novo assembly and functional annotation”, DOI 10.1186/s12864-019-6102-6. I act as the first author of the manuscript and contributed as follows; performed the whole experiment, analyzed the data, and drafted the manuscript. The copyright of this work is retained by the authors. All authors are acknowledged and approved the re-use of the work for this academic purpose.



PHONGTHANA PASOOKHUSH

TABLE OF CONTENTS

	Page
ABSTRACT.....	D
ACKNOWLEDGEMENTS	E
TABLE OF CONTENTS	G
LIST OF TABLES.....	M
LIST OF FIGURES.....	O
CHAPTER 1.....	1
INTRODUCTION	1
Background.....	1
Objective	4
Research hypotheses.....	4
Scopes	5
CHAPTER 2.....	6
LITERATURE REVIEW.....	6
<i>Macrobrachium rosenbergii</i> (Giant River Prawn)	6
Scientific classification	7
Biological features.....	7
Habitat and life cycle	8
<i>Macrobrachium rosenbergii</i> 's Nodavirus (MrNV)	9
Clinical signs.....	11
Histopathology	12
Transmission	13

The Immune System of Shrimp.....	14
Pattern recognition receptors (PRRs).....	14
Immune signaling pathways	15
RNA interference (RNAi) pathway.....	16
Hemocytes and hematopoiesis.....	17
Clotting, antimicrobial peptides, and prophenol oxidase system (proPO).....	17
Phagocytosis.....	18
Apoptosis	19
Translational control of tumor protein (TCTP).....	21
Protein structure.....	21
Regulation.....	22
Biological function.....	24
TCTP in shrimp.....	26
Rapid Amplification of cDNA Ends (RACE)	27
RNA interference (RNAi).....	30
RNAi mechanism.....	30
Initiator step	30
Effector step.....	32
Amplification of the silencing	32
Sequencing-by-synthesis: Illumina sequencing technology	33
NGS in shrimp.....	40
CHAPTER 3.....	43
MATERIALS & METHODS.....	43

1. Molecular cloning and identification of <i>MrTCTP</i> cDNA using Rapid amplification of cDNA ends (RACE).....	44
1.1 RNA extraction	44
1.2 First-Strand cDNA synthesis	45
1.3 Polymerase chain reaction using degenerate primers.....	47
1.4 Molecular cloning and identification of partial <i>MrTCTP</i> cDNA.....	49
1.5 Preparation of 3' and 5'-RACE-Ready cDNA	53
1.6 Rapid amplification of 3' and 5' cDNA ends (RACEs).....	54
1.7 Molecular cloning and identification of <i>MrTCTP</i> cDNA.....	58
2. Bioinformatics analysis and sequence confirmation of <i>MrTCTP</i> cDNA	58
2.1 Polymerase chain reaction (PCR) for the re-identification of <i>MrTCTP</i>	59
2.2 Molecular cloning and re-identification of <i>MrTCTP</i>	60
2.3 Protein composition analysis of <i>MrTCTP</i>	63
2.4 Phylogenetic analysis of <i>MrTCTP</i>	63
3. Tissue expression and distribution analysis of <i>MrTCTP</i> gene	64
3.1 Tissue collection and RNA extraction	64
3.2 Semi-quantitative reverse transcription PCR.....	65
4. Immune challenge experiment using <i>Macrobrachium rosenbergii</i> nodavirus (<i>MrNV</i>)	67
4.1 Preparation of the <i>MrNV</i>	67
4.2 Viral nucleic acid extraction and RT-PCR for the detection of <i>MrNV</i>	67
4.3 Preparation of the <i>MrNV</i> inoculum and immune challenge.....	70
6. <i>MrTCTP</i> knockdown experiment using RNA interference	71
6.1 Construction of DNA template for <i>in vitro</i> transcription.....	71

6.2 <i>in vitro</i> transcription and dsRNA purification.....	72
6.3 Validation of dsRNA	73
6.3.1 DNA digestion using DNase I	73
6.3.2 ssRNA digestion using RNase A.....	74
6.3.3 dsRNA digestion using RNase III.....	74
6.4 <i>MrTCTP</i> knockdown experiment using dsRNA injection.....	75
6.5 <i>MrTCTP</i> knockdown experiment combined with <i>MrNV</i> challenge	76
7. Transcriptomic analysis (RNAseq) of <i>M. rosenbergii</i> post-larvae in response to <i>M. rosenbergii</i> nodavirus (<i>MrNV</i>) infection.....	77
7.1 Preparation of <i>MrNV</i> infected post-larvae prawn	77
7.2 RNA extraction	77
7.3 Library preparation.....	78
7.4 Library denaturation and sequencing	80
7.5 Data analysis pipeline	81
7.6 Quantitative RT-PCR analysis.....	84
CHAPTER 4.....	89
RESULTS	89
1. Molecular cloning and characterization of <i>MrTCTP</i> cDNA	89
1.1 Molecular cloning and identification of partial <i>MrTCTP</i> cDNA using degenerate primers	89
1.2 Molecular cloning and identification of 5' and 3' ends of <i>MrTCTP</i> cDNA using Rapid amplification of cDNA ends (RACE).....	90
1.3 Sequence confirmation of full-length <i>MrTCTP</i> cDNA	91
1.4 Characterization of <i>MrTCTP</i> cDNA.....	92

1.5 Phylogenetic relationship analysis of <i>MrTCTP</i>	96
1.6 Tissue distribution analysis of <i>MrTCTP</i>	97
2. Response of <i>MrTCTP</i> after <i>MrNV</i> challenge	98
2.1 Preparation and RT-PCR for the detection of <i>MrNV</i>	98
2.2 Expression analysis of <i>MrTCTP</i> after <i>MrNV</i> challenge	99
3. <i>RNA interference</i> experiment	101
3.1 Construction of DNA template for <i>in vitro</i> transcription	101
3.2 Validation of dsRNA	102
3.3 <i>In vivo</i> knockdown of <i>MrTCTP</i> using dsRNA-mediated RNA interference ...	103
3.4 Cumulative mortalities of <i>MrTCTP</i> -knockdown prawn after the viral injection	104
4. Validation of the data analysis pipeline	106
5. Samples preparation, library preparation, and Illumina sequencing	108
5.1 Preparation of <i>MrNV</i> infected post-larvae prawn	108
5.2 Library preparation	108
5.3 Library denaturation and sequencing	110
6. <i>De novo</i> transcriptome assembly and annotation	112
7. Differential expression analysis	119
8. Quantitative RT-PCR validation of selected genes	125
CHAPTER 5	128
DISCUSSION	128
Molecular cloning and characterization of <i>MrTCTP</i>	129
Conclusion	134

Transcriptomic analysis of <i>M. rosenbergii</i> post-larvae in response to <i>MtNV</i> infection	134
Data analysis pipeline	134
<i>De novo</i> assembly and annotation.....	135
Differential expression analysis.....	137
Conclusion	144
REFERENCES	145
VITA	172



LIST OF TABLES

	Page
Table 1 Components of carrier RNA working solution (100 µL).....	44
Table 2 Components of rDNase reaction mixture.....	45
Table 3 Components of RNA mixture for first-strand cDNA synthesis.....	46
Table 4 Components of 2X reaction mix for first-strand cDNA synthesis.....	46
Table 5 Degenerate primers used in the PCR reaction.....	47
Table 6 Components of the PCR reaction for partial cloning.....	48
Table 7 Components of pCR™2.1-TOPO® ligation mixture.....	50
Table 8 Components of RNA mixture for RACE-Ready cDNA synthesis.....	53
Table 9 Components of RACE-Ready cDNA synthesis reaction mix.....	53
Table 10 Primers used in the RACE-PCR reaction.....	55
Table 11 Components of RACE-PCR reaction.....	55
Table 12 Components of nested RACE-PCR reaction.....	57
Table 13 Primers used for the re-identification of MrTCTP.....	59
Table 14 Components of the PCR reaction for MrTCTP.....	59
Table 15 Components of pCR®-Blunt II-TOPO® ligation mixture.....	61
Table 16 TCTP proteins from other organisms.....	63
Table 17 Primers used in the RT-PCR reaction.....	65
Table 18 Components of RT-PCR reaction.....	65
Table 19 Components of working solution.....	68
Table 20 Primers for the detection of MrNV.....	68
Table 21 RT-PCR reaction for the detection of MrNV.....	69

Table 22 Primers used in the PCR reaction for in vitro transcription.....	71
Table 23 Components of in vitro transcription mixture.....	72
Table 24 Components of DNase I digestion mixture	73
Table 25 Components of RNase A digestion mixture	74
Table 26 Components of RNase III digestion mixture.....	75
Table 27 Primers used in the RT-PCR reaction for knockdown experiment	76
Table 28 Components of DNase I reaction mix	78
Table 29 Components of the PCR reaction for determine optimal cycle for library amplification.....	79
Table 30 Primers used in the qRT-PCR experiment.....	85
Table 31 Components of cDNA mastermix for first-strand cDNA synthesis	86
Table 32 Components of RT-PCR reaction	87
Table 33 Summary of the transcriptome assembly and post-processing comparisons between the results from the pipeline and from (Rao et al., 2015)	107
Table 34 The library concentration and average size distribution	109
Table 35 Number of read pairs prior and after trimming	111
Table 36 Summary of the transcriptome assembly and quality assessment	112
Table 37 Summary of the transcriptome assembly, annotation and differential expression analysis.....	119
Table 38 List of DEG transcripts involved in immune system	120
Table 39 Comparison of fold change in gene expression between qRT-PCR and RNAseq.....	125

LIST OF FIGURES

	Page
Figure 1 <i>Macrobrachium rosenbergii</i> (De Man, 1879).....	6
Figure 2 3D Reconstruction of <i>Macrobrachium rosenbergii</i> nodavirus (MrNV)	10
Figure 3 Genomic organization of <i>Macrobrachium rosenbergii</i> nodavirus (MrNV).....	11
Figure 4 WTD-infected <i>M. rosenbergii</i> juvenile showing whitish muscles	12
Figure 5 An area of necrotic muscles in WTD-infected shrimp.....	13
Figure 6 Diagram of a cell undergoing apoptosis	19
Figure 7 Multiple sequence alignment, ribbon diagram and functional mapping of TCTP	23
Figure 8 Biological functions and regulation of TCTP	25
Figure 9 5'-Rapid amplification of cDNA ends.....	28
Figure 10 3'-Rapid amplification of cDNA ends.....	29
Figure 11 Dicer and RISC (RNA-induced silencing complex)	31
Figure 12 Illumina NextSeq® 500/550 High Output Kit v2 flow cell	33
Figure 13 Four major steps of Illumina sequencing platform	34
Figure 14 Tagmentation technique in Nextera® DNA Library Preparation Kits	35
Figure 15 cDNA library generation in Lexogen's SENSE mRNA-Seq Library Prep Kit V2	36
Figure 16 Cluster generation and sequencing-by-synthesis	37
Figure 17 Sequencing-by-synthesis	39
Figure 18 Overview of the studies	43
Figure 19 Multiple sequence alignment of TCTP protein	48

Figure 20 Features of the pCR™2.1-TOPO® vector.....	51
Figure 21 Features of the pCR®-Blunt II-TOPO®vector	62
Figure 22 The overviews of analysis pipeline.	84
Figure 23 PCR product of partial MrTCTP using degenerate primers	89
Figure 24 RACE-PCR products of MrTCTP.....	90
Figure 25 Cloning of MrTCTP-CDS PCR products.....	91
Figure 26 Full-length cDNA, deduced amino acid and sequence analysis of MrTCTP ..	92
Figure 27 Sequence alignment of MrTCTP protein.....	93
Figure 28 Ribbon diagram and protein family of MrTCTP protein.....	94
Figure 29 Identity and similarity of TCTP proteins	95
Figure 30 Phylogenetic relationship analysis of MrTCTP.....	96
Figure 31 Tissue distribution analysis of MrTCTP	97
Figure 32 Cloning of MrNV729PCR products	98
Figure 33 The RT-PCR detection of MrNV in immune challenge experiment	99
Figure 34 Expression of MrTCTP after MrNV challenge.....	100
Figure 35 PCR product of DNA template for in vitro transcription	101
Figure 36 Validation of dsRNA using three difference nucleases.....	102
Figure 37 Expression of MrTCTP after in vivo knockdown.....	103
Figure 38 The RT-PCR detection of MrNV in RNAi experiment.....	104
Figure 39 Cumulative mortalities of MrTCTP-silenced prawns after MrNV injection	105
Figure 40 Summary of DEG comparisons between the results from the pipeline and (Rao et al., 2015)	107
Figure 41 The RT-PCR detection of MrNV in NGS experiment	108

Figure 42 Electropherogram of the cDNA library.....	109
Figure 43 Electropherogram of the pooled cDNA library.....	110
Figure 44 Average Phred score of both raw and trimmed read	111
Figure 45 Transcriptome quality assessment results.....	113
Figure 46 Top 10 species distribution of Blastx results from different databases	115
Figure 47 GO distribution (level 2) of annotated unigenes based on UniProt database	116
Figure 48 EggNOG classifications of annotated unigenes based on UniProt database	117
Figure 49 KEGG orthology of annotated unigenes based on UniProt database	118
Figure 50 Principle component analysis of twelve samples (84,092 transcripts)	123
Figure 51 Heatmap of top 100 differentially expressed transcripts	124
Figure 52 Comparison of fold change in gene expression between qRT-PCR and RNAseq.....	126

CHAPTER 1

INTRODUCTION

Background

Shrimp aquaculture is one of the main industry that drives world's economic growth especially in India, China, and southeastern Asia (Destoumieux-Garzon et al., 2001). According to Food and Agriculture Organization of the United Nations, shrimp aquaculture has grown exponentially since 1980s due to high market demand (Flegel, Lightner, Lo, & Owens, 2008). Therefore, crustaceans such as giant river prawn (*Macrobrachium rosenbergii*) and penaeid shrimps have become important aquaculture products worldwide.

M. rosenbergii is one of the main species cultured in southeastern Asia and has worldwide production of 200,000 tonnes per year (FAO fishery statistic, 2017). Due to high market demand, farmers were being forced to increase culturing density which can lead to many problems especially infectious diseases caused by virus, bacteria, and fungi (Lightner & Redman, 1998). One of the most serious threats to *M. rosenbergii* is white tail disease (WTD) caused by *Macrobrachium rosenbergii* nodavirus (MrNV). The prominent clinical sign of WTD-infected larvae, post larvae (PL), and early juvenile is whitish muscles particularly in abdominal region. The mortalities may reach 100 percent within 7-15 days after the infection or 3-5 days after the appearance of the first gross signs which causes great economic losses (Sahul Hameed, Yoganandhan, Sri Widada, & Bonami, 2004). There is no report on control and prevention of WTD. There are only preventive procedures such as screening of brood stock and PL, good farm management, and good practices (OIE, 2009).

As a crustacean, shrimp's immune system is solely relied on innate immune system which consists of humoral and cellular responses. Pattern recognition receptors (PRRs) such as Toll receptors lead to the activation of humoral and cellular immune responses by the recognition of pathogens or pathogen-associated molecular patterns (PAMPs) (F. Li & Xiang, 2013). Humoral immune responses include prophenol oxidase

system (ProPO), clotting proteins, melanization and antimicrobial peptides(Soderhall & Cerenius, 1998). On the other hand, cellular immune responses involve hemocytes which capable of neutralizing pathogens by phagocytosis, apoptosis, nodule formation, and encapsulation(Jiravanichpaisal, Lee, & Soderhall, 2006).

Apoptosis or programmed cell death is a cellular process for removing harmful cell that carrying genetic damage or having uncontrolled proliferation. Apoptosis is also considered as an important cellular response that limit viral replication and eliminate viral-infected cells in multicellular organisms (Everett & McFadden, 1999; Koyama, Fukumori, Fujita, Irie, & Adachi, 2000). There are several apoptosis regulators in crustacean that have been reported including an initiator caspase (L. Wang, Zhi, Wu, & Zhang, 2008), effector caspases (J.H. Leu, Lin, Huang, Chen, & Lo, 2013; P. H. Wang, Wan, Chen, et al., 2013), inhibitor of apoptosis protein (J. H. Leu, Kuo, Kou, & Lo, 2008), the mitochondrial-related voltage-dependent anion channel (VDAC) (Shoshan-Barmatz & Ben-Hail, 2012), and translationally controlled tumor protein (TCTP) or fortilin (J.H. Leu et al., 2013).

TCTP or fortilin is highly conserved protein among eukaryotes(Thomas, Thomas, & Luther, 1981) that plays important roles in many biological processes including cell growth (Gachet et al., 1999), cell cycle control (Cans et al., 2003), and has anti-apoptotic activities (H. Liu, Peng, Cheng, Yuan, & Yang-Yen, 2005). There are several studies that identified *TCTP* cDNA in shrimp and suggested that TCTP might play critical roles in shrimp's anti-viral immunity (Bangrak, Graidist, Chotigeat, & Phongdara, 2004; S. Wang, Zhao, & Wang, 2009; W. Wu et al., 2013). Bangrak and others reported that PmTCTP mRNA expression from *Penaeus monodon* is significantly up-regulated after the infection of white spot syndrome virus (WSSV) and significantly decreased in WSSV-infected moribund shrimp (Bangrak et al., 2004). In 2008, Wang and others identified *FcTCTP* from *Fenneropenaeus chinensis* and found that *FcTCTP* expression is increased after the exposure of WSSV (S. Wang et al., 2009). Another study from Wu and others in 2013 has been reported that silencing of *LvTCTP* from *Litopenaeus vannamei* using RNAi technology led to increase of WSSV copies (W. Wu et al., 2013). To date, there is no

information about TCTP from *M. rosenbergii* in terms of immunological roles against *MrNV* infection. Here in, the objectives of this study were to clone and characterize TCTP from *M. rosenbergii* and examine its role in innate immunity against viral infection.

There are many ways to investigate host-pathogen interactions through gene expression (transcriptome profiling). In recent years, high-throughput technology such as next generation sequencing (NGS) has emerged and is widely used in both genomic and transcriptomic research. One of the most popular NGS platform in the market is Illumina Genome Analyzer. NGS technology can also be used to study differential gene-expression on various tissues or certain conditions such as stress and pathogen infection (Morozova & Marra, 2008). There are transcriptomic studies for penaeid shrimps such as *Peneaus monodon* (Huerlimann et al., 2018; Nguyen et al., 2016; Soonthornchai et al., 2016), *Litopenaeus vannamei* (K. Chen et al., 2015; C. Li et al., 2012; Yu et al., 2014), *Fenneropenaeus chinensis* (S. Li, Zhang, Sun, Li, & Xiang, 2013; X. Shi et al., 2018), *Fenneropenaeus merguensis* (Powell, Knibb, Remilton, & Elizur, 2015; W. Wang et al., 2017), and *Marsupeneaus japonicus* (Sellars, Trewin, McWilliam, Graves, & Hertzler, 2015) to investigate tissue-specific expression, the stress response, and viral infection. Moreover, many studies have performed on whole transcriptome sequencing of the hepatopancreas of *M. rosenbergii* in response to *Vibrio parahaemolyticus* infection (Rao et al., 2015), hepatopancreas and lymphoid organ in response to white spot syndrome virus (WSSV) (Cao et al., 2017; Rao et al., 2016), and intestinal tissue in response to WSSV or the viral PAMP mimic (poly I:C) (Z. Ding, Jin, & Ren, 2018). Most recently, transcriptomic analysis of hematopoietic tissue of *M. rosenbergii* adult prawn in response to *MrNV* infection has been studied. They also reported differentially expressed genes involved in *MrNV* infection in adult prawn (Jariyapong et al., 2019). Many of these genes were belonged to various immune mechanisms such as pattern-recognition receptors, antioxidants, and antimicrobial peptides (Jariyapong et al., 2019).

White tail disease caused by *MrNV* has direct impact on *M. rosenbergii* post-larvae culture. However, there is no transcriptomic data on *M. rosenbergii* post-larvae in response to the infection with *MrNV*. Therefore, this study was aimed to discover immune-

related genes of *M. rosenbergii* that respond to *MrNV* infection in post-larvae prawn, using NGS technology. Identifying these genes is crucial to understanding the mechanism by which *M. rosenbergii* combats a viral infection and provides manipulatable gene targets to test for disease prevention and spread.

Objective

1. To clone and characterize TCTP from *M. rosenbergii* (*MrTCTP*)
2. To analyze the tissue distribution of *MrTCTP* transcript among various tissues and responses against viral infection
3. To examine *MrTCTP* role in anti-viral immunity using RNA interference
4. To generate highly complete transcriptome of *M. rosenbergii* that can be used as reference transcriptome for the further gene expression analysis
5. To discover immune-related genes of *M. rosenbergii* in response to *MrNV* infection

Research hypotheses

1. *MrTCTP* is expected to be highly conserved among various TCTP proteins and expressed ubiquitously in every tissue examined.
2. The expression of *MrTCTP* is expected to be aberrantly expressed in response to viral infection and *MrTCTP*-knockdown prawn is expected to have higher mortality after the infection of *MrNV*.
3. Assembled transcriptome of *M. rosenbergii* is expected to be highly complete and well annotated with low level of redundancy.
4. Immune-related genes of *M. rosenbergii* regarding antiviral-immunity are expected to be aberrantly expressed in response to *MrNV* infection.
5. High correlation of the differentially expressed genes between RNAseq and qRT-PCR results using difference biological samples is expected.

Scopes

1. Clone *MrTCTP* using degenerate primers and rapid amplification of cDNA ends (RACEs) and characterize using multiple sequence alignment, homology search, and prediction software
2. Analyze the tissue distribution of *MrTCTP* transcript and responses against viral infection using semi-quantitative RT-PCR
3. Examine *MrTCTP* role in anti-viral immunity by monitoring cumulative mortalities of *MrTCTP*-knockdown prawn using RNA interference regarding viral infection
4. Generate high quality transcriptome of *M. rosenbergii* post-larvae using whole transcriptome sequencing and *de novo* transcriptome assembly software
5. Annotate the assembled transcriptome using homology search software and assess the quality of assembled transcriptome
6. Discover immune-related genes of *M. rosenbergii* post-larvae in response to *MNV* infection using alignment-based abundance estimation and differential expression analysis software
7. Validate the differential expression results using quantitative PCR (qRT-PCR) in separate biological samples

CHAPTER 2

LITERATURE REVIEW

Macrobrachium rosenbergii (Giant River Prawn)

Macrobrachium rosenbergii or giant river prawn is a large freshwater prawn native throughout the tropical and subtropical areas of the Indo-West Pacific, from India to Southeast Asia (Vietnam, Philippines,) and Northern Australia (Motoh & Kuronuma, 1980). *M. rosenbergii* is one of the largest freshwater prawn in the world and is commercially important. It has been introduced to various parts of Africa, Thailand, China, Japan, New Zealand, the Americas, and the Caribbean for aquaculture (New, 2000). Since then, global production of *M. rosenbergii* has increased and exceeded 200,000 tonnes in 2002 (FAO fishery statistic, 2017).

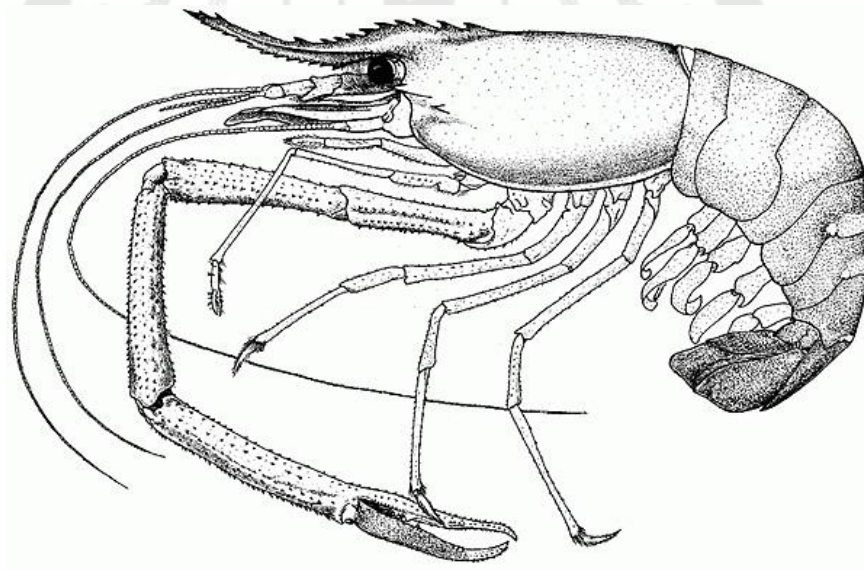


Figure 1 *Macrobrachium rosenbergii* (De Man, 1879)

Source: Food and Agriculture Organization of the United Nations (Online)

Scientific classification

Domain: Eukaryota

Kingdom: Metazoa

Phylum: Arthropoda

Subphylum: Crustacea

Class: Malacostraca

Order: Decapoda

Suborder: Natantia

Family: Palaemonidae

Genus: *Macrobrachium*

Species: *Macrobrachium rosenbergii*

Biological features

Males prawn are usually larger than the females, which can grow up to 320 mm whereas the females can grow up to 250 mm. The color of *M. rosenbergii* is usually greenish to brownish gray depending on habitat and diet. As a decapod crustacean, head (cephalon) and thorax are fused into a cephalothorax. The rostrum at the tip of the cephalothorax has 11-14 dorsal teeth and 8-10 ventral teeth. Cephalon part of cephalothorax contains eyes, antennulae, antennae, mandibles, maxillulae, and maxillae. Thorax part of cephalothorax contains three pairs of maxillipeds (mouthparts), and five pairs of pereopods (true legs). Abdomen contains five pairs of pleopods, and a pair of uropod (Holthuis, 2000). Anatomy sketch of *M. rosenbergii* is presented in Figure 1.

Macrobrachium means "large arms" which can justify by the second pair of walking legs. Especially in the males, the walking legs can be very powerful and twice the body length. The abdomen of the female is wider than that of the male as well as longer pleura (overlapping plates of cuticle) for incubating the eggs. Female genital pores are located at the third walking legs whereas the male genital is on the fifth walking legs (Holthuis, 2000).

Habitat and life cycle

M. rosenbergii lives in tropical freshwater environments adjacent to the brackish water typically in extremely turbid water. When mating, the males deposit spermatophores under the female's thorax, then the females perform egg extrusion. The fertilized eggs will be carried within the pleura until hatching. The gravid females migrate into estuaries and perform hatching. Larvae live in brackish water until metamorphose into post-larvae (PL). After the metamorphosis, the PL begin to migrate towards freshwater. The larvae feeds on zooplankton, tiny worms, and larvae of other crustacean whereas the PL and adults are omnivore which eat algae, plants, and other aquatic life (Motoh & Kuronuma, 1980). Males and females *M. rosenbergii* are differ in size and growth rates. The males are generally larger than females and have heterogeneous individual growth (HIG). There are three distinct male's morphotypes including small males (SM), orange claw males (OC), and blue claw males (BC) in which male's development generally follows this order. The presence of the BC delays the transition of the OC and suppress the growth of the SM. This allows the BC to dominate other morphotypes (A. Barki, Karplus, & Goren, 1991).

***Macrobrachium rosenbergii*'s Nodavirus (MrNV)**

White tail disease (WTD) is an infection disease of *M. rosenbergii* caused by *Macrobrachium rosenbergii* nodavirus (MrNV). This disease was first discovered in the Pointe Noire in Guadeloupe Island and then in Martinique, French West Indies in 1997 with the prominent clinical sign of whitish muscles particularly in abdominal region and up to 100 percent mortalities in post larvae (PL) hatchery (Arcier et al., 1999). Few years after the first discovery, MrNV has been identified as causative agent for this disease (Bonami, Shi, Qian, & Sri Widada, 2005). MrNV is also found in Taiwan (Tung, Wang, & Chen, 1999), China (Qian et al., 2003), India (Sahul Hameed et al., 2004), Thailand (Yoganandhan, Sri Widada, Bonami, & Sahul Hameed, 2005), and Australia (Owens, La Fauce, Juntunen, Hayakijkosol, & Zeng, 2009). MrNV has been found in brackish and freshwater and can be detected in infected larvae, PL, and early juvenile with whitish muscles sign whereas adult may act as a carrier (Sahul Hameed et al., 2004). It has been reported that extra small virus (XSV) is usually found in MrNV-infected prawn. XSV is a non-enveloped, icosahedral with 15 nm diameter bearing one ssRNA genome encoding capsid protein. Many studies suggested that XSV may be a satellite virus that utilize RdRP from MrNV for replication (Bonami et al., 2005; Murphy et al., 1995; Widada & Bonami, 2004). However, Zhang and others reported that MrNV is the major cause of the pathology and the relationship between MrNV and XSV is still unknown (H. Zhang et al., 2006).

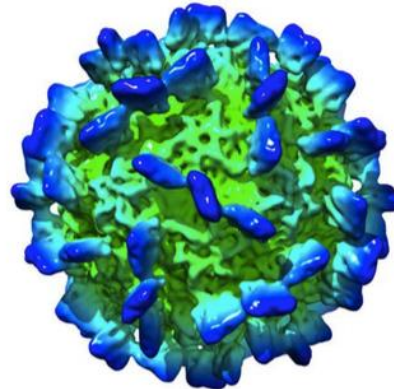


Figure 2 3D Reconstruction of *Macrobrachium rosenbergii* nodavirus (MrNV)

Source: Kok LH, Chare LK, Poay LB, Wen ST, David B. (2017). Cryo-Electron Microscopy Structure of the *Macrobrachium rosenbergii* Nodavirus Capsid at 7 Angstroms Resolution. *Scientific reports*, 7(2083).

As a member of nodaviruses, MrNV is a non-enveloped, icosahedral with 26-27 nm diameter (Figure 2) which comprises a nucleocapsid bearing two positive single-stranded RNA genomes (RNA-1 and RNA-2) (Figure 3). RNA-1 is 3202 bp positive ssRNA encoding protein A or RNA-dependent RNA polymerase (RdRp) (Widada & Bonami, 2004). Additionally, the 3' end of RNA-1 (sub-genomic of RNA-1 or known as RNA-3) also encodes protein B in different reading frame (+1 reading frame relative to protein A). Protein B2 is capable of inhibiting RNAi pathway in host cell by binding to dsRNA which prevents the degradation of RNA by RNAi (H. Li, Li, & Ding, 2002). RNA-2 is 1175 bp positive ssRNA encoding coat protein precursor alpha (known as capsid protein) which is then cleaved into protein beta and gamma after the provirions assembly (Bonami et al., 2005).

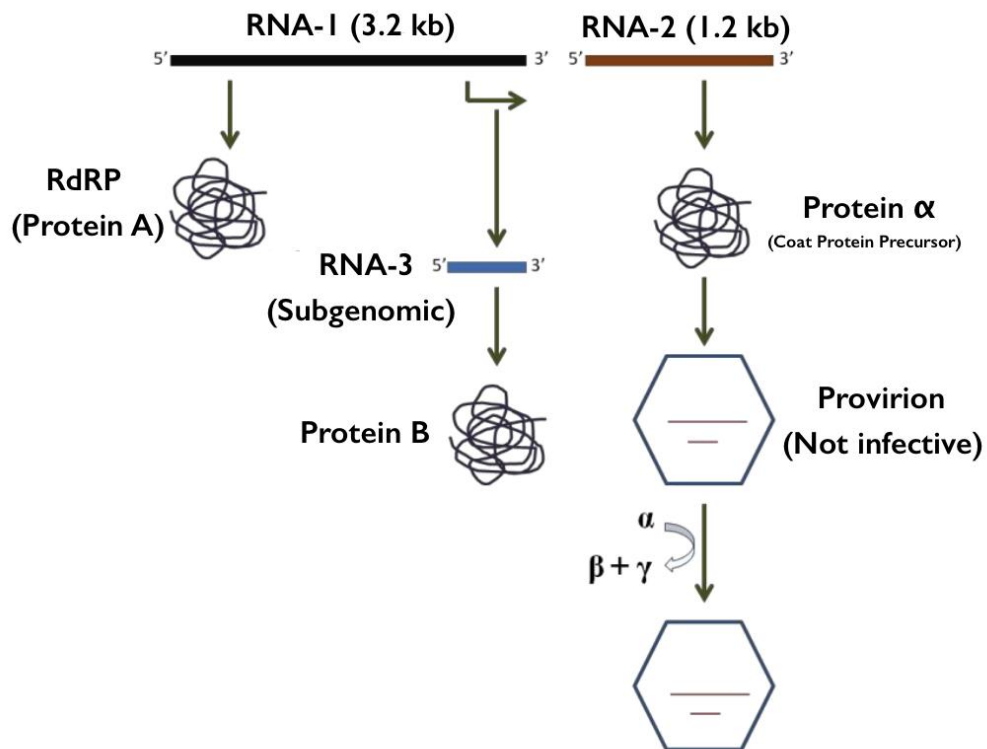


Figure 3 Genomic organization of *Macrobrachium rosenbergii* nodavirus (MrNV)

Source: Murphy FA, Fauquet CM, Bishop DHL, Ghabrial SA, Jarvis A, Martelli GP, et al. (1995). Virus Taxonomy: Classification and Nomenclature of Viruses. Springer-Verlag Wien. (Modified)

Clinical signs

The prominent clinical sign of WTD-infected larvae, post larvae (PL), and early juvenile is whitish muscles particularly in abdominal regions and abnormal molting (Figure 4). The whitish muscles are clearly visible against dark background (Arcier et al., 1999). The discoloration starts at the tail and spread towards the head and appears 2-3 days after the infection. Necrotic tissues are also found in the striated muscle. The mortality rate is up to 100 percent within 7-15 days after the infection or 3-5 days after the appearance of the first gross signs. However, very few infected PL with prominent signs can survive and grow normally (Sahul Hameed et al., 2004).



Figure 4 WTD-infected *M. rosenbergii* juvenile showing whitish muscles

Source: Owens L, La Fauce K, Juntunen K, Hayakijkosol O, Zeng C. (2009). *Macrobrachium rosenbergii* nodavirus disease (white tail disease) in Australia. *Dis Aquat Organ.* 23,85(3): 175-80.

Histopathology

MrNV mainly infects muscles and other mesodermal tissues (e.g. intratubular connective tissue of hepatopancrease). Necrotic muscles show high levels of eosinophilic and show the absence of striated appearance (Figure 5). The infected striated muscles show fibrosis and haemocytic infiltration which can be characterized by basophilic inclusion in the cytoplasm of the connective tissues. However, the viral inclusions are not detected in hepatopancreatic tubules and gut epitheliums (Arcier et al., 1999).

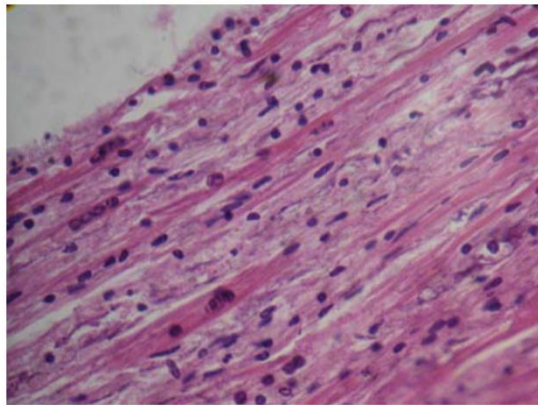


Figure 5 An area of necrotic muscles in WTD-infected shrimp

Source: Owens L, La Fauce K, Juntunen K, Hayakijkosol O, Zeng C. (2009). *Macrobrachium rosenbergii* nodavirus disease (white tail disease) in Australia. *Dis Aquat Organ.* 23, 85(3): 175-80.

Transmission

MrNV infects larvae, post larvae (PL), and early juvenile causing massive mortality in infected PL (Sahul Hameed et al., 2004). The viral replication occurs in connective tissue of the muscles as can be observed by basophilic inclusion in the cytoplasm. *MrNV* may transmit by both vertical and horizontal ways. The main route of transmission is the vertical which demonstrated in the brooders to progeny experiment and RT-PCR in ovarian tissues and fertilized eggs (Sudhakaran et al., 2007).

The Immune System of Shrimp

The immune system of shrimp is less developed compared to the finfish and other vertebrates which have ability to produce immunoglobulin (Roch, 1999). Therefore, shrimp's immune system is solely relied on innate immune system known as non-specific defense mechanisms which consist of humoral and cellular responses. Humoral defenses include activation and secretion of molecules stored within hemocytes such as prophenol oxidase system (ProPO), clotting proteins, melanization and antimicrobial peptides (Soderhall & Cerenius, 1998). On the other hand, cellular defenses include reactions conducted directly from hemocytes and other cells such as phagocytosis, apoptosis, nodule formation, and encapsulation (Jiravanichpaisal et al., 2006).

Pattern recognition receptors (PRRs)

Innate immune system in shrimp requires the recognition of the pathogens by the pattern recognition receptors (PRRs) to trigger the responses (Medzhitov & Janeway, 2000). PRRs are various groups of germ-line encoded proteins that can lead to rapid humoral and cellular immune response (X. W. Wang & Wang, 2013). There are PRRs that have been studied in shrimp including peptidoglycan recognition proteins (PGRPs), Gram-negative binding proteins (GNBP) or lipopolysaccharide and beta-1,3-glucan binding proteins (LGBPs), C-type lectins and Toll receptors (Amparyup, Sutthangkul, Charoensapsri, & Tassanakajon, 2012; C. Yang et al., 2008; L. S. Yang et al., 2007; Y. Zhang et al., 2009). Additionally, in insects, there are other groups of PRRs that have been identified including galectins, thioester containing proteins (TEPs), fibrinogen-related proteins (FREPs), scavenger receptors (SRs), and Down syndrome cell adhesion molecules (DSCAMs) (Christophides, Vlachou, & Kafatos, 2004; Nakamoto et al., 2012; Watson et al., 2005).

Unlike vertebrate antibodies, PRRs recognize pathogen associated molecular patterns (PAMPs) rather than specific epitope of the microbes. PAMPs are molecular patterns or molecular structures shared by pathogens which are the polysaccharides and glycoproteins that are not associated with the hosts such as lipopolysaccharide (LPS),

peptidoglycan, lipoteichoic acid, and glucan. In addition, PAMPs can be nucleic acids such as single stranded and double stranded RNA of viruses (Christophides et al., 2004; Jensen & Thomsen, 2012; X. W. Wang & Wang, 2013).

Immune signaling pathways

The recognition of pathogens or PAMPs by pattern recognition receptors (PRRs) triggers humoral and cellular immune responses via signal transductions (F. Li & Xiang, 2013). This signal transduction or immune signaling pathways includes binding of extracellular ligands to surface receptor that activates the molecular cascade inside the cells and triggers response against pathogens (Borregaard, Elsbach, Ganz, Garred, & Svejgaard, 2000).

The Toll and immune deficiency (IMD) signaling pathways are considered to be the most important immune signaling pathways in invertebrates (De Gregorio, Spellman, Tzou, Rubin, & Lemaitre, 2002). The toll receptor recognizes pathogens via cytokine-like ligand Spätzle whereas vertebrate Toll-like receptors (TLRs) recognize pathogens directly (Lemaitre & Hoffmann, 2007; P. H. Wang et al., 2012). Endogenous ligand Spätzle will be cleaved into mature form after the infections and then binds to the toll receptor. After the activation of NF-kappa-B family protein Dif/Dorsal by the binding to the toll receptor, expression of immune-related genes such as antimicrobial peptide genes (AMPs) are up-regulated (Lemaitre & Hoffmann, 2007). The IMD pathway functions parallel to the toll signaling pathway. The IMD pathway induces immune-related genes expression in response to the pathogen particularly to the Gram-negative bacteria (Lemaitre & Hoffmann, 2007). The JAK-STAT signaling pathway is also an important pathway in antiviral response. This pathway is activated by the inflammation and production of type I interferon (IFN) induced by the viral infection, resulting in the up-regulation of interferon-stimulated genes (ISGs) (de Veer et al., 2001; Sadler & Williams, 2008).

RNA interference (RNAi) pathway

RNA interference (RNAi) or post-transcriptional gene silencing (PTGS) is a biological process which is conserved in many eukaryotes. RNAi pathway involves two types of small RNA molecule including, microRNA (miRNA) and small interfering RNA (siRNA) that are capable of inhibiting gene expression by neutralizing mRNA (Saurabh, Vidyarthi, & Prasad, 2014). Many studies found that administration of synthetic dsRNA/siRNA can protect shrimp from viral infection suggesting that RNAi pathway has a crucial role in crustacean antiviral immunity (Tirasophon, Roshorm, & Panyim, 2005; J. Xu, Han, & Zhang, 2007; Yodmuang, Tirasophon, Roshorm, Chinnirunvong, & Panyim, 2006).

RNAi pathway involves cleavage of foreign double-stranded RNA (dsRNA) molecules (e.g. from viral infection) into short double-stranded fragments of 21-30 nucleotides siRNA. The siRNA is then bounded to the RNA-induced silencing complex (RISC) which can cleave RNA that is complemented to the siRNA (Kupferschmidt, 2013). There are numerous studies revealed that administration of dsRNA or siRNA in shrimp can inhibit viral replication (Tirasophon et al., 2005; J. Xu et al., 2007; Yodmuang et al., 2006). The dsRNA can also be formed during replication of both RNA (e.g. taura syndrome virus (TSV) and yellow head virus (YHV)) and DNA viruses (e.g. white spot syndrome virus (WSSV)). These dsRNA will engage the RNAi pathway and then trigger the antiviral responses (T. Huang & Zhang, 2013b).

The miRNAs are germ-line encoded RNAs that regulate gene expression, especially during growth and development by binding to the RISC and inhibit the translation of the mRNA. Huang and Zhang revealed that there are 31 miRNAs that expressed differentially in response to WSSV infection (25 miRNAs were up-regulated while 6 miRNAs were down-regulated) suggesting that these miRNAs could mediate immune signaling pathway and involved in innate immunity (T. Huang & Zhang, 2013a). Moreover, Yang and others identified a total number of 24 miRNAs that involve in innate immune system including phagocytosis, proPO system, and apoptosis (G. Yang, Yang, Zhao, Wang, & Zhang, 2012).

Hemocytes and hematopoiesis

Most of crustaceans have three different types of hemocyte including, hyaline cells (HC), semigranular cells (SGCs) and granular cells (GCs) which play a crucial role in protecting the animal against the infection (Jiravanichpaisal et al., 2006). The hyaline cells are responsible for cellular response such as phagocytosis (Johansson, Keyser, & Sritunyalucksana, 2000). The granular cells contain granule with several immune substances such as the proPO-activating enzymes and crustins, whereas the semigranular cells are responsible for both cellular and humoral responses (Sricharoen, Kim, Tunkijjanukij, & Soderhall, 2005). Hematopoiesis or hemocytes formation in shrimp is occurred in the hematopoietic tissues (HPTs) which made of lobules covered by connective tissue and located at the dorsal side of the stomach, and at the start of the maxillipeds (van de Braak et al., 2002).

Clotting, antimicrobial peptides, and prophenol oxidase system (proPO)

Clotting is one of the humoral responses that preventing hemolymph loss and microbial spread during the injury (Maningas, Kondo, & Hirono, 2013). The blood coagulation in crustacean involves cross-linking aggregates of clotting proteins (CPs) by a calcium-dependent transglutaminase (TGase) produced by hemocyte during microbe invasion or injury. The TGase forms crosslinks between glutamine and lysine of the CPs which cause blood clotting (Hall, Wang, van Antwerpen, Sottrup-Jensen, & Soderhall, 1999). Recent report showed that lysosome and crustin are significantly down-regulated in TGase depleted shrimp suggesting that clotting system is linked with the expression of antimicrobial peptides (AMPs) (Fagutao, Maningas, Kondo, Aoki, & Hirono, 2012).

Antimicrobial peptides (AMPs) are very important components of innate immune system. AMPs are usually small cationic, amphipathic, germ-line encoded proteins that have rapid and efficient antimicrobial effects against broad spectrum of microorganisms including Gram-positive, Gram-negative, yeast, fungi, and some viruses. AMPs's antimicrobial mechanisms are differ in structural conformation, charge, and amphipaticity (Bulet et al., 1991; Yount, Bayer, Xiong, & Yeaman, 2006). It seems to be that AMPs disrupt

the membrane integrity of the target. The cationic charge of AMPs firstly attach to the negatively charged membrane and then destroy microbes by membrane destabilization or pore formation (Brogden, 2005; Yount et al., 2006). To date, there are four major types of crustacean AMPs that have been identified including single-domain linear alpha-helical, single-domain containing cysteine, multi-domain or chimeric, and unconventional AMPs (Rosa & Barracco, 2010).

Prophenol oxidase system or proPO-activating system participates in innate immunity by association with other responses such as melanization, opsonization, hemocyte induction, encapsulation, and nodule formation (Cerenius & Soderhall, 2004; Soderhall & Cerenius, 1998; Soderhall, Cerenius, & Johansson, 1994). The proPO-activating system is controlled by an immune signaling pathway which requires recognition of PAMPs by PRRs that leads to activation of serine proteinases cascade (SPs) and finally to the proteolytic cleavage of the proPO zymogen into active PO enzyme. The active PO enzyme produces polymeric melanin around invading pathogens resulting in melanization at the infection site (Cerenius & Soderhall, 2004).

Phagocytosis

Phagocytosis is an important part in innate immune system. Phagocytosis is a highly conserved mechanisms among multicellular organisms involving ingestion of microparticles including microbial pathogens, and cellular debris from apoptosis and necrosis (Stuart & Ezekowitz, 2008). In crustacean, this process begins with the recognition of PAMPs by PRRs and then triggers the responses via immune signaling pathway. The responses include rearrangement of the cell's cytoskeleton, membrane remodeling, maturation of phagosomes, and production of cytokines. Consequently, phagosomes, lysosome, and endosome are fused into mature phagolysosomes which have acidic and hydrolytic properties and capable of digest the microparticles after being ingested (Stuart & Ezekowitz, 2008).

Apoptosis

Apoptosis or programmed cell death is a cellular process for removing harmful cell that carrying genetic damage or having uncontrolled proliferation. Apoptosis is also considered as an important cellular response that limit viral replication and eliminate viral-infected cells in multicellular organisms (Everett & McFadden, 1999; Koyama et al., 2000). The mechanisms of apoptosis include blebbing (protrusion of cell membrane), cell shrinkage, nuclear fragmentation (karyorrhexis), chromosomal fragmentation, chromatin condensation (pyknosis), and mRNA degradation (Figure 6) (Karam, 2009). Unlike necrosis, apoptosis is well-controlled process that causes no harm to the organisms. Apoptosis produces cell fragments called “apoptotic bodies” that being immediately engulfed and processed by the phagocytes causing zero damage to the surrounding cells (Alberts et al., 2008).

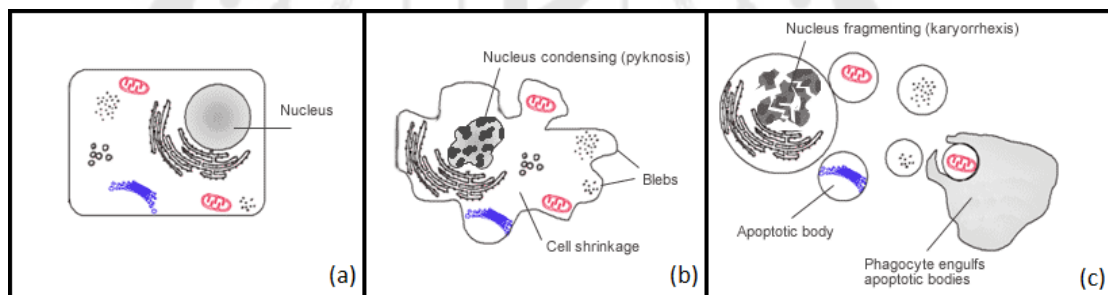


Figure 6 Diagram of a cell undergoing apoptosis

(a) Normal cell, (b) Cell starts shrinking and blebbing and nucleus starts condensing (pyknosis), (c) Nucleus fragmentation (karyorrhexis) occurs and cell breaks into apoptotic body which being engulfed and processed by the phagocyte

Source: Apoptosis, Emma Farmer (Online)

Due to well-regulated and well-controlled of this process, apoptosis can be triggered by two distinct pathways, intrinsic and extrinsic pathways. The extrinsic pathway is activated by ligands binding to cell-surface death receptors and transmission of death signal. This pathway involves in elimination of cells during growth and development, cell differentiation, and tissue remodeling (Tran, Meinander, & Eriksson, 2004). On the other hand, the intrinsic pathway involves responses to disturbance of intracellular homeostasis by cellular stress such as hypoxia, anoxia, viral or bacterial proteins, reactive oxygen species (ROS), radiation, and malfunctioned proteins (Ferri & Kroemer, 2001). The mitochondrial signaling plays an important part in the both pathways and amplification of the death signal (Hand & Menze, 2008).

Both extrinsic and intrinsic pathways trigger the activation of the apoptosis hallmark called “caspases” (Menze, Fortner, Nag, & Hand, 2010). Caspases are highly conserved cysteine protease that involve in the execution of cell death. Caspases are divided into two types, the initiator (Caspase 2, 8, 9, 10, 11, and 12) and the effector (Caspase 3, 6, and 7). The initiator caspases are activated by oligomerization at a specific oligomeric activator protein such as apoptotic protease activating factor 1 (APAF-1). The effector caspases are then activated through proteolytic cleavage that triggered by the activated initiator. The active effector caspases then degrade intracellular proteins and trigger the cell death program (Kumar, 2007).

There are several apoptosis regulators in crustacean that have been reported including an initiator caspase (L. Wang et al., 2008), effector caspases (J.H. Leu et al., 2013; P. H. Wang, Wan, Chen, et al., 2013), inhibitor of apoptosis protein (J. H. Leu et al., 2008), the mitochondrial-related voltage-dependent anion channel (VDAC) (Shoshan-Barmatz & Ben-Hail, 2012), and translationally controlled tumor protein (TCTP) or fortilin (J.H. Leu et al., 2013). In addition, Bangrak and others reported that *PmTCTP* mRNA expression from *Penaeus monodon* is significantly up-regulated after the infection of white spot syndrome virus (WSSV) and significantly decreased in WSSV-infected moribund shrimp (Bangrak et al., 2004). This results confirmed that TCTP play a role in anti-apoptotic

activities (H. Liu et al., 2005) and might play critical roles in shrimp's anti-viral immunity (Bangrak et al., 2004).

Translationally controlled tumor protein (TCTP)

Translationally controlled tumor protein (TCTP) was first discovered in 1980s by three research groups and first named P21, Q23, and P23 (Gachet et al., 1999). In the late 1980s, the name translationally controlled tumor protein was originated because this protein was identified from a human tumour and is regulated at the translational level (Gross, Gaestel, Boehm, & Bielka, 1989). TCTP is also called histamine releasing factor (HRF), and fortilin due to extracellular function as an anti-apoptotic protein and histamine releasing factor (F. Li, Zhang, & Fujise, 2001; MacDonald, Rafnar, Langdon, & Lichtenstein, 1995).

Protein structure

TCTP is a 18-20 kDa hydrophilic protein (approximately 170 amino acid residues) which highly conserved among eukaryotes (Thomas et al., 1981). The TCTP family does not share similarity with any proteins. Multiple sequence alignment of TCTP revealed that approximately 9% of amino acid sequences are conserved (9 amino acid residues and another 6 amino acid residues with one mismatch) (Figure 7A). Most of the conserved residues are located in the beta-stranded core domain indicating the importance of interaction with other molecules. The other two domains specific for TCTP are the flexible loop and the helical domain. The flexible loop contains highly conserved areas which have been listed in the prosite database as TCTP signature 1 and 2 (Bommer & Thiele, 2004). The helical loop contains two molecular function motifs which are the tubulin-binding region and the Ca^{2+} binding area (Gachet et al., 1999; Kim, Jung, Lee, & Kim, 2000). Ribbon diagram containing three major domains of TCTP from fission yeast is shown in Figure 7B.

Regulation

TCTP is ubiquitously expressed in all eukaryotic organisms and in every tissues and cell types investigated. TCTP is present in both cytosol and nucleus. The summary of TCTP regulation and biological functions is presented in Figure 8. The expression levels of TCTP vary according to cell/tissue types and developmental stages. In addition, TCTP is preferentially expressed in highly mitotic tissue rather than less mitotic ones (e.g. brain) (Thiele, Berger, Skalweit, & Thiele, 2000). There are numerous studies reported that the expression levels of TCTP are mainly regulated by various extracellular signals such as growth signals (Bommer et al., 2002) and cytokines (Nielsen, Johnsen, Sanchez, Hochstrasser, & Schlotz, 1998; Teshima, Rokutan, Nikawa, & Kishi, 1998). Moreover, TCTP expression can also be regulated by cellular conditions including starvation (Bommer et al., 2002; Bonnet et al., 2000), heat shock, heavy metals, calcium stress (A. Xu, Bellamy, & Taylor, 1999), or pro-apoptotic/cytotoxic signals (Oikawa et al., 2002).

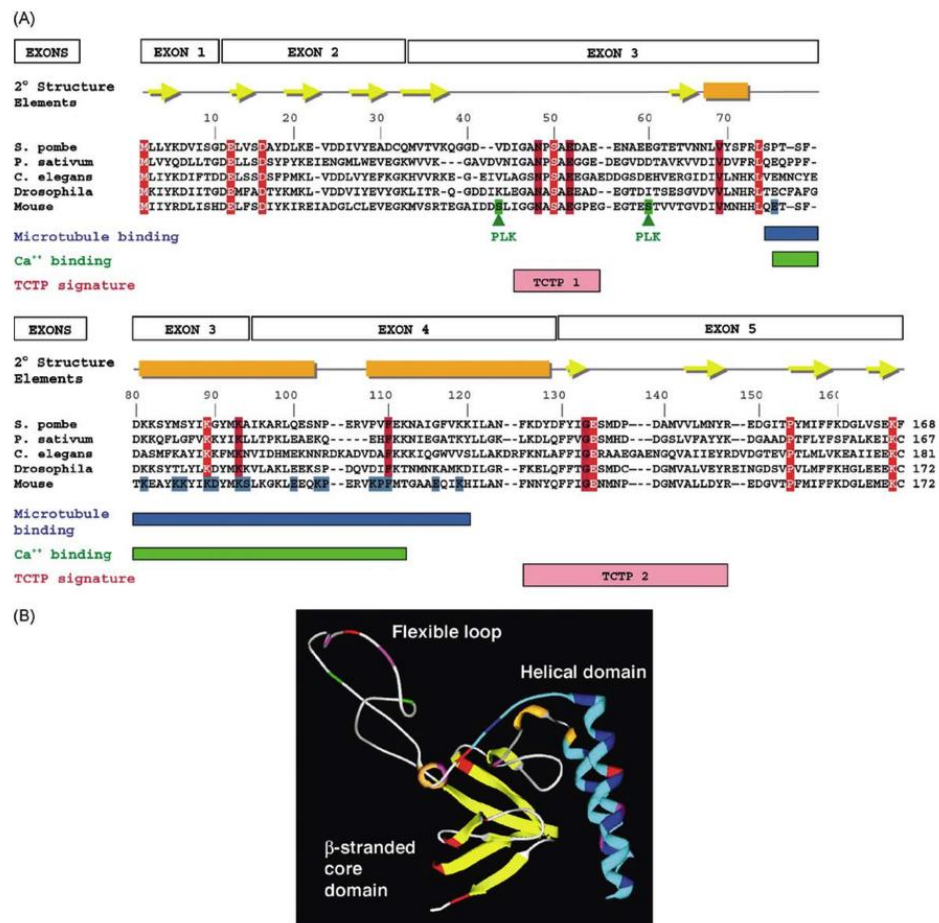


Figure 7 Multiple sequence alignment, ribbon diagram and functional mapping of TCTP

(A) Multiple sequence alignment of TCTP. Conserved residues are labelled in red, the nine absolute conserved residues are in white letter while the six conserved with one mismatch are in the black letter. The secondary structure elements of fission yeast TCTP are represented as follows, beta-stranded core domain: yellow arrows, helices: orange bars, coiled regions: grey line. The tubulin-binding region and the Ca²⁺ binding area are shown in the blue and green bar, respectively. The TCTP signature 1 and 2 are indicated by the pink boxes. Serine residues in the mouse sequence (highlighted in green) are phosphorylated by the Plk mitotic kinase (Yarm, 2002). (B) Ribbon diagram of fission yeast TCTP (Thaw et al., 2001). The color coding is the same as in (A).

Source: Bommer, U. A., & Thiele, B. J. (2004). The translationally controlled tumour protein (TCTP). *Int J Biochem Cell Biol*, 36(3), 379-385.

Biological function

TCTP or fortilin has been reported to play important roles in many biological processes including cell growth and cell cycle control (Cans et al., 2003; Gachet et al., 1999), microtubule stabilization (Yarm, 2002), inflammation (MacDonald et al., 1995), chemo-resistance (Sinha et al., 2000), and anti-apoptotic mechanisms (H. Liu et al., 2005). The summary of biological functions and regulation of TCTP is presented in Figure 9.

From the fact that TCTP is preferentially expressed in highly mitotic tissue, TCTP is believed to be crucial for cell growth, and cell division (Cans et al., 2003; Gachet et al., 1999). This conclusion was agreed by following reports which demonstrated that: (1) down-regulation of TCTP was associated with reversion of the tumour cells and slow-growth phenotype (Kamath et al., 2003; Tuynder et al., 2002)., (2) over-expression of TCTP can cause growth retardation and delayed cell cycle progression (Gachet et al., 1999). (3) TCTP is bound microtubules during most of the cell cycle and detached after metaphase (Yarm, 2002). Moreover, phosphorylation of TCTP by the mitotic polo-like kinase (Plk) may cause the detachment of TCTP and the microtubules and mutation of phosphorylation sites for mitotic Plk protein kinase cause the incomplete mitosis (Yarm, 2002).

As the calcium-binding region was mapped, TCTP has calcium-binding activity which prevent cytosolic Ca^{2+} to cause mitochondrial swelling and activate Ca^{2+} -dependent apoptosis pathway (Kim et al., 2000). TCTP was also reported to function as histamine releasing factor (MacDonald et al., 1995). Following studies suggested that TCTP displays cytokine-like activities in which TCTP is able to induce interleukins-8 (IL-8) production from eosinophils and IL-4, IL-13 and histamine production from basophils (Bheekha-Escura, MacGlashan, Langdon, & MacDonald, 2000; MacDonald et al., 2001). TCTP can be induced by certain type of cytokines and acts as a growth factor for B-cell (Kang et al., 2001). Although the signal sequence of TCTP is absence, TCTP is believed to be secreted via exosome (non-classical pathway) with an assistance of H,K-ATPase and TSAP6 (Amzallag et al., 2004). This hypothesis was supported by the inhibition of

TCTP secretion using proton pump inhibitors (PPIs) *in vivo* (Choi, Min, Kim, Hwang, & Lee, 2009).

The expression levels of TCTP are also regulated by cellular conditions including cellular stress which are consistent with association between increasing TCTP expression and increasing chemo-resistance (Sinha et al., 2000). Moreover, in cancer cell lines, TCTP was reported to be critical survival factor that preventing oxidative stress-induced cell death. Up-regulation of TCTP was observed in survived cell after the treatment of hydrogen peroxide (Nagano-Ito, Banba, & Ichikawa, 2009).

Later on, numerous studies demonstrated protein interaction of TCTP which correlated with anti-apoptotic mechanisms as follows: (1) destabilization of p53 by TCTP which associated with equilibrium between p53 and TCTP and apoptotic homeostasis (H. Liu et al., 2005; Rho et al., 2011), (2) interaction with anti-apoptotic protein, myeloid cell leukemia 1 protein (MCL1), as a chaperone for stabilization of TCTP, another anti-apoptotic protein (D. Zhang, Li, Weidner, Mnjoyan, & Fujise, 2002), (3) binding between N-terminal of TCTP and Bcl-xL which required for anti-apoptotic activity of TCTP (Y. Yang et al., 2005), and (4) inhibition of TCTP secretion by caspase-3 (Sirois et al., 2011).

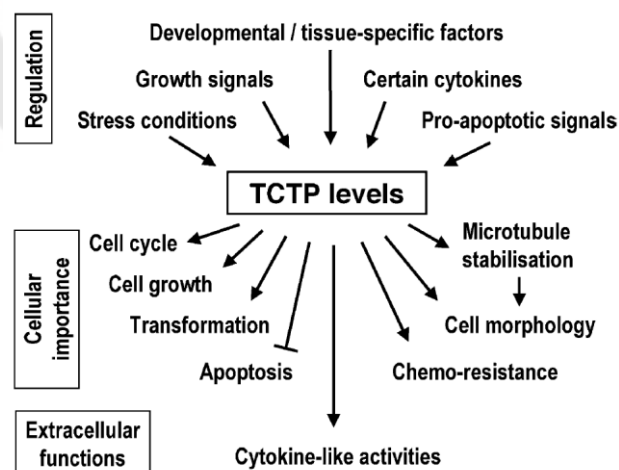


Figure 8 Biological functions and regulation of TCTP

Source: Bommer, U. A., & Thiele, B. J. (2004). The translationally controlled tumour protein (TCTP). *Int J Biochem Cell Biol*, 36(3), 379-385.

TCTP in shrimp

Since TCTP involves in many biological processes including anti-apoptotic mechanisms (H. Liu et al., 2005; Thomas et al., 1981), several studies identified TCTP from various shrimp species and examined TCTP roles in shrimp's anti-viral immunity (Bangrak et al., 2004; S. Wang et al., 2009; W. Wu et al., 2013). In 2004, Bangrak and others identified *PmTCTP* from *Penaeus monodon* and performed semi-quantitative RT-PCR to investigate *PmTCTP* response against WSSV infection. The results showed that *PmTCTP* mRNA expression in hemocytes was significantly up-regulated after the infection of white spot syndrome virus (WSSV) and significantly decreased in WSSV-infected moribund shrimp (Bangrak et al., 2004). Later in 2008, Wang and others cloned *FcTCTP* from *Fenneropenaeus chinensis* and investigated *FcTCTP* expression in hepatopancreas after the infection of WSSV using time-course semi-quantitative RT-PCR analysis. The results revealed that *FcTCTP* expression was increased after the exposure of WSSV (S. Wang et al., 2009). Wu and others in 2013 identified *LvTCTP* from *Litopenaeus vannamei* reported that *LvTCTP* expression in gills was up-regulated at 8 to 48 hours after the infection of WSSV using real-time RT-PCR analysis. Wu and others also reported that silencing of *LvTCTP* using RNAi technology led to the increasing of WSSV copies in gills at 48 hours post infection (W. Wu et al., 2013).

Furthermore, there are reports that studied TCTP's roles in innate immune system in terms of protection against viral infection and immune modulation (Rajesh, Kamalakannan, & Narayanan, 2014; Sinthujaroen, Tonganunt, Eurwilaichitr, & Phongdara, 2015; Tonganunt et al., 2008). In 2008, Tonganunt and others administered *PmTCTP* into *P. monodon* shrimp via oral and intramuscular route and found that survival rate was increased after WSSV infection. Additionally, using PCR detection, the WSSV copies in moribund shrimps were notably higher than that of survived shrimps (Tonganunt et al., 2008). Later in 2014, Rajesh and others cloned *FiTCTP* from *Fenneropenaeus indicus* and examine protective effect of *FiTCTP* using immunological parameters determination including reactive oxygen species (ROS), phenoloxidase activity and mitochondrial

membrane potential (MMP). *F. indicus* shrimps were injected and oral administered by recombinant *FitTCTP* followed by the exposure of WSSV. The results showed that *FitTCTP* pretreatment reduced ROS, mitochondrial damage and respiratory burst during the infection of WSSV (Rajesh et al., 2014). Recently in 2015, Sinthujaroen and others investigated protection of recombinant *PmTCTP* using injection and oral administration. *P. monodon* were injected and oral administered by *PmTCTP* and sonicated yeast harboring *PmTCTP* followed by the injection of WSSV. The cumulative mortality results revealed that recombinant *PmTCTP* has clearing effect on WSSV infection. In addition, shrimp injected with *PmTCTP* dsRNA demonstrated lower survival rates compared with those injected with *LacZ* dsRNA (Sinthujaroen et al., 2015).

Rapid Amplification of cDNA Ends (RACE)

Rapid Amplification of cDNA Ends (RACE) is a molecular biology technique used to identify full-length cDNA of a gene in which partial sequence of the gene is identified. RACE procedures consist of reverse transcription (RACE-ready cDNA preparation) and polymerase chain reaction (RACE-PCR) followed by sequencing of the PCR product. The partial sequence of the gene of interest is required to generate the Gene Specific Primers (GSPs) and nested GSPs (NGSPs) for the RACE-PCR and nested PCR (Frohman, 1994). The use of nested PCR is important for reducing the amplification of non-specific products since the specificity of RACE-PCR is generally low compared to the conventional PCR because of the use of one gene specific primer and one universal primer in the reaction (Oladapo & Michael, 2011).

5'- RACE begins with reverse transcription of the mRNA using anti-sense (reverse) GSP followed by addition of homopolymeric tail from terminal deoxynucleotidyl transferase (TdT) at the 3'-end of the cDNA. The PCR reaction is then being performed using second anti-sense GSP and sense (forward) universal primer that specific to the homopolymeric tail (Figure 9) (F. Li et al., 2001).

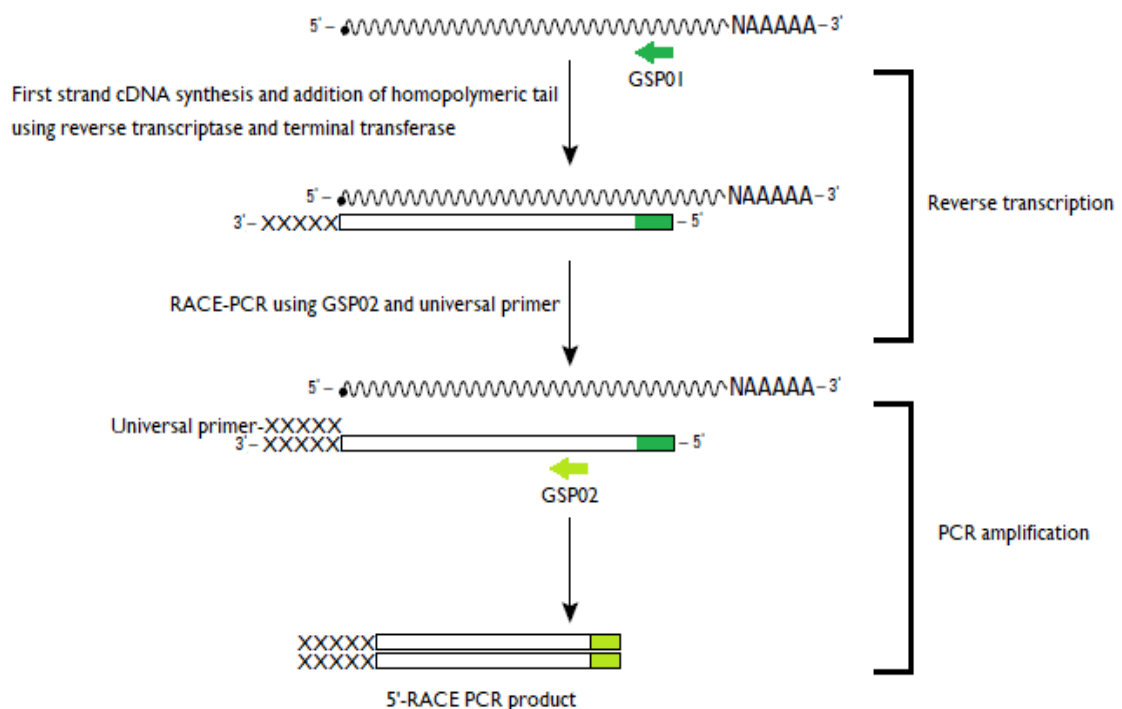


Figure 9 5'-Rapid amplification of cDNA ends

In case of 3'-RACE, reverse transcription of the mRNA uses Oligo-dT-adaptor primer which complementary to the polyA tail. The PCR reaction then uses sense GSP and anti-sense universal primer that specific to the adaptor sequence (Figure 10) (F. Li et al., 2001).

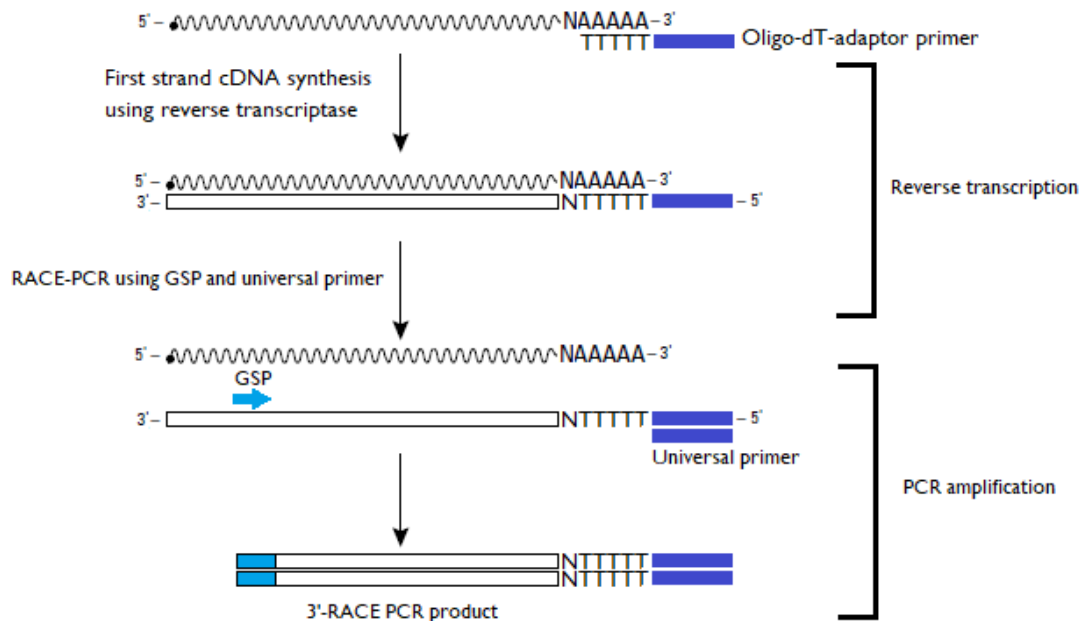


Figure 10 3'-Rapid amplification of cDNA ends

RNA interference (RNAi)

RNA interference (RNAi) is gene regulatory mechanism in which gene expression is inhibited by the mRNA degradation or translational inhibition. This process was formerly known as co-suppression, post-transcriptional gene silencing (PTGS), and quelling (Saurabh et al., 2014). RNAi is conserved in many eukaryotes. RNAi pathway involves two types of small RNA molecule including, microRNA (miRNA) and small interfering RNA (siRNA) that capable of inhibiting gene expression by neutralizing mRNA (Saurabh et al., 2014).

RNAi mechanism

RNAi mechanism involves cleavage of foreign double-stranded RNA (dsRNA) molecules (e.g. from viral infection) into short double-stranded fragments of 21-30 nucleotides siRNA. The 21 nucleotides siRNAs are two strand of 21 nucleotides in which 19 nucleotides are paired into dsRNA and the other two are unpaired nucleotides at both of 3'-and. The siRNAs are then bounded to the RNA-induced silencing complex (RISC) which can cleave RNA that complemented to the siRNA (Kupferschmidt, 2013). In case of miRNA, miRNAs are generated from endogeneous hairpin RNA precursor called short hairpin RNA (shRNA). The miRNAs are germ-line encoded RNAs that regulate gene expression, especially during growth and development by bound to the RISC and inhibit the translation of the mRNA(T. Huang & Zhang, 2013a).

Initiator step

RNAi mechanism is initiated by the cleavage of dsRNA into 21-30 nucleotides siRNA with 2 to 3 nucleotides overhang at 3'-hydroxy terminal ends and 5'-phosphate terminal ends (S.M. Elbashir, W. Lendeckel, & T. Tuschl, 2001). The enzyme that is responsible for the cleavage is RNase III-like enzyme called "Dicer" (Gregory, 2002). Dicer contains four domains including amino-terminal helicase domain, dual RNase III motifs, dsRNA binding domain (dsBRD) and PAZ domain (Piwi, Argo, Zwille/Pinhead like protein) (Bernstein, Caudy, Hammond, & Hannon, 2001). Dicer unwinds and cleaves

dsRNA into 21-30 nucleotides siRNA with 2 to 3 nucleotides overhang at 3'-ends. Bacterial RNase III normally cleaves dsRNA into 9 to 11 nucleotides. Based on this knowledge, Dicer is believed to work as a dimer. Cleavage by Dicer is catalyzed by two active RNase III motifs from each monomer resulting in about 22 nucleotides products (Blaszczyk et al., 2001). The siRNAs are then proceeded to the effector step by bound to the RNA-induced silencing complex (RISC).

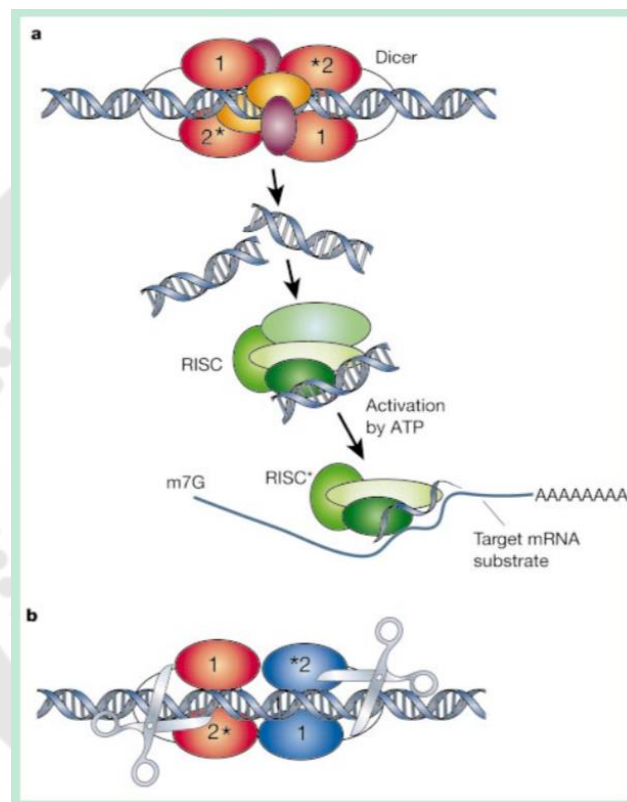


Figure 11 Dicer and RISC (RNA-induced silencing complex)

(A) RNAi mechanism is initiated by the cleavage of dsRNA into 21-30 nucleotides by RNase III-like enzyme called “Dicer”. The siRNAs are then proceeded to the effector step by bound to the RNA-induced silencing complex (RISC) (B) Dicer is believed to work as a dimer. Cleavage by Dicer is catalyzed by two active RNase III motifs from each monomer resulting in about 22 nucleotides products. The defective Dicer domains are shown with asterisk.

Source: Gregory, J. H. (2002). RNA interference. *Nature*, 418, 244-251.

Effector step

After the siRNA was generated, siRNAs are unwound and sense strand of siRNAs are incorporated into RNA-induced silencing complex (RISC) which begins the effector step of RNAi (Nykanen, Haley, & Zamore, 2001). RISC recognizes and degrades target mRNA which represses the expression of the target genes. The endonucleolytic cleavage by RISC complex is occurred at one specific site between siRNA and target mRNA. The degradation by exonucleases is then occurred to cleave mRNA into small fragments. RISC consists of AGO2 which is member of the Argonaute family. AGO2 is 130 kDa protein containing PAZ domain and PIWI domain which is the characteristic of this protein family. The presence of PAZ domain in both AGO2 and Dicer is believed to be associated with RISC assembly (Bernstein et al., 2001). Argonaute proteins are also homologue to RDE1 which required for RNAi mechanisms in *C. elegans* (Fagard, Boutet, Morel, Bellini, & Vaucheret, 2000).

Amplification of the silencing

RNAi mechanism is very effective gene regulation pathway. Small amount of dsRNA is capable for degradation of continuously transcribed mRNA. The amplification of the silencing RNA is caused by two independent processes; cleavage of long dsRNA into many small siRNA, and polymerization by RdRP (RNA-dependent RNA polymerase). Since the former process is not sufficient for spreading proper amount siRNA for mRNA degradation, the latter process is mainly responsible for continuous mRNA degradation (Agrawal et al., 2003).

Lipardi and others demonstrated that single-stranded target mRNA and dsRNA acted as template for generating new molecule of dsRNA by RdRP. The newly formed dsRNA were rapidly generated, cleaved, and proceeded into RNAi pathway. Additionally, they also found that RdRP specifically recognizes siRNA that only contain 3'-hydroxy terminal ends and 5'-phosphate terminal ends (Lipardi, Wei, & Paterson, 2001). In 2002, Sijen and others proposed a term "transitive RNAi" which is movement of silencing signal along target gene from 3'-end to 5'-end. The movement of silencing signal is caused by

activity of RdRP that generate secondary siRNA while slightly move the signal toward 5'-end. For example, in *C. elegans* experiment, targeting GFP in 5'-UNC22-GFP-3' fusion transcript resulted in white and uncoordinated phenotype (white color and abnormal locomotive phenenotype). Whereas targeting GFP in 5'-GFP-UNC22-3' fusion transcript resulted in white phenotype only. This result showed movement of silencing signal toward 5'-end of target mRNA which caused by RdRP-mediated activity (Sijen et al., 2001).

Sequencing-by-synthesis: Illumina sequencing technology

Sequencing-by-synthesis technology was originally developed by Shankar Balasubramanian and David Klenerman, founders of Solexa company, at the University of Cambridge (Bentley et al., 2008). Illumina Inc. subsequently purchased Solexa Company, built and improved their sequencing technology and then became one of the most successful next-generation sequencing (NGS) provider in the market. The Solexa/Illumina sequencing technology utilizes reversible dye terminators, modified dNTP with fluorescent dye and terminators, therefore only single base can be used in the polymerization and then detected by the camera (Mardis, 2013). Millions sequencing reaction occurred simultaneously on the microfluidic glass slide called flow cell. Flow cell contains one, two, four, or eight separate lanes (Figure 12) coated with lawn of adaptor-complimentary oligos (Illumina, 2017).



Figure 12 Illumina NextSeq® 500/550 High Output Kit v2 flow cell

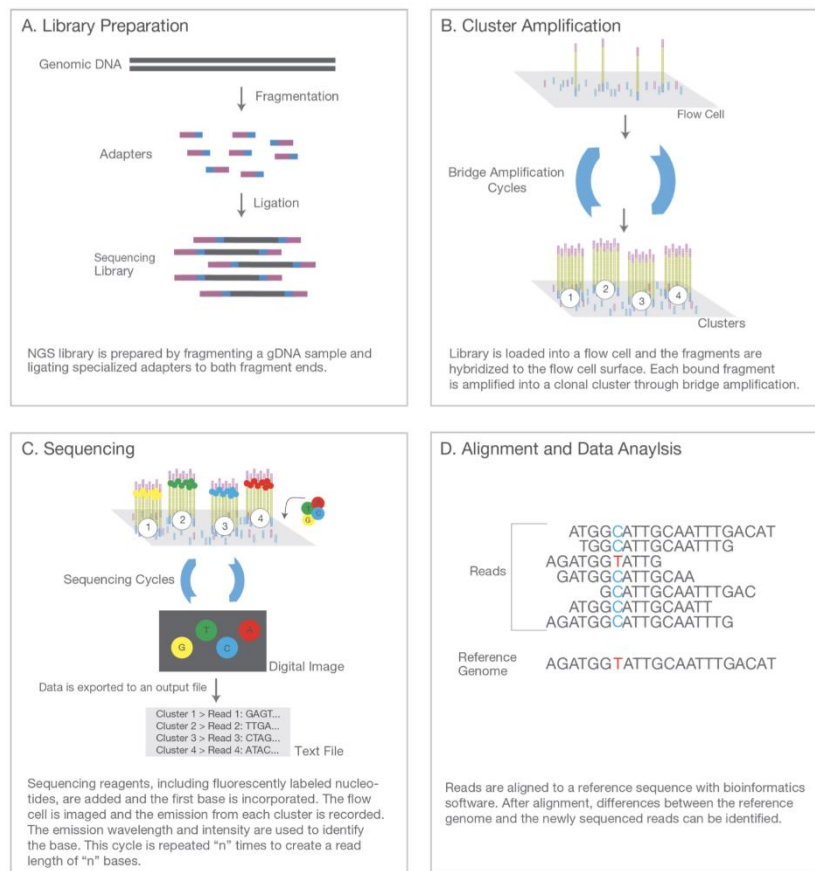


Figure 13 Four major steps of Illumina sequencing platform

Source: Illumina, Inc. (Online)

The Illumina sequencing include four steps: library preparation, cluster generation, sequencing-by-synthesis, and data analysis (Figure 13). Library preparation step involves random fragmentation of DNA or cDNA sample followed by 5' and 3' adaptor ligation (Illumina, 2017). Fragmentation and ligation steps can occurred simultaneously as in Nextera[®] DNA Library Preparation Kits. This technique is called "tagmentation" in which Tn5 transposase and read 1 and 2 primer sequence are employed in the reaction. Transposomes with read 1 or 2 sequence cleave DNA or cDNA sample resulting in fragmented-tagged sample in a single step. A PCR reaction is then carried out generating sequencing-ready-fragment (Figure 14) (Illumina, 2016).

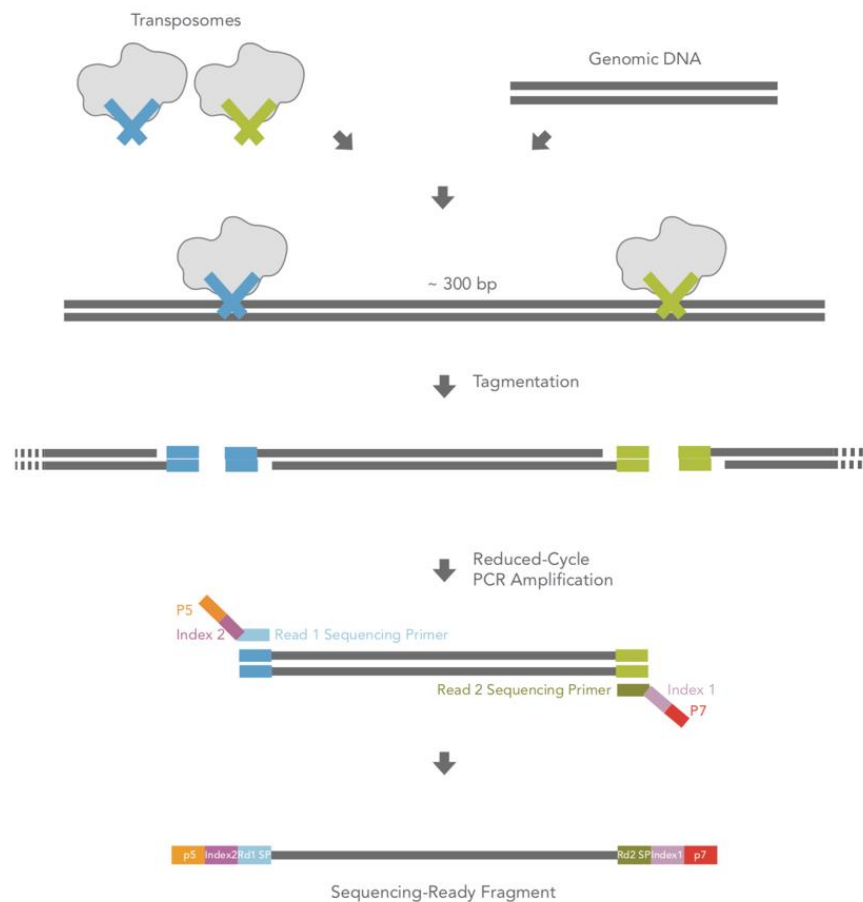


Figure 14 Tagmentation technique in Nextera[®] DNA Library Preparation Kits

Source: Illumina, Inc. (Online)

In case of cDNA library generation, fragmentation and ligation steps can also be performed simultaneously as in Lexogen's SENSE mRNA-Seq Library Prep Kit V2 for Illumina sequencing. After poly (A) selection of mRNA, library generation starts with random hybridization of starter/stopper heterodimers to the poly (A) RNA. The starter/stopper heterodimers contain Illumina-compatible linker sequences. First strand cDNA synthesis extends the starter to the stopper of the next heterodimer and ligation of the stopper occurred. Second strand synthesis is then carried out resulting in fragmented-double-stranded cDNA library. Finally, library amplification is performed using oligo primers with adaptors for Illumina sequencing (Figure 15) (GmbH, 2018).

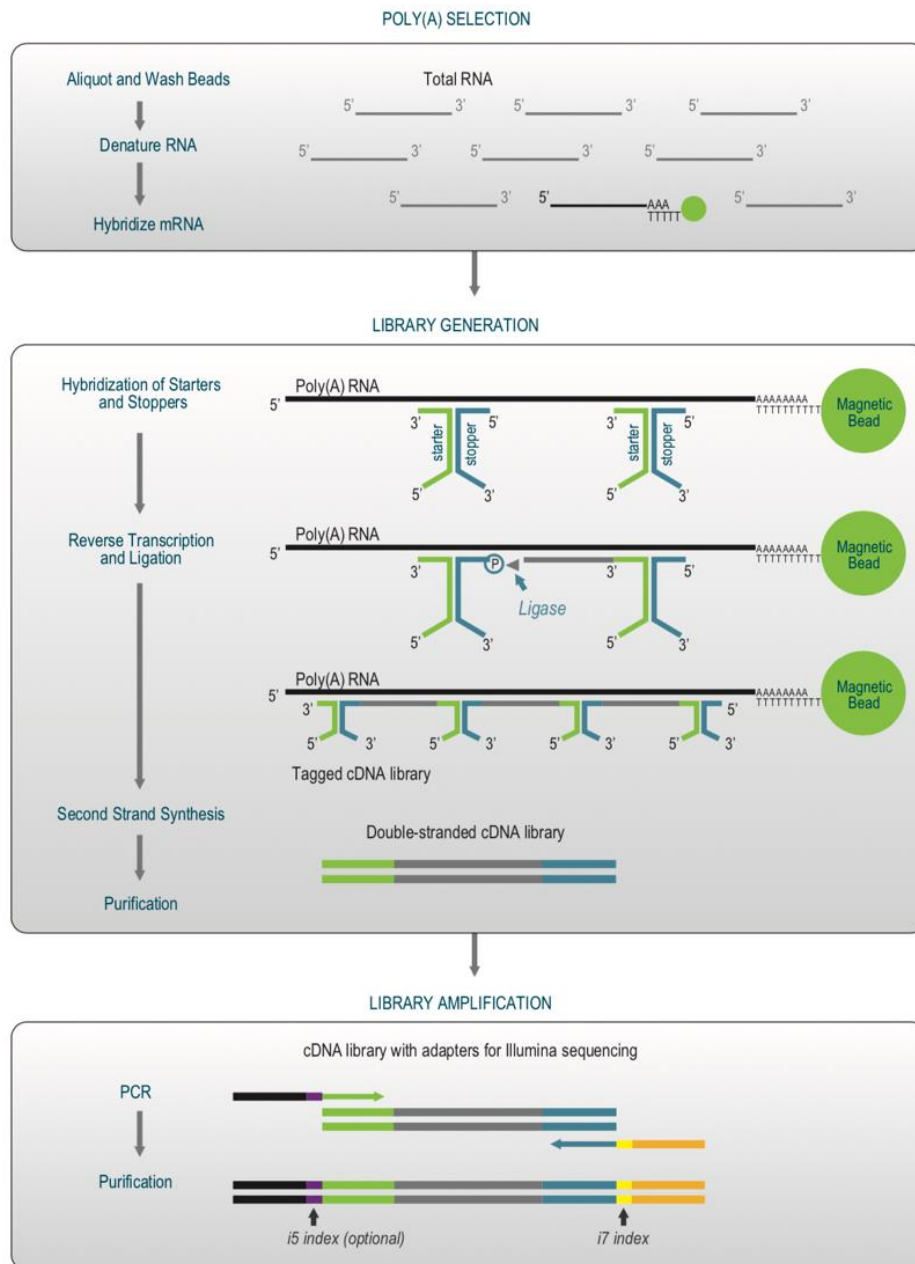


Figure 15 cDNA library generation in Lexogen's SENSE mRNA-Seq Library Prep Kit V2

Source: Lexogen GmbH (Online)

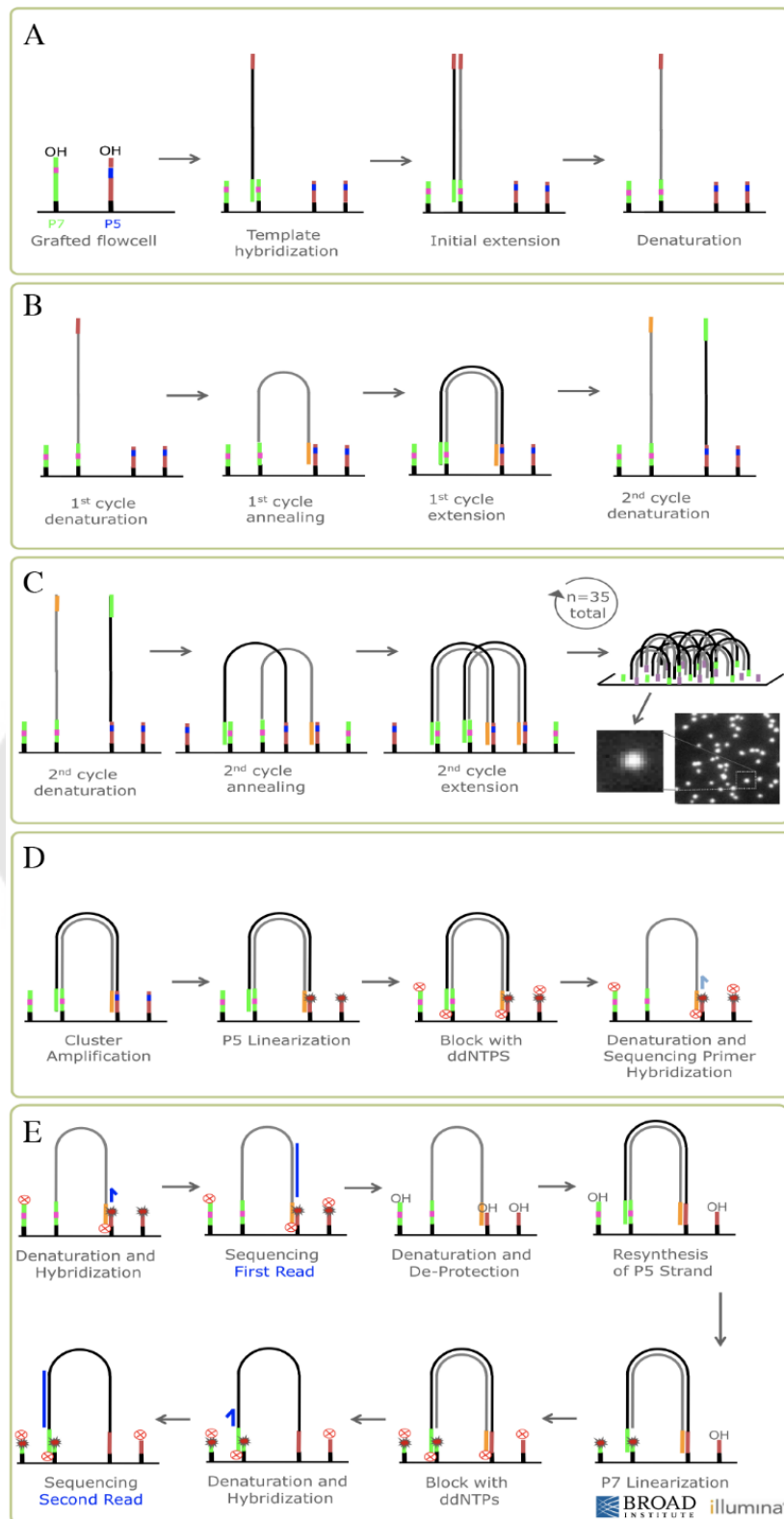


Figure 16 Cluster generation and sequencing-by-synthesis

Source: Broad Institute (Online)

Cluster amplification involves hybridization of the library onto a flow cell, followed by clonal cluster amplification through bridge amplification (Illumina, 2017). Briefly, P7c region of the library hybridizes to P7 on the flow cell and then the first cycle of amplification is occurred (Figure 16A). The library is then washed resulting in grafted library on a flow cell (Figure 16A). Next, bridge amplification occurs through annealing of P5c of the grafted library and P5 on the flow cell (Figure 16B). This process is then carried out in total of 35 cycles resulting in sequencing-ready template (Figure 16C). Before the sequencing, P5 linearization occurs to wash out the reverse strand of the template and blocking occurs in 3'-OH position preventing base incorporation during the sequencing (Figure 16D). In case of paired-end (PE) sequencing, after read 1 is sequenced, 3'-OH blocking is removed and P5 strand is resynthesized. The blocking and sequencing processes for read 2 is then carried out (Figure 16E). The sequencing is performed in this order; read 1 sequencing, i7 index sequencing (optional), read 2 sequencing (PE sequencing), and i5 index sequencing (optional).

Sequencing-by-synthesis occurs repeatedly (up to 300 cycles) in this following order: 1) modified dNTP with reversible dye terminators is added by the polymerase, 2) unincorporated dNTPs are washed out, 3) fluorescence signals are recorded after laser excitation, 4) fluorescent and 3'-OH-terminator are removed (Figure 17B) (Mardis, 2008). This cycle of reactions occurs simultaneously on the flow cell as demonstrated in Figure 17A.

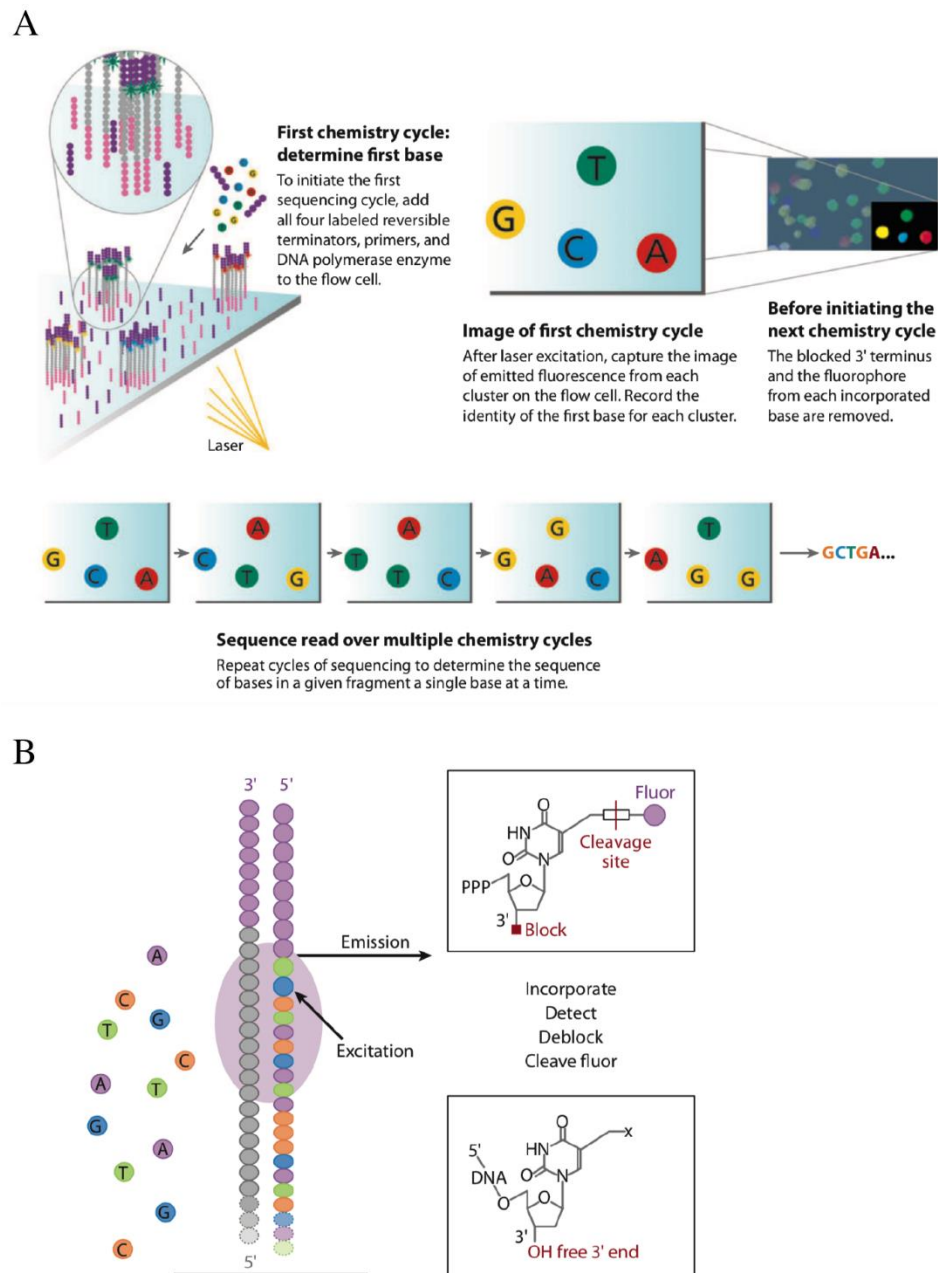


Figure 17 Sequencing-by-synthesis

(A) Overview of sequencing-by-synthesis on a flow cell

(B) Sequencing-by-synthesis

Source: (Mardis, 2008, 2013) (Modified)

NGS in shrimp

Numerous studies have been performed on whole transcriptome sequencing of penaeid shrimps including *P. monodon* (Huerlimann et al., 2018; Nguyen et al., 2016; Soonthornchai et al., 2016), *L. vannamei* (K. Chen et al., 2015; C. Li et al., 2012; Yu et al., 2014), *F. chinensis* (S. Li et al., 2013; X. Shi et al., 2018), *F. merguensis* (Powell et al., 2015; W. Wang et al., 2017), and *M. japonicus* (Sellars et al., 2015). In case of *P. monodon*, Nguyen and others have performed whole transcriptome in four different tissues of *P. monodon* and identified growth-related genes specifically expressed in heart, muscle, hepatopancreas, and eyestalk (Nguyen et al., 2016). Later on, Soonthornchai and others performed whole transcriptome sequencing in stomach of *P. monodon* and identified 141 immune-related genes that differentially expressed in response to the infection of *V. parahaemolyticus* acute hepatopancreatic necrosis disease (AHPND) strain (Soonthornchai et al., 2016). Recently in 2018, Huerlimann and others reported assembled transcriptome and expression patterns of *P. monodon* on nine adult tissues and eight early-life stages as well as identified genes specific to each life stage and tissue (Huerlimann et al., 2018). In 2012, Li and others were the first to perform whole transcriptome sequencing in *L. vannamei* using whole *L. vannamei* larvae (C. Li et al., 2012). Later in 2014, Yu and others reported assembled transcriptome and discovered a total of 96,040 single nucleotide polymorphisms (SNPs) from *L. vannamei* larvae at mysis stage using publicly-available read data (larvae at 20 days post spawning) (Yu et al., 2014). Moreover, Chen and others identified 855 genes that were aberrantly expressed under salinity stress in *L. vannamei* and validated the expression results of 20 randomly selected genes by qRT-PCR (K. Chen et al., 2015). Transcriptome analyses on *F. chinensis* during the infection of WSSV have been performed by two research groups (S. Li et al., 2013; X. Shi et al., 2018). Li and others identified 805 differentially expressed genes which were categorized into 11 functional groups (S. Li et al., 2013), whereas Shi and others identified 896 differentially expressed genes and validated the results using 8 selected genes by qRT-PCR (X. Shi et al., 2018). Powell and others performed whole transcriptome sequencing on *F. merguensis* tissues and reported list of genes

associated with reproduction, sex determination and development as well as expression of each gene in examined tissues (Powell et al., 2015). Later in 2017, Wang and others reported transcriptome from *F. merguensis* gill and 9190 differentially expressed genes under ammonia stress which were mostly involved in cytoskeleton remodeling and immune response (W. Wang et al., 2017). In case of *M. japonicus*, Sellars and others performed transcriptome sequencing on animal pole and vegetal pole of *M. japonicus* and identified genes involved in sex determination, germ line, mesoderm, and other developmental processes (Sellars et al., 2015).

In addition, many studies performed whole transcriptome sequencing on *M. rosenbergii* tissues and investigated gene expression responses to several pathogens including *V. parahaemolyticus* (Rao et al., 2015), WSSV (Cao et al., 2017; Rao et al., 2016), as well as the viral PAMP mimic (poly I:C) challenges (Z. Ding et al., 2018). In 2015, Rao and others performed transcriptome sequencing on *M. rosenbergii* hepatopancreas of control and *V. parahaemolyticus* infected prawn using Illumina sequencing and Trinity *de novo* transcriptome assembler resulting in 59,050 and 73,946 unigenes (Rao et al., 2015). Both transcriptome were clustered into 64,411 standard unigenes and functional annotated against several databases such as NCBI non-redundant, Swiss-Prot, Kyoto Encyclopaedia of Genes and Genome pathway (KEGG) and Orthologous Groups of Proteins (COG) databases. Using fragments per kb per million fragments (FPKM) method, they identified 14,569 aberrantly expressed unigenes with 11,466 up-regulated and 3,103 down-regulated genes. Among those, many immune-related genes were categorized into 11 functional groups and validated 7 of those genes using qRT-PCR (Rao et al., 2015). Later in 2016, the same research group performed transcriptomic study on *M. rosenbergii* hepatopancreas in response to WSSV infection using the same methodologies (Rao et al., 2016). Total of 63,584 unigenes were obtained from 59,050 unigenes and 65,625 unigenes of control and WSSV infected prawn, respectively. They identified 14,416 differentially expressed unigenes with 8,443 and 5,973 up and down-regulated gene, respectively, in which 74 genes were listed as immune-related genes. The expression of ten of those immune-related genes were validated using qRT-PCR (Rao et al., 2016). In

2017, Cao and others performed transcriptome sequencing on *M. rosenbergii* lymphoid organ in response to WSSV infection using similar approaches as in Rao and other's reports (Cao et al., 2017). Total of 73,658 and 72,374 unigenes from control and WSSV infected group were clustered into 57,921 universal unigenes which were then functional annotated against several database. FPKM method showed that 4,055 unigenes were up-regulated whereas 896 were down-regulated during WSSV challenge. They also reported 12,308 simple sequence repeats (SSRs) using the MISA software, which can be used as potential functional markers (Cao et al., 2017). In 2018, Ding, Jin, and Ren performed whole transcriptome sequencing on *M. rosenbergii* intestines under WSSV and poly (I:C) challenges (Z. Ding et al., 2018). Total of 65,340, 71,241, and 70,614 unigenes were generated from control, WSSV, and poly (I:C) group, respectively, and then clustered into 88,412 universal unigenes. Differential expression analysis using FPKM method revealed 2,604 up-regulated and 2,192 down-regulated genes in WSSV group, whereas the poly (I:C) group showed 2,480 up-regulated and 1,928 down-regulated genes. They also identified SSRs using the MISA software and single nucleotide polymorphisms (SNP) markers using Genome Analysis Toolkit (GATK) (Z. Ding et al., 2018) Most recently, in 2019, Jariyapong and others performed transcriptomic analysis on adult *M. rosenbergii* hematopoietic tissue at two time points after the infection of *MiNV* (Jariyapong et al., 2019). Total of 63,894 unigenes were obtained from 17.3M reads from control, 6 hours post infection and 24 hours post infection. Using EdgeR, they discovered up-regulation of 281 genes and down-regulation of 181 genes at 6 hours post infection. Among those, 18 differentially expressed genes were associated with immune system and cell growth regulation. They also reported top 20 up- and down-regulated genes at 6 hours post infection (Jariyapong et al., 2019).

CHAPTER 3

MATERIALS & METHODS

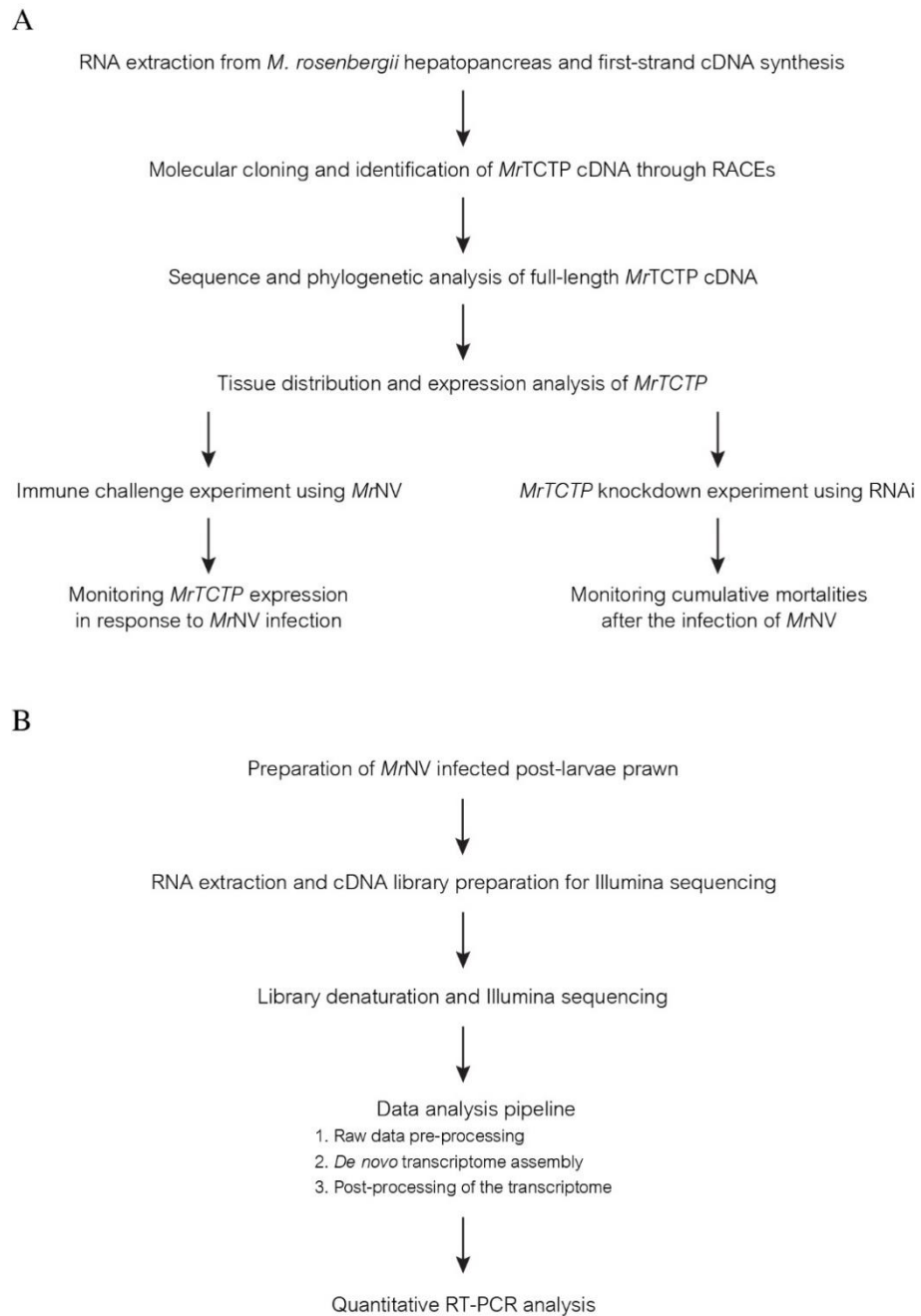


Figure 18 Overview of the studies

(A) Molecular cloning and characterization of TCTP from *M. rosenbergii*.

(B) Transcriptomic analysis of *M. rosenbergii* post-larvae in response to *MrNV* infection.

1. Molecular cloning and identification of *MrTCTP* cDNA using Rapid amplification of cDNA ends (RACE)

In this study, the full-length of *MrTCTP* cDNA was identified. The partial sequence of *MrTCTP* cDNA was isolated using degenerate primers designed from conserved regions of related species. The remaining 3' and 5' ends were further identified using SMARTer™ RACE cDNA Amplification Kit (Clontech, USA). The fresh water prawn (approximately 40-50 g) was purchased from local farm at Suphan Buri province, Thailand and hepatopancreas was collected. The total RNA was extracted from collected hepatopancreases using NucleoSpin® RNA XS total RNA isolation kit (Macherey-Nagel, Germany). The extracted RNA was subjected to cDNA synthesis for the identification of partial *MrTCTP* cDNA using degenerate primers. The 3'-RACE and 5'-RACE for identification of the remaining 3' and 5' ends were performed.

1.1 RNA extraction

The total RNA was extracted using NucleoSpin® RNA XS total RNA isolation kit (Macherey-Nagel, Germany) according to manufacturer's protocol. Briefly, the collected hepatopancreas (5 mg) was homogenized in 200 µL of RA1 buffer and 4 µL of TCEP (tris(2-carboxyethyl)phosphine) and was mixed with 5 µL of Carrier RNA working solution as listed in Table 1.

Table 1 Components of carrier RNA working solution (100 µL)

Components	Volume (µL)
Carrier RNA stock solution (100 ng/ µL)	1
RA1 buffer	99
Total volume	100

After the tissues were mixed and briefly centrifuged, the mixtures were filtrated through NucleoSpin® Filter using centrifugation at 11,000 x g for 30 seconds. The filtrated

was gently mixed with 200 μL of 70% ethanol and then transferred to NucleoSpin[®] RNA XS column. Next, the column was centrifuged at 11,000 $\times g$ for 30 seconds, added with 100 μL of MDB and then centrifuged (11,000 $\times g$ for 30 seconds). After the column was dried, the column was added with 25 μL of rDNase reaction mixture as listed in Table 2 and incubated at room temperature for 15 minutes.

Table 2 Components of rDNase reaction mixture

Components	Volume (μL)
rDNase	3
Reaction Buffer for rDNase	27
Total volume	30

After incubation, the column was added with 100 μL of RA2 buffer, incubated at room temperature for 2 minutes, and then centrifuged. The column was washed twice with 400 μL and 200 μL of RA3 buffer using centrifugation (11,000 $\times g$ for 30 seconds and 2 minutes for the second wash). Finally, the total RNA was eluted with 10 μL of RNase-free H_2O using centrifugation (11,000 $\times g$ for 30 seconds). The extracted RNA was quantified using NanoDrop Lite Spectrophotometer (Thermo Fisher Scientific, USA) and stored at -70°C until use.

1.2 First-Strand cDNA synthesis

The first-strand cDNA was synthesized using SuperScript[®] III First-Strand Synthesis System for RT-PCR (Invitrogen, USA) according to manufacturer's protocol. Firstly, the RNA mixture was prepared as listed in Table 3 using extracted RNA as described in section 1.1.

Table 3 Components of RNA mixture for first-strand cDNA synthesis

Components	Volume (μL)
Total RNA from hepatopancreases	8
50 μM Oligo(dT) ₁₂₋₁₈	1
10 mM dNTP	1
Total volume	10

Next, the mixture was incubated at 65°C for 5 minutes, then placed on-ice at least 1 minute. After that, the 2X reaction mix was prepared as listed in Table 4.

Table 4 Components of 2X reaction mix for first-strand cDNA synthesis

Components	Volume (μL)
RNA mixture (Table 3)	10
10X RT Buffer	2
25 mM MgCl ₂	4
0.1 M DTT	2
RNaseOUT™ (40 U/ μL)	1
SuperScript® III RT (200 U/ μL)	1
Total volume	20

After preparation of the reaction mixture, the reaction mixture was incubated at 42°C for 50 minutes followed by 85°C for 5 min using the Thermal Cycler (Bio-Rad, USA). After the termination, the reaction mixture was placed on-ice at least 1 minute. Finally, the

reaction mixture was added with 1 μ L of *E. coli* RNase H (2 U/ μ L) and incubated at 37°C for 20 minutes. The cDNA was stored at -20°C until use.

1.3 Polymerase chain reaction using degenerate primers

To identify partial sequence of *Mr*TCTP cDNA, multiple sequence alignment was constructed using TCTP proteins from related organisms as follow; *M. japonicus* (ABZ90155.1), *F. chinensis* (ABB05535.1), *F. indicus* (ACR58988.1), *P. monodon* (AY186580.1), and *L. vannamei* (ABY55541.1). Two degenerate primers were designed based on conserved regions of the sequence alignment (Figure 12) as listed in Table 5.

Table 5 Degenerate primers used in the PCR reaction

Primer name	Sequence
TCTPdegF	5'-GTG GAT GAT GCC TTC TAC ATG-3'
TCTPdegR	5'-TAG ACC RTA TTT TGG GAA RTA-3'

The PCR was carried out using Platinum™ *Taq* DNA Polymerase (Invitrogen, USA) and cDNA from section 1.2 as DNA template. Firstly, the PCR reaction was prepared as listed in Table 6.

```

M._japonicus_ABZ90155.1      MKVFKDILTGDEMFTDTYKYEEVDDAFYMVIGKDVTVTEGNIELEGANPSAEEAEGTDS
F._chinensis_ABB05535.1     MKVFKDMLTGDEMFTDTYKYEEVDDAFYMVIGKNITITEDNIELEGANPSAEEAEGTDT
F._indicus_ACR58988.1       MKVFKDMLTGDEMFTDTYKYEEVDDAFYMVIGKNITITEDNIELEGANPSAEEAEGTDT
P._monodon_AY186580.1       MKVFKDMLTGDEMFTDTYKYEEVDDAFYMVIGKNITVTEDNIELEGANPSAEEAEGTDT
L._vannamei_ABY55541.1      MKVFKDMLTGDEMFTDTYKYEEVDDAFYMVIGKNITVTEDNIELEGANPSAEEAEGTDT
*****:*****:*****:*****:*****:*****:*****:*****:*****:*****:
M._japonicus_ABZ90155.1      NTQSGVDVVLYMRLQETGFQVKDYLAYMKEYLKNVKAKLEGTPeASKLTSIQKPLTDLL
F._chinensis_ABB05535.1     NSQSGVDVVIYMRLQETGFQVKDYLAYMKEYLKNVKAKLEGTPeASKLTSIQKPLTDLL
F._indicus_ACR58988.1       TSQSGVDVVIYMRLQETGFQVKDYLAYMKEYLKNVKAKLEGTPeASKLTSIQKPLTDLL
P._monodon_AY186580.1       TSQSGVDVVIYMRLQETGFQVKDYLAYMKEYLKNVKAKLEGTPeASKLTSIQKPLTDLL
L._vannamei_ABY55541.1      TSQSGVDVVIYMRLQETGFQVKDYLAYMKEYLKNVKAKLEGTPeASKLTSIQKPLTDLL
.:*****:*****:*****:*****:*****:*****:*****:*****:*****:
M._japonicus_ABZ90155.1      KKFkDLQFFtGESMDPDGMVLMdYKDIgEERpVLYYFPKYGLQEEKL
F._chinensis_ABB05535.1     KKFkDLQFFtGESMDPDGMVIMdYKDIgEERpVLYYFPKYGLTEeKL
F._indicus_ACR58988.1       KKFkDLQFFtGESMVPDGMVLMdYKDIgEERpVLYYFPKYGLTEeKL
P._monodon_AY186580.1       KKFkDLQFFtGESMDPDGMVLMdYKDIgEERpVLYYFPKYGLTEeKL
L._vannamei_ABY55541.1      KKFkDLQFFtGESMDPDGMVLMdYKDIgEERpVLYYFPKYGLTEeKL
***** ***** .:*****.*****:***** *****

```

Figure 19 Multiple sequence alignment of TCTP protein

Multiple sequence alignment was constructed using TCTP proteins from related organisms as follow; *M. japonicus* (ABZ90155.1), *F. chinensis* (ABB05535.1), *F. indicus* (ACR58988.1), *P. monodon* (AY186580.1), and *L. vannamei* (ABY55541.1). Red letter indicates conserved region used for forward degenerate primer design whereas blue letter is for reverse degenerate primer design.

Table 6 Components of the PCR reaction for partial cloning

Components	Volume (µL)
10X PCR Buffer, - Mg	5
2.5 mM dNTP	4
50 mM MgCl ₂	1.5
50 µM TCTPdegF	1
50 µM TCTPdegR	1
cDNA from section 1.2	2
Platinum™ Taq DNA Polymerase (2.5 U/µL)	0.5
Deionized H ₂ O	35
Total volume	50

After the preparation, the reaction was placed in the Thermal Cycler (Bio-Rad, USA) and the PCR was performed. The PCR program followed the protocol from Platinum™ *Taq* DNA Polymerase (Invitrogen, USA) with some modification as described below.

Step 1	Denaturation	94 °C for 30 seconds
Step 2	Annealing	50 °C for 30 seconds
Step 3	Extension	72 °C for 30 seconds
Step 4	Repeat Step (1), (2) and (3) for 34 cycles	

The results were analyzed by agarose gel electrophoresis using 2% agarose gel followed by SYBR™ safe staining (Invitrogen, USA) and visualized by Gel Doc™ XR+ Gel Documentation System (Bio-Rad, USA). The product with expected size was excised and extracted using NucleoSpin® Gel and PCR clean-up (Macherey-Nagel, Germany) according to manufacturer's protocol. Briefly, the product was mixed with 200 µL of Buffer NTI per 100 mg gel and incubated at 50 °C for 5 minutes or until the gel was completely dissolved. After that, the mixture was loaded into NucleoSpin® Gel and PCR clean-up column and centrifuged at 11,000 x *g* for 30 seconds. Next, the column was washed using 700 µL of Buffer NT3 with centrifugation at 11,000 x *g* for 30 seconds. After drying the column, the product was eluted using 15 µL of Buffer NE with centrifugation at 11,000 x *g* for 1 minute. The extracted product was stored at -20 °C until use.

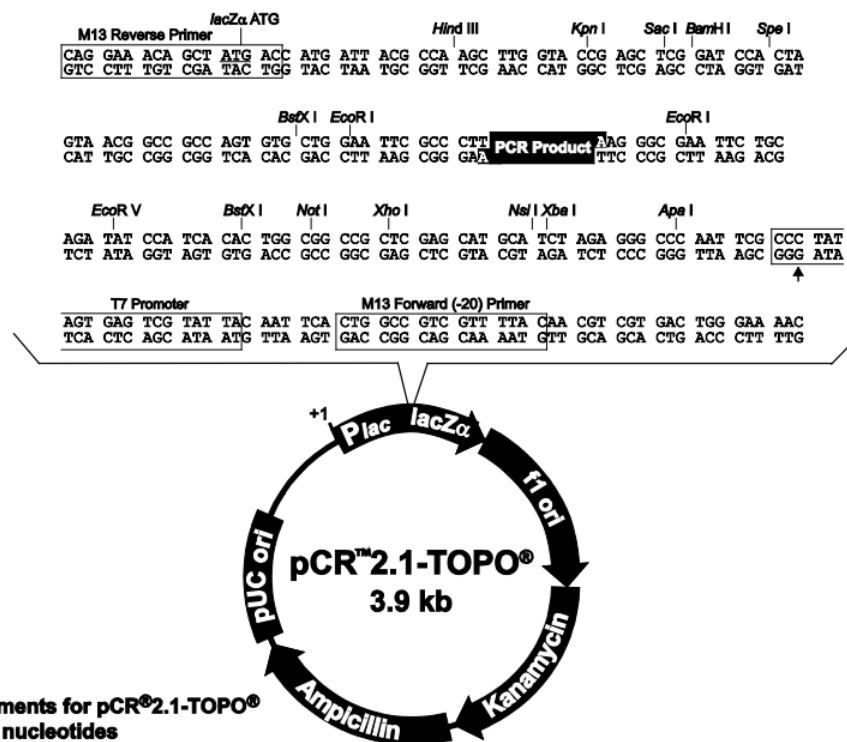
1.4 Molecular cloning and identification of partial *MrTCTP* cDNA

To identify partial sequence of *MrTCTP* cDNA, the PCR products from section 1.3 were cloned into pCR™2.1-TOPO® (Figure 13) using TOPO® TA Cloning® Kit (Invitrogen, USA), transformed into *E. coli* TOP10 strain, and then sequenced. Briefly, the ligation mixture was prepared according to manufacturer's protocol as listed in Table 7.

Table 7 Components of pCR™2.1-TOPO® ligation mixture

Components	Volume (μL)
PCR products (Section 1.3)	1
Salt solution	1
pCR™2.1-TOPO®	1
Deionized H ₂ O	3
Total volume	6

After the preparation of the ligation mixture, the mixture was incubated at 22 °C for 30 minutes and subjected to the transformation into *E. coli* (TOP10). The incubated ligation mixture was transformed into *E. coli* (TOP10) using heat-shock transformation. Firstly, the ligation mixture was transferred into chemically competent *E. coli* TOP10 strain (200 μL) and then incubated on ice for 30 minutes. After the incubation, the *E. coli* was heat-shocked at 42 °C for 2 minutes and then immediately placed on ice for 20 minutes. Next, the *E. coli* was added with 600 μL of LB broth and incubated at 37 °C for 2 hours with agitation (225 rpm). Finally, total volume of 100 μL of transformed *E. coli* was spread on LB agar plate supplemented with ampicillin at final concentration of 100 μg/mL, 40 μg/mL X-gal, and 50 μg/mL IPTG. The LB agar plate was incubated at 37 °C overnight and then stored at 4 °C until use.



Comments for pCR™2.1-TOPO®
3931 nucleotides

LacZα fragment: bases 1-547
M13 reverse priming site: bases 205-221
Multiple cloning site: bases 234-357
T7 promoter/priming site: bases 364-383
M13 Forward (-20) priming site: bases 391-406
f1 origin: bases 548-985
Kanamycin resistance ORF: bases 1319-2113
Ampicillin resistance ORF: bases 2131-2991
pUC origin: bases 3136-3809

Figure 20 Features of the pCR™2.1-TOPO® vector

Source: TOPO® TA Cloning® Kit. (Invitrogen, USA)

The bacteria that harbored vector with PCR products grew into white colony on the LB-ampicillin supplemented with X-gal and IPTG agar, whereas the bacteria harbored vector without the insert grew into blue colony. The white colony was sub-cultured into 4 mL of LB broth supplemented with ampicillin at final concentration of 100 µg/mL at 37 °C for 16 hours with agitation (225 rpm).

The plasmid was extracted from the culture using NucleoSpin[®] Plasmid Kit (Macherey-Nagel, Germany) according to manufacturer's protocol. Briefly, the culture was transferred into sterile microcentrifuge tube and centrifuged at 11,000 x *g* for 30 seconds to collect the pellet. Then, the pellet was resuspended with 250 μ L of Buffer A1 by vortexing. After the pellet was completely resuspended, the tube was added with 250 μ L of Buffer A2. The tube was gently mixed by inverting the tube and incubated at room temperature for 5 minutes to lyse the bacteria. After the bacteria were completely lysed, the lysate was added with 300 μ L of Buffer A3 and mixed by inverting the tube. The tube was then centrifuged at 11,000 x *g* for 10 minutes. Next, the supernatant was loaded into a NucleoSpin[®] Plasmid Column and centrifuged 11,000 x *g* for 1 minute. The column was then washed with 600 μ L of Buffer A4 using centrifugation (11,000 x *g* for 1 minute). After the column was dried, the plasmid was eluted using 50 μ L of Buffer AE with centrifugation at 11,000 x *g* for 1 minute.

The extracted plasmid was further sequenced to identify the PCR products using M13 Reverse primer (5'-CAG GAA ACA GCT ATG AC-3'). The obtained sequencing data was eliminated the plasmid regions on both 3' end and 5' end and then identified using BLASTX program (<https://blast.ncbi.nlm.nih.gov/blast/Blast.cgi>). The identified partial sequence of *MrTCTP* was used for the identification of the remaining 3' and 5' end of *MrTCTP*.

1.5 Preparation of 3' and 5'-RACE-Ready cDNA

The 3' and 5'-RACE-Ready cDNA were synthesized using SMARTer™ RACE cDNA Amplification Kit (Clontech, USA) according to manufacturer's protocol. Firstly, the RNA mixture was prepared as listed in Table 8 using extracted RNA as described in section 1.1.

Table 8 Components of RNA mixture for RACE-Ready cDNA synthesis

Components	Volume (μL)
Total RNA from hepatopancreases	2
12 μM 3'-RACE CDS Primer A or 5'-RACE CDS Primer A	1
Deionized H ₂ O	0.75
Total volume	3.75

* 3'-RACE CDS Primer A : 5'-AAGCAGTGGTATCAACGCAGAGTAC(T)₃₀ V N-3'

5'-RACE CDS Primer A : 5'-(T)₂₅ V N-3' (N = A, C, G, or T; V = A, G, or C)

Next, the mixture was incubated at 72°C for 3 minutes, then cooled at 42°C for 2 minutes using the Thermal Cycler (Bio-Rad, USA). After cooling, the RACE-Ready cDNA synthesis reaction mix was prepared as listed in Table 9. SMARTer II A Oligonucleotide was used in case of 5'-RACE-Ready cDNA synthesis.

Table 9 Components of RACE-Ready cDNA synthesis reaction mix

Components	Volume (μL)
RNA mixture (Table 8)	3.75
5X First-Strand Buffer	2
20 mM DTT	1

Table 9 (Continued)

10 mM dNTP Mix	1
12 μ M SMARTer II A Oligonucleotide (in case of 5'-RACE ready cDNA) 5'-AAGCAGTGGTATCAACGCAGAGTACXXXX-3'	1
RNase inhibitor (40 U/ μ L)	0.25
SMARTScribe Reverse Transcriptase (100 U)	1
Total volume	10

After the reaction mix was prepared, the reaction mix was incubated at 42°C for 90 minutes followed by 70°C for 10 minutes using the Thermal Cycler (Bio-Rad, USA). Finally, the cDNA mixture was diluted with 20 μ L of Tricine-EDTA Buffer (10 mM Tricine-KOH (pH 8.5) 1.0 mM EDTA) if less than 200 ng of total RNA are used. The RACE Ready cDNA was stored at -20°C until use.

1.6 Rapid amplification of 3' and 5' cDNA ends (RACEs)

To identify the remaining 3' and 5' end of *MrTCTP* cDNA, four oligonucleotide primers were designed based on the partial sequence. The primers used in the RACE-PCR reaction consisted of 4 gene specific primers and 2 universal primers (provided by SMARTer™ RACE cDNA Amplification Kit) for RACE-PCR and nested RACE-PCR reaction as listed in Table 10. The GSP002 and NGSP002 were designed for 3'-RACE-PCR and nested 3'-RACE-PCR, whereas the GSP001 and NGSP001 were designed for 5'-RACE-PCR and nested 5'-RACE-PCR, respectively.

Table 10 Primers used in the RACE-PCR reaction

Primer name	Sequence
GSP001	5'-GCA GGA AGC TTG TCA GCA GCT GGG GTT CCC TC-3'
NGSP001	5'-TGT TTC CAA AGC CAG TCT CCT GGA GGC GC-3'
GSP002	5'-GCA AGC TAG AGG GAA CCC CAG CTG CTG-3'
NGSP002	5'-GAA CCC TGA TGG TAT GGT TGC AAT TGG CG-3'
UPM	
Long (0.4 μ M)	5'-CTA ATA CGA CTC ACT ATA GGG CAA GCA GTG GTA TCA ACG CAG AGT-3'
Short (2 μ M)	5'-CTA ATA CGA CTC ACT ATA GGG C-3'
NUP	5'-AAG CAG TGG TAT CAA CGC AGA GT-3'

The RACE-PCR was carried out using Advantage[®] 2 Polymerase Mix (Clontech, USA) and RACE-Ready cDNA from section 1.5 as DNA template. Firstly, the RACE-PCR was prepared as listed in Table 11.

Table 11 Components of RACE-PCR reaction

Components	Volume (μ L)
10X Advantage 2 PCR Buffer	5
10 mM dNTP mix	1
10 μ M GSP001 or GSP002	1
10X UPM	5
RACE-Ready cDNA from section 1.5	2.5
50X Advantage 2 Polymerase Mix	1

Table 11 (Continued)

Deionized H ₂ O	34.5
Total volume	50

After the preparation, the reaction was placed in the Thermal Cycler (Bio-Rad, USA) and the touchdown PCR was performed. The touchdown PCR program followed the protocol from SMARTer™ RACE cDNA Amplification Kit (Clontech, USA) as described below.

Step 1	Denaturation	94 °C	for 30 seconds
Step 2	Annealing and Extension	72 °C	for 3 minutes
Step 3	Repeat Step (1) and (2) for 4 cycles		
Step 4	Denaturation	94 °C	for 30 seconds
Step 5	Annealing	70 °C	for 30 seconds
Step 6	Extension	72 °C	for 3 minutes
Step 7	Repeat Step (4), (5) and (6) for 4 cycles		
Step 8	Denaturation	94 °C	for 30 seconds
Step 9	Annealing	68 °C	for 30 seconds
Step 10	Extension	72 °C	for 3 minutes
Step 11	Repeat Step (9), (10) and (11) for 24 cycles		

The results were analyzed by agarose gel electrophoresis using 2% agarose gel followed by SYBR™ safe staining (Invitrogen, USA) and visualized by Gel Doc™ XR+ Gel Documentation System (Bio-Rad, USA). After confirmation of the product, the PCR product was diluted 50 times with Tricine-EDTA buffer (10 mM Tricine-KOH (pH 8.5), 1.0 mM EDTA). The diluted PCR product was used as a template in the nested RACE-PCR reaction as listed in Table 12.

Table 12 Components of nested RACE-PCR reaction

Components	Volume (μL)
10X Advantage 2 PCR Buffer	5
10 mM dNTP mix	1
10 μM NGSP001 or NGSP002	1
10 μM NUP	1
Diluted RACE-PCR product	5
50X Advantage 2 Polymerase Mix	1
Deionized H ₂ O	36
Total volume	50

After the preparation of the nested RACE-PCR reaction, the reaction was placed in the Thermal Cycler (Bio-Rad, USA) and the PCR was performed using the program as described below.

Step 1	Denaturation	94 °C	for 30 seconds
Step 2	Annealing	65 °C	for 30 seconds
Step 3	Extension	72 °C	for 3 minutes
Step 4	Repeat Step (1), (2) and (3) for 29 cycles		

The results were analyzed by agarose gel electrophoresis using 2% agarose gel followed by SYBR™ safe staining (Invitrogen, USA) and visualized by Gel Doc™ XR+ Gel Documentation System (Bio-Rad, USA). The product with expected size was excised and extracted using NucleoSpin® Gel and PCR Clean-up (Macherey-Nagel, Germany) as described in section 1.3.

1.7 Molecular cloning and identification of *MrTCTP* cDNA

To identify the 3' and 5' end of *MrTCTP* cDNA, the nested RACE-PCR products from section 1.6 were cloned into pCR™2.1-TOPO® using TOPO® TA Cloning® Kit (Invitrogen, USA), transformed into *E. coli* XL1-Blue strain, and then sequenced as described in section 1.4.

The incubated ligation mixture was transformed into *E. coli* (TOP10) using heat-shock transformation. The bacteria that harbored vector with nested RACE-PCR products grew into white colony on the LB-ampicillin supplemented with X-gal and IPTG agar, whereas the bacteria harbored vector without the insert grew into blue colony. The white colony was sub-cultured into 4 mL of LB broth supplemented with ampicillin at final concentration of 100 µg/mL at 37 °C for 16 hours with agitation (225 rpm).

The plasmid was extracted from the culture using NucleoSpin® Plasmid Kit (Macherey-Nagel, Germany) as described in section 1.4. The extracted plasmid was further sequenced to identify the nested 5'-RACE-PCR products using M13 Reverse primer (5'-CAG GAA ACA GCT ATG AC-3'). The obtained sequencing data was eliminated the plasmid regions on both 3' end and 5' end and then identified using BLASTX program (<https://blast.ncbi.nlm.nih.gov/blast/Blast.cgi>). The identified 3' and 5' end of *MrTCTP* was aligned and combined with the partial sequence of *MrTCTP* cDNA as mentioned earlier using overlapping region to obtain the full-length *MrTCTP* cDNA.

2. Bioinformatics analysis and sequence confirmation of *MrTCTP* cDNA

To confirm the sequence of *MrTCTP* cDNA, *MrTCTP* cDNA was re-identified using designed primers that cover the coding sequence of *MrTCTP* cDNA. After obtaining the confirmed full-length *MrTCTP* cDNA, the deduced amino acid sequence of *MrTCTP* was generated from the *MrTCTP* cDNA using Translate tool (<http://web.expasy.org/translate/>). The *MrTCTP* protein was further studied the evolutionary relationships of *MrTCTP* among other organisms and the protein composition using prediction programs.

2.1 Polymerase chain reaction (PCR) for the re-identification of *MrTCTP*

For the re-identification of *MrTCTP*, total number of 2 oligonucleotide primers were designed (Table 13). The primers used in the PCR reaction covered all of the coding sequence from start codon to stop codon. The forward and reverse primer were designed to recognize slightly upstream of the start codon and downstream of the stop codon, respectively.

Table 13 Primers used for the re-identification of *MrTCTP*

Primer name	Sequence
TCTPcdsF	5'-CCA ACC TAG GCC AAT TTT TCT ACC-3'
TCTPcdsR	5'-CCG ATG TTA ATG GAT GAC TGG AAT AC-3'

The PCR was carried out using Platinum™ *Pfx* DNA Polymerase (Invitrogen, USA) and cDNA from section 1.2 as DNA template. Firstly, the PCR reaction was prepared as listed in Table 14.

Table 14 Components of the PCR reaction for *MrTCTP*

Components	Volume (μL)
10X <i>Pfx</i> Amplification Buffer	5
2.5 mM dNTP	6
50 mM MgSO ₄	1
50 μM TCTPcdsF	1
50 μM TCTPcdsR	1
cDNA from section 1.2	5

Table 14 (Continued)

Platinum™ Pfx DNA Polymerase (2.5 U/μL)	0.4
Deionized H ₂ O	30.6
Total volume	50

After the preparation, the reaction was placed in the Thermal Cycler (Bio-Rad, USA) and the PCR was performed. The PCR program followed the protocol from Platinum™ Pfx DNA Polymerase (Invitrogen, USA) with some modification as described below.

Step 1	Denaturation	94 °C for 30 seconds
Step 2	Annealing	55 °C for 30 seconds
Step 3	Extension	72 °C for 1 minute
Step 4	Repeat Step (1), (2) and (3) for 29 cycles	

The results were analyzed by agarose gel electrophoresis using 2% agarose gel followed by SYBR™ safe staining (Invitrogen, USA) and visualized by Gel Doc™ XR+ Gel Documentation System (Bio-Rad, USA). The product with expected size was excised and was extracted using NucleoSpin® Gel and PCR Clean-up (Macherey-Nagel, Germany) as described in section 1.3.

2.2 Molecular cloning and re-identification of *MrTCTP*

The *MrTCTP* CDS from section 1.2 was cloned into pCR®-Blunt II-TOPO® using Zero Blunt® TOPO® PCR Cloning Kit (Invitrogen, USA). Firstly, the ligation mixture was prepared according to manufacturer's protocol as listed in Table 15.

Table 15 Components of pCR[®]-Blunt II-TOPO[®] ligation mixture

Components	Volume (μL)
PCR product (Section 2.1)	1
Salt solution	1
pCR [®] -Blunt II-TOPO [®]	1
Deionized H ₂ O	3
Total volume	6

After the preparation of the ligation mixture, the mixture was incubated at 22 °C for 30 minutes and subjected to the transformation into *E. coli* (TOP10). The incubated ligation mixture was transformed into *E. coli* (TOP10) using heat-shock transformation as described in section 1.4. Transformed *E. coli* was spread on LB agar plate supplemented with kanamycin at final concentration of 100 μg/mL, 40 μg/mL X-gal, and 50 μg/mL IPTG. The LB agar plate was incubated at 37 °C overnight and then stored at 4 °C until use.

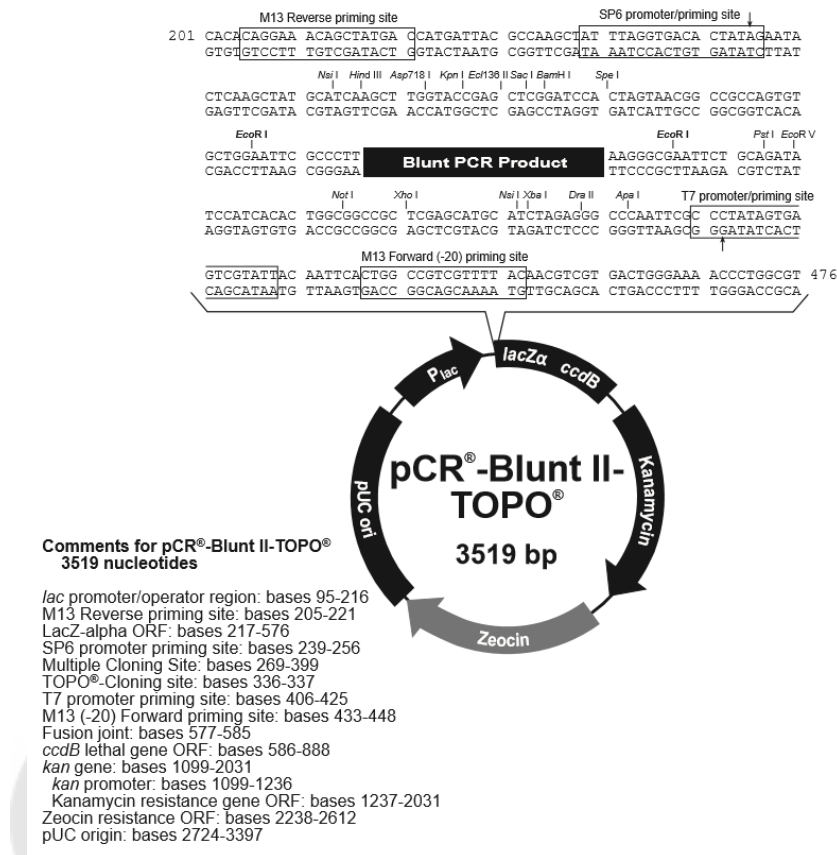


Figure 21 Features of the pCR[®]-Blunt II-TOPO[®] vector

Source: TOPO[®] TA Cloning[®] Kit. (Invitrogen, USA)

The bacteria that harbored vector with *MtTCTP* grew into white colony on the LB-kanamycin supplemented with X-gal and IPTG agar, whereas the bacteria harbored vector without the insert grew into blue colony. The white colony was sub-cultured into 4 mL of LB broth supplemented with kanamycin at final concentration of 100 µg/mL at 37 °C for 16 hours with agitation (225 rpm). The plasmid was extracted from the culture using NucleoSpin[®] Plasmid Kit (Macherey-Nagel, Germany) as described in section 1.4.

The extracted plasmid was further sequenced (Sanger sequencing) to confirm the *MtTCTP* insert using M13 Reverse primer (5'-CAG GAA ACA GCT ATG AC-3'). The obtained sequencing data was eliminated the plasmid regions on both 3' end and 5' end and then aligned with *MtTCTP* cDNA's sequence from section 1.4 to confirm the CDS.

2.3 Protein composition analysis of *MrTCTP*

The obtained full-length *MrTCTP* cDNA was translated into *MrTCTP* protein. The *MrTCTP* protein was analyzed the molecular weight and isoelectric point using Compute pI/Mw tool (web.expasy.org/compute_pi/), domain and protein family using Simple Modular Architecture Research Tool (SMART) (smart.embl-heidelberg.de/), and potential N-Glycosylation sites using NetNGlyc 1.0 Server (cbs.dtu.dk/services/NetNGlyc/). The three-dimension structure of *MrTCTP* protein was generated using SWISS-MODEL (swissmodel.expasy.org/interactive/sGdhRB/models/).

2.4 Phylogenetic analysis of *MrTCTP*

The *MrTCTP* was studied evolutionary relationships among other crustaceans and organisms using the Molecular Evolutionary Genetics Analysis (MEGA) version X beta (<http://www.megasoftware.net/>). The phylogenetic tree was constructed using the *MrTCTP* and TCTP proteins from other organisms as listed in Table 16. The maximum likelihood algorithm with 200 replicates of bootstrap analysis was used to construct the phylogenetic tree.

Table 16 TCTP proteins from other organisms

Common name	Species	Accession number
Fission yeast	<i>Schizosaccharomyces pombe</i>	Q10344
Zebrafish	<i>Danio rerio</i>	NP937783.1
Human	<i>Homo Sapiens</i>	NP003286.1
Domestic dog	<i>Canis lupus familiaris</i>	XP005633960.1
Common rat	<i>Rattus norvegicus</i>	P63029
Rainbow smelt	<i>Osmerus mordax</i>	ACO09085.1
Rohu	<i>Labeo rohita</i>	AAK27316.1

Table 16 (Continued)

Honey bee	<i>Apis mellifera</i>	XP395299.2
Fruit fly	<i>Drosophila melanogaster</i>	AAF54603.1
Whiteleg shrimp	<i>Litopenaeus vannamei</i>	ABY55541.1
Indian shrimp	<i>Fenneropenaeus indicus</i>	FJ890311.1
Giant tiger prawn	<i>Penaeus monodon</i>	AAO61938.1
Banana shrimp	<i>Fenneropenaeus merguensis</i>	AY700595.1
Chinese white shrimp	<i>Fenneropenaeus chinensis</i>	DQ205420.1
Chinese mitten crab	<i>Eosimias sinensis</i>	AEF32710.1

3. Tissue expression and distribution analysis of *MtTCTP* gene

3.1 Tissue collection and RNA extraction

The analysis of *MtTCTP* transcript was performed in order to determine the tissue distribution among various tissues. The water prawn (approximately 40-50 g) was purchased from local farm in Suphan Buri provinces, Thailand. The tissue from various organs were collected including gill, hepatopancreas, heart, hemocyte, muscle, stomach, and intestine. The hemocyte was collected from hemolymph according to Song and Hsieh (Song & Hsieh, 1994) with some modification. Briefly, the hemolymph was collected from prawn and mixed with 1 volume of Alsever's solution (0.055% citric acid, 0.8% sodium citrate, 2.05% D-glucose, and 0.42% sodium chloride (w/v)). The mixture was centrifuged at 4000 x *g* for 5 minutes and washed twice with 1 volume of Alsever's solution using centrifugation at 4000 x *g* for 5 minutes. Total RNA from the collected tissues was extracted using NucleoSpin[®] RNA XS total RNA isolation kit (Macherey-Nagel, Germany) as described in section 1.1. The extracted RNA was quantified using NanoDrop Lite Spectrophotometer (Thermo Fisher Scientific, USA) and stored at -70°C until use.

3.2 Semi-quantitative reverse transcription PCR

The reverse transcription PCR (RT-PCR) was performed using SuperScript[®] III One-Step RT-PCR System with Platinum[®] Taq DNA Polymerase (Invitrogen, USA). Two sets of primer were used in the RT-PCR reaction including *MrTCTP* specific primers and beta-actin specific primers from Lu and others (Lu, Huang, Lee, & Sung, 2006) as listed in Table 17.

Table 17 Primers used in the RT-PCR reaction

Primer name	Sequence
TCTPexpF	5'-ATG AGG GCA CAG AAT CCA AC-3'
TCTPexpR	5'-TAG CAG GAA GCT TGT CAG CA-3'
beta-actin-F	5'-CCC AGA GCA AGA GAG GTA-3'
beta-actin-R	5'-GCG TAT CCT TCG TAG ATG GG-3'

The RT-PCR was carried out using SuperScript[®] III One-Step RT-PCR System with Platinum[®] Taq DNA Polymerase (Invitrogen, USA) and total RNA extracted from each organ as described in section 3.1 as RNA template. The total RNA from various organs were used in two RT-PCR reactions (using TCTPexp and beta-actin primer sets) to determine relative expression between *MrTCTP* and the housekeeping gene (*beta-actin*). Firstly, the RT-PCR reaction was prepared as listed in Table 18.

Table 18 Components of RT-PCR reaction

Components	Volume (μL)
2X Reaction Mix	12.5
10 μM TCTPexpF or beta-actin-F	0.5

Table 18 (Continued)

10 μ M TCTPexpR or beta-actin-R	0.5
1 ng/ μ L of total RNA from each organ (section 3.1)	5
SuperScript™ III RT/Platinum™ Taq Mix	0.5
DEPC-treated H ₂ O	6
Total volume	25

After the preparation, the reaction was placed in the Thermal Cycler (Bio-Rad, USA) and the RT-PCR was performed. The RT-PCR program followed the protocol from SuperScript® III One-Step RT-PCR System with Platinum® Taq DNA Polymerase (Invitrogen, USA) as described below.

Step 1	cDNA synthesis	50 °C	for 30 minutes
Step 2	Pre-denaturation	94 °C	for 5 minutes
Step 3	Denaturation	94 °C	for 30 seconds
	Annealing	55 °C	for 30 seconds
Step 5	Extension	72 °C	for 30 seconds
Step 6	Repeat Step (4), (5) and (6) for 34 cycles		
Step 7	Final extension	72 °C	for 10 minutes

The PCR products were analyzed by agarose gel electrophoresis using 2% agarose gel followed by SYBR™ safe staining (Invitrogen, USA) and visualized by Gel Doc™ XR+ Gel Documentation System (Bio-Rad, USA). The experiment was performed in triplicate and the relative expression between *MrTCTP* and *beta-actin* was calculated using Image Lab™ Software (Bio-Rad, USA).

4. Immune challenge experiment using *Macrobrachium rosenbergii* nodavirus (*MrNV*)

The immune challenge experiment was conducted by injection of *MrNV* into a prawn and monitoring the *MrTCTP* expression compared with that of the control group using semi-quantitative RT-PCR. The experiment was performed in order to study the role of *MrTCTP* against the viral infection.

4.1 Preparation of the *MrNV*

The post-larvae prawn (PL 25-30) was purchased from local farm at Suphan Buri provinces, Thailand. The PL was kept in the glass tank with dechlorinated freshwater and continuous aeration at room temperature (28-20°C). After one day of acclimation, the *MrNV*-infected PL was homogenized in a TN buffer (20 mM Tris-HCl and 0.4 M NaCl, pH 7.4) using sterile homogenizer (10% w/v). The homogenate was centrifuged at 11,000 x g, 4°C for 20 minutes and filtered through a 0.45 µm pore membrane to obtain the viral suspension. The PL was challenged with viral suspension at 0.1% of the total rearing medium (1mL/L) (Sahoo et al., 2012). After the immersion, the PL with prominent signs of infection (whitish muscles in the abdominal region) was collected and the infection of *MrNV* was confirmed using viral nucleic acid extraction and RT-PCR. The *MrNV*-infected PL was stored at -70°C until use.

4.2 Viral nucleic acid extraction and RT-PCR for the detection of *MrNV*

The viral nucleic acid was extracted from the PL using High Pure Viral Nucleic Acid Kit (Roche, Switzerland) according to the manufacturer's protocol. Briefly, the PL was homogenized in lysis buffer (10mM Tris-HCl, 5mM EDTA, and 0.5% SDS, pH 8.0) using sterile homogenizer. The homogenate was then centrifuged at 4,000 x g for 5 minutes. After the centrifugation, the supernatant was mixed with working solution as listed in Table 19 and incubated at 72°C for 10 minutes.

Table 19 Components of working solution

Components	Volume (μL)
Binding buffer (Green cap)	196
Poly (A) solution	4
Proteinase K	50
Total volume	250

After incubation, the mixture was added with 100 μL of isopropanol and gently inverted 6-8 times. Next, the mixture was transferred into a High Pure filter column and centrifuged 8,000 $\times g$ for 1 minute. The column was washed with 500 μL of Inhibition Removal Buffer and then washed twice with 450 μL of wash buffer using centrifugation (8,000 $\times g$ for 1 minute). After the column was dried, the viral nucleic acid was eluted using 50 μL of elution buffer with centrifugation at 8,000 $\times g$ for 1 minute. The viral nucleic acid was kept at -20°C until use.

Table 20 Primers for the detection of MrNV

Primer name	Sequence
Mr-RdRP-F	5'-GCA TTT GTG AAG AAT GAA CCG-3'
Mr-RdRP-R	5'-CAT GTT CAA CTT TCT CCA CGT-3'

For the RT-PCR, *MrNV*-specific primers from Senapin and others (Senapin et al., 2012) were used for the detection of *MrNV* (Table 20). The RT-PCR was carried out using SuperScript[®] III One-Step RT-PCR System with Platinum[®] Taq DNA Polymerase (Invitrogen, USA) and viral nucleic acid extracted from the PL as described earlier as RNA template. Firstly, the RT-PCR was prepared as listed in Table 21.

Table 21 RT-PCR reaction for the detection of *MnV*

Components	Volume (μL)
2X Reaction Mix	12.5
50 μM Mr-RdRP-F	1
50 μM Mr-RdRP-R	1
Viral nucleic acid (template)	2
SuperScript™ III RT/Platinum™ Taq Mix	0.5
DEPC-treated H ₂ O	8
Total volume	25

After the preparation, the reaction was placed in the Thermal Cycler (Bio-Rad, USA) and the RT-PCR was performed. The RT-PCR program followed the protocol from SuperScript® III One-Step RT-PCR System with Platinum® Taq DNA Polymerase (Invitrogen, USA) as described below.

Step 1	cDNA synthesis	50 °C for 30 minutes
Step 2	Pre-denaturation	94 °C for 5 minutes
Step 3	Denaturation	94 °C for 1 minute
Step 4	Annealing	55 °C for 45 seconds
Step 5	Extension	72 °C for 1 minute
Step 6	Repeat Step (4), (5) and (6) for 34 cycles	
Step 7	Final extension	72 °C for 10 minutes

The PCR products were analyzed by agarose gel electrophoresis using 2% agarose gel followed by SYBR™ safe staining (Invitrogen, USA) and visualized by Gel Doc™ XR+ Gel Documentation System (Bio-Rad, USA).

4.3 Preparation of the *MrNV* inoculum and immune challenge

The *MrNV* inoculum was prepared according to Ravi and others (Ravi, Nazeer Basha, Taju, Ram Kumar, & Sahul Hameed, 2010) with some modifications. Firstly, the *MrNV*-infected PL was homogenized in a TN buffer (20 mM Tris-HCl and 0.4 M NaCl, pH 7.4) using sterile homogenizer (10% w/v). The homogenate was centrifuged at 11,000 x g, 4°C for 20 minutes and filtered through a 0.45 µm pore membrane. The *MrNV* inoculum was freshly prepared for the immune challenge experiment.

The adult prawn (3-4 g body weight) was purchased from local farm in Suphan Buri provinces, Thailand. The prawn was subjected to random sampling for the detection of *MrNV* using pleopod sample. The prawn was kept in cement tank with dechlorinated freshwater and continuous aeration at room temperature (28-30°C). The prawn was fed once a day with commercial pellet feed. After three days of acclimation, the prawn was injected intramuscularly into the third abdominal segment with the *MrNV* inoculum (50 µL per each) using 1-ml insulin syringe. Control prawn was injected with 50 µL of TN buffer (20 mM Tris-HCl and 0.4 M NaCl, pH 7.4). Muscle samples were collected from both of *MrNV*-injected and control group (3 prawns per time point) at 0, 1, 2, 3, 4, 5, 6, 7 day-post-injection. Muscle samples were subjected to the RT-PCR using the same methodology as described in section 3.

The experiment was performed in triplicate and the results were presented as relative expression between *MrTCTP* and beta-*actin*. The relative expression from *MrNV*-injected and control group was compared. Difference among the *MrNV*-injected and control group was analyzed by Student's t-test using Microsoft Excel 2013. Differences were defined as statistical significance at $p < 0.05$.

6. *MrTCTP* knockdown experiment using RNA interference

To further examine *MrTCTP* role in innate immune system, dsRNA was used for the knockdown experiment. The *MrTCTP* expression was suppressed using the injection of dsRNA followed by *MrNV* injection and mortality rate was observed.

6.1 Construction of DNA template for *in vitro* transcription

To construct DNA template for *in vitro* transcription, four oligonucleotide primers were designed based on the coding sequence. The first two primers were designed using E-RNAi Webservice (<http://www.dkfz.de/signaling/e-rnai3/>). The other two primers contained T7 promoter at the 5'-end for the *in vitro* transcription (Table 22). For control experiment, an exogenous gene, RNA-directed RNA polymerase (RdRP) gene of infectious myonecrosis virus (IMNV) was used (EF061744) (Senapin, Phewsaiya, Briggs, & Flegel, 2007).

Table 22 Primers used in the PCR reaction for *in vitro* transcription

Primer name	Sequence
F-TCTP-RNAi	5'-GTG GGG ATG AGA TGT TCA CC-3'
R-TCTP-RNAi	5'-TAG CAG GAA GCT TGT CAG CA -3'
F-TCTP-RNAiT7	5'-GGA TCC TAA TAC GAC TCA CTA TAG G GTG GGG ATG AGA TGT TCA CC-3'
R-TCTP-RNAiT7	5'-GGA TCC TAA TAC GAC TCA CTA TAG G TAG CAG GAA GCT TGT CAG CA-3'

The PCR was carried out using Platinum™ *Pfx* DNA Polymerase (Invitrogen, USA). In order to generate two templates for *in vitro* transcription (sense and antisense), two PCR reactions were performed separately using one T7-added primer and one normal primer (e.g. F-TCTP-RNAiT7 combined with R-TCTP-RNAi) The PCR was carried out as

described in section 2.1 using plasmid with confirmed sequence of *MtTCTP* from section 2.2 as DNA template. Both of the products with expected size were excised and extracted using NucleoSpin® Gel and PCR Clean-up (Macherey-Nagel, Germany) as described in section 1.3. The extracted products were quantified using NanoDrop Lite Spectrophotometer (Thermo Fisher Scientific, USA) and stored at -20°C until use.

6.2 *in vitro* transcription and dsRNA purification

To synthesize dsRNA, *in vitro* transcription was performed using T7 RiboMAX™ Express Large Scale RNA Production System (Promega, USA) according to manufacturer's protocol. Firstly, two *in vitro* transcription mixtures (sense and antisense) were prepared separately as listed in Table 23.

Table 23 Components of *in vitro* transcription mixture

Components	Volume (μL)
RiboMAX™ Express T7 2X Buffer	10
DNA template (sense or antisense) (1 μg)	1-8
Nuclease-free water	0-7
Enzyme Mix, T7 Express	2
Total volume	20

The mixtures were mixed gently and incubated at 37°C for 30 minutes. After the incubation, the two mixtures were mixed together, denatured at 70°C for 10 minutes and gradually cool-down into 25°C within about 20 minutes to allow the annealing. Next, the mixture was added with 2 μL of RQ1 DNase (RNase free) and incubated at 37°C for 30 minutes. After that, dsRNA was extracted using 42 μL of phenol:chloroform:isoamyl alcohol (125:24:1) (Sigma-Aldrich, USA), 1 minute of vortexing, and centrifugation at 14,000 x g, 4°C for 15 minutes. After the centrifugation, aqueous phase containing dsRNA

was transferred into new tube and added with 4.2 μL of 3M Sodium acetate (NaOAc) and 42 μL of isopropanol. The mixture was mixed gently, incubated at -20°C for 20 minutes followed by centrifugation at $14,000 \times g$, 4°C for 15 minutes. Finally, the pellet was washed with 1 mL of 70% ethanol and centrifuged at $14,000 \times g$, 4°C for 15 minutes. The pellet was dried at room temperature and stored at -70°C until use.

6.3 Validation of dsRNA

After the dsRNA was obtained, integrity of the dsRNA was validated. The dsRNA was subjected to three difference nuclease digestions including DNA digestion, ssRNA digestion, and dsRNA digestion using DNase I, RNase A, and RNase III, respectively. The digested product was analyzed by agarose gel electrophoresis using 2% agarose gel followed by DNA Stain G staining (SERVA Electrophoresis, Germany) and visualize by Gel Doc™ XR+ Gel Documentation System (Bio-Rad, USA). The valid dsRNA will be intact after the DNA and ssRNA digestion but not after the dsRNA digestion.

6.3.1 DNA digestion using DNase I

The DNA digestion was conducted to ensure that the DNA is completely digested after the addition of RQ1 DNase (section 6.2). The DNase I digestion mixture was prepared as listed in Table 24 using DNase I, RNase-free (Thermo Fisher Scientific, USA). The mixture was mixed gently and incubated at 37°C for 30 minutes. After the incubation, the reaction was terminated by the addition of 2 μL of 0.5 M EDTA and followed by incubation at 65°C for 10 minutes.

Table 24 Components of DNase I digestion mixture

Components	Volume (μL)
dsRNA (1 μg)	5
10X reaction buffer with MgCl_2	1

Table 24 (Continued)

Nuclease-free water	3.5
DNase I, RNase-free (1 U/ μ L)	0.5
Total volume	10

6.3.2 ssRNA digestion using RNase A

The ssRNA digestion was conducted to ensure that the synthesized sense and antisense RNA are annealed completely. Under low salt condition (less than 100 mM NaCl), RNase A cleaves all of dsRNA, ssRNA, and RNA strand in DNA:RNA hybrid. On the other hand, under high salt condition (more than 300 mM NaCl), RNase A cleaves ssRNA only. The RNase A digestion mixture was prepared as listed in Table 25 using RNase A, DNase and protease-free (Thermo Fisher Scientific, USA). The mixtures was mixed gently and incubated at room temperature for 15 minutes.

Table 25 Components of RNase A digestion mixture

Components	Volume (μ L)
dsRNA (1 μ g)	5
20X SSC	1
Nuclease-free water	3.5
RNase A, DNase and protease-free (10 mg/mL)	0.5
Total volume	10

6.3.3 dsRNA digestion using RNase III

The dsRNA digestion was conducted to verify the validity of dsRNA. The RNase III digestion mixture was prepared as listed in Table 26 using ShortCut[®] RNase III (New

England Biolabs, USA). The mixture was mixed gently and incubated at 37°C for 30 minutes. After the incubation, the reaction was terminated by the addition of 1 µL of 10X EDTA solution.

Table 26 Components of RNase III digestion mixture

Components	Volume (µL)
dsRNA (1 µg)	5
10X ShortCut [®] Reaction Buffer	1
10X MnCl ₂	1
Nuclease-free water	2.5
ShortCut [®] RNase III (2 U/µL)	0.5
Total volume	10

6.4 *MrTCTP* knockdown experiment using dsRNA injection

The juvenile prawn (1-2 g body weight) was purchased from local farm at Suphan Buri province, Thailand. The prawn was subjected to random sampling for the detection of *MrNV* using pleopod sample. The prawn was kept in cement tank with dechlorinated freshwater and continuous aeration at room temperature (28-20°C). The prawn was fed once a day with commercial pellet feed. For *MrTCTP* knockdown experiment, the prawn was divided into three groups including dsRNA-*MrTCTP*, dsRNA-*IMNV*, and 2X PBS group (n=30) which was then injected intramuscularly into the third abdominal segment with 5 µg of dsRNA-*MrTCTP*, 5 µg of dsRNA-*IMNV*, and 2X PBS (50 µL per each), respectively using 1-ml insulin syringe.

Muscle samples were collected from all of the three groups (3 prawns per time point) at 0, 1, 2, 3, 4, 5, 6, 7 day post-injection. Muscle samples were subjected to the RT-PCR for monitoring *MrTCTP* knockdown using primers that cover the whole dsRNA region for preventing the amplification of dsRNA (Table 27). The experiment was performed in

triplicate. The day in which *MrTCTP* is completely knockdown was further used in the knockdown experiment combined with *MrNV* challenge.

Table 27 Primers used in the RT-PCR reaction for knockdown experiment

Primer name	Sequence
TCTPKnock-F	5'-GGA TCT GAT CAG TGG GGA TG-3'
TCTPKnock-R	5'-CCA TCA GGG TTC ATG GAT TC-3'

6.5 *MrTCTP* knockdown experiment combined with *MrNV* challenge

To further examine *MrTCTP* role in innate immune system, the juvenile prawn was divided into three groups including dsRNA-*MrTCTP*, dsRNA-IMNV, and 2X PBS group and further divided into two subgroups (n=15 for each subgroup). In each group, the prawn was injected with 5 µg dsRNA or PBS using the same methodology as described in section 6.4 and then injected with *MrNV* inoculum (section 4.3) or TN buffer after the day that *MrTCTP* is completely knockdown.

For example, in case of dsRNA-*MrTCTP* group, 40 prawns were injected with 5 µg of dsRNA-*MrTCTP*. At the day in which *MrTCTP* is completely knockdown, 20 prawns were injected with *MrNV* inoculum and other 20 prawns were injected with TN buffer (50 µL per each). The moribund prawns were collected and subjected to RT-PCR for the detection of *MrNV* (section 4.2) using pleopod samples. The cumulative mortalities were observed every 24 hours after the second injection. The experiment was conducted in triplicates and the results were presented as cumulative mortalities and were compared using line chart. Differences among each experimental group were analyzed by one-way ANOVA (analysis of variance) with post-hoc Tukey HSD (honestly significant difference). Differences were defined as statistical significance at $p < 0.05$.

7. Transcriptomic analysis (RNAseq) of *M. rosenbergii* post-larvae in response to *M. rosenbergii* nodavirus (*MrNV*) infection

7.1 Preparation of *MrNV* infected post-larvae prawn

The post-larvae prawn (PL 25-30) were purchased from local farm at Suphan Buri provinces, Thailand. The PL was subjected to random sampling for the detection of *MrNV* using muscle and pleopod sample. The PL were kept in the glass tank with dechlorinated freshwater and continuous aeration at room temperature (25-27°C). The PL were confirm the absence of *MrNV* infection using viral nucleic acid extraction and RT-PCR. After one day of acclimation, the PL were divided into two groups including control and *MrNV* group. In the *MrNV* group, the PL were challenged with *MrNV*-infected PL homogenate using the same methodology as described earlier, whereas the control group were challenged with TN buffer. After four days of immersion, for the *MrNV* group, the PL with prominent signs of infection were collected and the infection of *MrNV* will be confirmed using viral nucleic acid extraction and RT-PCR. The *MrNV*-infected PL and the PL from control group were 10 subgroups (10 PL per each subgroup). Six subgroups were used in Illumina sequencing, whereas four subgroups were used in quantitative RT-PCR experiment. The PL samples were immersed in DNA/RNA Shield (Zymo Research, USA) and stored at -80°C until RNA extraction.

7.2 RNA extraction

The total RNA were extracted using Quick-RNA™ MiniPrep (Zymo Research, USA) according to manufacturer's protocol. Briefly, the PL samples (10 PL per subgroup) were homogenized in 600 µL of RNA lysis buffer. After the PL samples were homogenized and centrifuged, the homogenates were filtrated through Spin-Away™ Filter using centrifugation at 11,000 x g for 1 minute. The filtrates were mixed with 600 µL of EtOH. The columns were then transferred to Zymo-Spin™ III CG Column and centrifuged at 11,000 x g for 1 minute. After one wash with 400 µL of RNA Wash Buffer, total of 80 µL of DNase I reaction mix (as listed in Table 28) were added to the column and incubated at RT for 15 minutes.

Table 28 Components of DNase I reaction mix

Components	Volume (μL)
DNase I	5
DNA Digestion Buffer	75
Total volume	80

After that, the columns were washed with 400 μL of RNA Prep Buffer once, and with 600 μL of RNA Wash Buffer twice using centrifugation. Finally, the total RNA were eluted with 50 μL of Nuclease-Free water using centrifugation. The extracted RNA were quantified using DropSense 16 Micro-volume spectrophotometer (Unchained Labs, USA) and stored at -80°C until use.

7.3 Library preparation

The cDNA library was prepared using SENSE mRNA-Seq Library Prep Kit V2 (Lexogen, USA). The preparation was performed according to manufacturer's protocol which includes poly-A selection, library generation, and library amplification. Library generation steps include reverse transcription and ligation, second strand synthesis, and purification. Library amplification steps include polymerase chain reaction and purification. The purification steps were conducted using the purification module with magnetic beads (Lexogen, USA). Each library was indexed by 6-nucleotide-long i7 indices during PCR amplification step.

Firstly, the oligo-dT magnetic beads (MB) were washed twice using 200 μL of wash buffer (BW) and resuspended in 10 μL of RNA Hybridization Buffer (HYB). For the poly-A selection, 10 μL of extracted RNA (500 ng) was denatured at 60°C for 1 min and held at 25°C , and then mixed with 10 μL of washed beads. The beads was incubated at RT, 1,250 rpm for 20 min. The beads were washed twice with 100 μL of BW by incubating at RT for 5 min and removing supernatant using magnetic rack.

For the library generation steps, the beads were added with 15 μL of Reverse Transcription and Ligation Mix (RTL) and 2 μL of Starter/Stopper Mix (ST) and incubate at RT, 1,250 rpm for 5 min. Then, the beads were added with 3 μL of Enzyme Mix (E1), incubate at RT, 1,250 rpm for 2 min and 37 °C, 1,250 rpm for 1 hr. After the incubation, the beads were the beads were washed twice with 100 μL of BW. Next, the beads were resuspended with 17 μL of Second Strand Synthesis Mix (SSM) and 1 μL of Enzyme Mix 2 (E2). The second strand were generated using one cycle of thermo cycling (98 °C for 90 sec, 65 °C for 60 sec, and 72 °C for 5 min). The double-stranded cDNA library was then purified using magnetic beads. Briefly, the beads were added with 14 μL of Purification Beads (PB) and 2 μL of Purification Solution (PS), and incubating at RT for 5 min. The beads were the resuspended with 50 μL of Elution Buffer (EB), and incubating at RT for 2 min. After the incubation, the beads were added with 70 μL of PS, and incubating at RT for 5 min. Next, the beads were washed twice with 120 μL of freshly prepared 80 % EtOH. Finally, the cDNA library was eluted using 20 μL of EB.

For the library amplification, real-time PCR was preliminary performed to determine optimal cycle for library amplification using 1.7 μL of purified library (one tenth). The qPCR reaction will be prepared as listed in Table 29.

Table 29 Components of the PCR reaction for determine optimal cycle for library amplification

Components	Volume (μL)
PCR	7
E2	1
P7 primer without index (7000)	5
SYBR Green I	1.2
Elution Buffer (EB)	14.1
Eluted library	1.7
Total volume	30

The PCR conditions were initial denaturation at 98 °C for 30 sec followed by 40 cycles of 98 °C for 10 s, 65 °C for 20 s, and 72 °C for 30 s, and final extension at 72 °C for 1 min. The cycle for library amplification was the cycle that has 50 % maximum amplification curved subtracted by three ($\sim 2^3$ compensation from one tenth amount). After the cycle for the amplification was determined, total of 17 μL of purified library was added with 7 μL of PCR Mix (PCR), 1 μL of Enzyme Mix 2 (E2), and 5 μL of i7 index (7001 to 7012). The mixtures were then subjected to PCR reaction using the optimal cycle. Finally, the amplified library was subjected to purification steps using 30 μL of PB and the same methodology as described earlier. The prepared cDNA library was subjected to quality assessment using Qubit 4 Fluorometer (Invitrogen, USA) and LabChip GX Touch 24 microfluidic nucleic acid analyzer (PerkinElmer, USA).

7.4 Library denaturation and sequencing

Before denaturation, total of 20 fmol from each cDNA library (calculated from Qubit 4 and LabChip results) were pooled together and re-purified using magnetic beads as described earlier. The re-purified library was qualified using Qubit 4 Fluorometer (Invitrogen, USA) and LabChip GX Touch 24 (PerkinElmer, USA) and then diluted into 2 nM. The diluted library was subjected to denaturation steps according to NextSeq System Denature and Dilute Libraries Guide (Illumina, USA) using Standard Normalization Method (Protocol A). Briefly, Total of 10 μL of diluted library was mixed with 10 μL of freshly prepared 0.2 M NaOH and incubated at RT for 5 min. Finally, the mixture was added with 10 μL of Resuspension Buffer (RSB), and 970 μL of prechilled HT1 solution resulting in 20 pM of denatured library.

A 1.8 pM of denatured library (total of 1,300 μL) was loaded into NextSeq 500/550 High Output Reagent Cartridge v2 150 cycles (Illumina, USA). Cluster generation and paired-end sequencing with 75 bp were performed on a NextSeq 550 sequencer (Illumina, USA).

7.5 Data analysis pipeline

Snakemake tool was used to create reproducible and scalable automated data analysis pipeline (Koster & Rahmann, 2012). The pipeline was written in python based language using Atom v 1.33.1. The transcriptome assembly pipeline contained three major sections including raw data pre-processing, transcriptome assembly, and post-processing of the transcriptome. The overviews of analysis pipeline are summarized in Figure 22. Raw read pairs were subjected to preliminary quality assessment using FastQC v 0.11.5 (Andrew, 2010). FastQC provides useful quality metrics regarding GC content, adaptor contamination, size distribution, and N base ratio. The FastQC results from each sample were then compiled using MultiQC v 1.8 (Ewels, Magnusson, Lundin, & Kaller, 2016).

The pre-processing steps included trimming low quality bases, adapters, and removing small reads using Trimmomatic v 0.36 (Bolger, Lohse, & Usadel, 2014). Trimmomatic software orderly performed these following actions; trim the first 9 bases of the both reads (according to Lexogen's recommendation), remove N base and leading and trailing bases if the quality is below 3, scan and cutting 4-base wide if the average quality per base drops below 15, and remove small reads below the 36 bases long. The trimmed reads were subjected to quality assessment using FastQC and MultiQC and then merged together for transcriptome assembly using merge command.

The *de novo* transcriptome assembly was performed using Trinity software v 2.8.0 with default parameters (Grabherr et al., 2011). Trinity software combines three software module including Inchworm, Chrysalis, and Butterfly to process RNAseq reads into transcripts. Before Trinity assembly, *in-silico* normalization was performed within Trinity using default parameters. *In-silico* normalization was recommended for large RNAseq data sets (exceeding 300M pairs) in order to reduce hardware requirements and time consumption for the assembly (Grabherr et al., 2011). Trinity assembly is based on constructed *De Bruijn* graphs from sequence data using k-mer-based method. Firstly, Inchworm reconstructs the best representative transcript using greedy k-mer-based method. Then, Chrysalis builds complete *De Bruijn* graphs from Inchworm's output.

Finally, Butterfly constructs full-length linear transcripts from Chrysalis's component into assembled transcripts. This process resulted in transcripts with relatively high redundancy. To remove the redundancy, transcripts that have more than 95 % of identity were clustered together using CD-HIT software (W. Li & Godzik, 2006) resulting in unigene transcripts which will be used for downstream analysis.

The post-processing steps consisted of three major parts including transcriptome quality assessment, differential expression analysis, and annotation. For the transcriptome quality assessment, the assembled transcripts were used to calculate the fragment mapping rates by mapping reads back to the transcripts using Bowtie 2 v 2.3.0 (Langmead & Salzberg, 2012). The assembled transcripts were also examined orthologs completeness using BUSCO v 3 (Simao, Waterhouse, Ioannidis, Kriventseva, & Zdobnov, 2015) by pairing the transcripts against 1,066 complete universal single copy orthologous gene from arthropoda_odb9 database (https://busco.ezlab.org/datasets/arthropoda_odb9.tar.gz). Finally, the assembled transcripts were used to generate Nx (x% of the transcripts that have at least Nx base pair in length) and ExN50 statistics (top x% most expressed transcripts that have at least N50 length) using 'contig_ExN50_statistic.pl' script within Trinity assembler.

To identify differentially expressed transcripts, edgeR was used in this pipeline (Robinson, McCarthy, & Smyth, 2010). EdgeR uses the trimmed mean of M-values normalization method (TMM) to calculate the transcript expression levels (Robinson & Oshlack, 2010) with the Benjamini-Hochberg method for multiple p -value correction (Benjamini & Hochberg, 1995). The transcripts that had at least two-fold change with a false discovery rate (FDR or adjusted p -value) less than 0.05 was considered as differentially expressed transcripts. The raw counts for each transcript from each sample were calculated by RSEM software (B. Li & Dewey, 2011) using 'align_and_estimate_abundance.pl' script within Trinity assembler. The raw counts were used to generate expression matrix using 'abundance_estimates_to_matrix.pl' script which were then used to identify differentially expressed transcripts by EdgeR using 'run_DE_analysis.pl' script within Trinity assembler.

For the transcripts annotation, the assembled transcripts were used to search sequence homology by aligning against UNIPROT (https://data.broadinstitute.org/Trinity/Trinotate_v3_RESOURCES/uniprot_sprot.pep.gz) and NCBI's non-redundant arthropod database (https://ftp.ncbi.nlm.nih.gov/blast/db/v5/nr_v5.*.tar.gz) using Blastx. Only top-hit matches with E-value less than $1e-5$ were kept. The results from Blastx against UNIPROT database were then used to obtain functional annotation from EggNOG (Evolutionary Genealogy of Genes: Non-supervised Orthologous Groups), KEGG (Kyoto Encyclopedia of Genes and Genomes), and GO (Gene Ontology) database using Trinotate v 3.0.2 (Bryant et al., 2017). Gene ontology is bioinformatic database for unifying the representative of gene and gene product along with functional annotation across variety of organisms. GO database divided into three domains including cellular component, molecular function, and biological process (Gene Ontology, 2008). EggNOG is a public database containing orthologous groups (OG) of across different taxonomic levels with functional annotations. EggNOG is based on cluster of orthologous (COG) principles which were comparing the protein sequences of complete genomes and applies this principle to non-supervised OG from numerous organisms (Huerta-Cepas et al., 2016). KEGG database is a resource for utilizing genomic, chemical and functional information to understand higher-level systemic functions of the cell, the organism and the ecosystem. KEGG orthology (KO) is a pathway-based functional ortholog database which is a part of genomic information concept of KEGG database (Kanehisa & Goto, 2000).

The data analysis pipeline was tested using RNAseq sample data from *M. rosenbergii* in response to *V. parahaemolyticus* infection (Rao et al., 2015) which were deposited into NCBI's Short Read Archive (SRA) under the accession number SRR1424572 and SRR1424574 for control and *Vibrio*-infected group, respectively. This pipeline including Snakefile, config.yaml, samples.txt (sample configuration file) are available on GitHub at https://github.com/prawnseq/Mrosenbergii_MrNV_RNAseq.

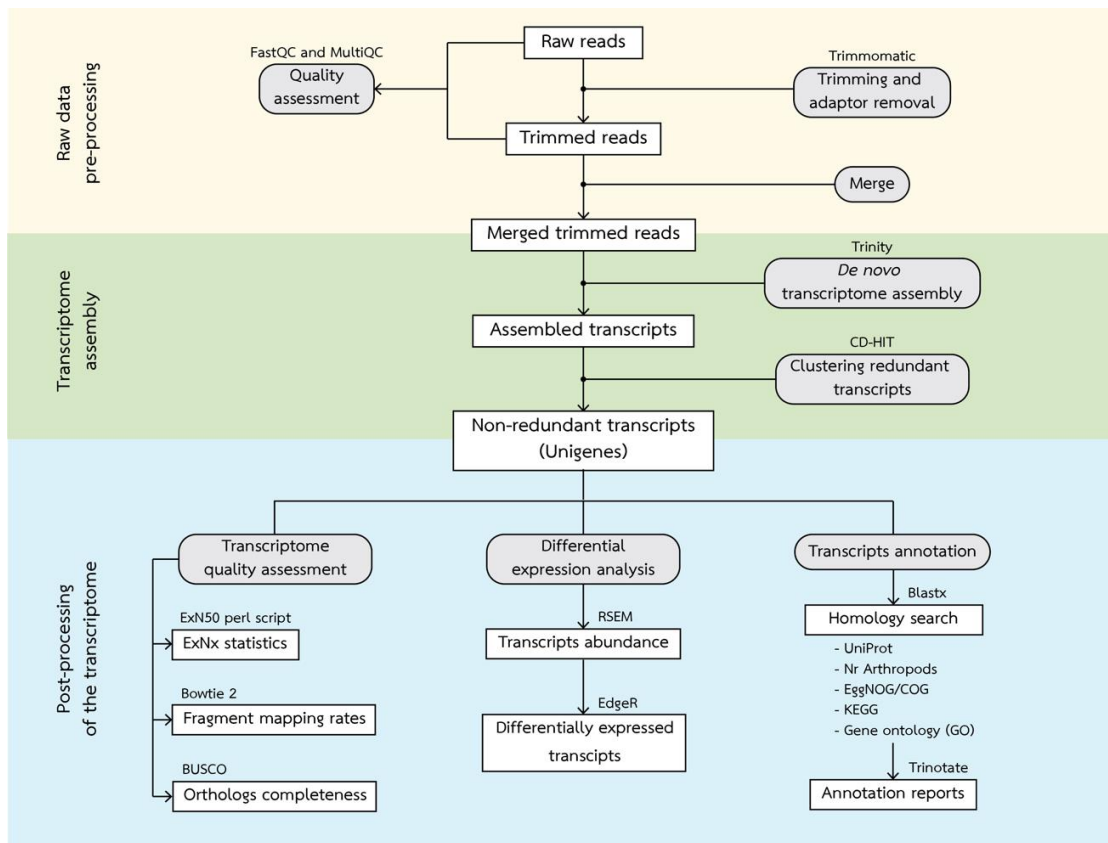


Figure 22 The overviews of analysis pipeline.

The pipeline is divided into three major parts including rawdata pre-processing, transcriptome assembly, and post-precessing of the transcriptome which indicated by area of different colors. Boxes represent datasets. Rounded boxes represent analyses. The software for each analysis is indicated at the top of the box whereas the database for homology search are listed under the box.

7.6 Quantitative RT-PCR analysis

To validate differential expression results, total of nine differentially expressed unigenes were selected for quantaltive RT-PCR (qRT-PCR) including *anti-lipopolysaccharide factor 1 (ALF1)*, *Spatzle (Spz)*, *copper/zinc superoxide dismutase 3 (CuZnSOD3)*, *caspase (CASP)*, *antiviral protein (Anv)*, *dicer (DICER)*, *hemicentin-1-like (HMCN1)*, *ADP ribosylation factors (ARF)*, and *prophenoloxidase (ProPO)*. The two-step qRT-PCR was carried out using extracted RNA from separate biological replicates and

elongation factor1-alpha (EF1-alpha) as an internal reference gene (Dhar, Bowers, Licon, Veazey, & Read, 2009). Oligonucleotide primers were designed using Primer3Plus webserver (<http://www.bioinformatics.nl/cgi-bin/primer3plus/primer3plus.cgi>) with qPCR default settings as listed in Table 30.

Before qRT-PCR validation, designed primers were subjected to the primer efficiency testing using two-fold dilution of cDNA ranging from 200 ng to 12.5 ng. The standard curves were plotted using Log quantities and average Ct values. The efficiency of primers was calculated using the following formula "Efficiency (100%) = $(10^{(-1/\text{Slope}-1)}) * 100$ ". Primers with efficiency score between 90-110 % will be used in the qRT-PCR validation.

Table 30 Primers used in the qRT-PCR experiment

Primer name	Sequence	Efficiency (%)	R ²
ALF1-F	5'-CTG GTG ACG GAA GAA GAA GC-3'	98.13	0.9975
ALF1-R	5'-CTT AAC CAG GCC ATT CCT CA-3'		
Spz-F	5'-CGA CGGA ATA CCC GAC CTA CA-3'	92.27	0.9926
Spz-R	5'-TGT CGG TTT TGC AGA CGT AG-3'		
CuZnSOD3-F	5'-GGG AGA CCT AGG GAA CAT CC-3'	95.33	0.9920
CuZnSOD3-R	5'-GTG GAT GAC CAC GGC TCT AT-3'		
CASP-F	5'-CTG CCC TGA ATT CCT CTC TG-3'	105.24	0.9885
CASP-R	5'-CGA AGG TGG TAT GGA GCA AT-3'		
Anv-F	5'-AAT GGT GGT ATC AGC CTT GC-3'	94.53	0.9885
Anv-R	5'-TTA GAG GGT CGA CCA TGA GG-3'		
DICER-F	5'-CAC TCG AGC ATC CTG TTT CA-3'	107.80	0.9969
DICER-R	5'-ACC AAT CCC CAT CCA ATG TA-3'		

Table 30 (Continued)

HMCN1-F	5'-TAA GGC AAC CGA CCA CTA CC-3'	107.85	0.9940
HMCN1-R	5'-GAC GTA GAG ACT GGC GGA AG-3'		
ARF-F	5'-CCC ATT ACA GTG GTC CTG CT-3'	95.22	0.9928
ARF-R	5'-CAG AAC CCT TCC CTT CAC AA-3'		
ProPO-F	5'-AAC AAC CTG AGA ACC GGA TG-3'	93.46	0.9899
ProPO-R	5'-CGG CAG GGT TGG CAT AAT CT-3'		
EF1a-F	5'-TGC GCT GTG TTG ATT GTA GC-3'	103.19	0.9834
EF1a-R	5'-ACA ATG AGC TGC TTG ACA CC-3'		

The total RNA were extracted using Quick-RNA™ MiniPrep (Zymo Research, USA) as described earlier. The first-strand cDNA was synthesized using SensiFAST™ cDNA Synthesis Kit (Bioline, UK) according to manufacturer's protocol. Briefly, cDNA mastermix was prepared as listed in Table 31.

Table 31 Components of cDNA mastermix for first-strand cDNA synthesis

Components	Volume (μL)
Total RNA (250 ng/μL)	4
5X TransAmp Buffer	4
Reverse Transcriptase	1
Nuclease-free water	11
Total volume	20

Finally, the mastermix was incubated at 25°C for 5 minutes, 45°C for 15 minutes, and 85°C for 5 minutes. After the termination, the mastermix was chilled on-ice at least 1 minute. The synthesized cDNA were quantified using DropSense 16 Micro-volume spectrophotometer (Unchained Labs, USA) and stored at -20°C until use.

The qPCR was carried out using SensiFAST™ SYBR® Lo-ROX Kit (Bioline, UK) and synthesized cDNA as described earlier as DNA template. The cDNA from each sample were used in ten qPCR reactions (nine gene of interests and one internal control). Firstly, the qPCR reactions were prepared as listed in Table 32.

Table 32 Components of RT-PCR reaction

Components	Volume (μL)
2X SensiFAST™ SYBR® Lo-ROX Mix	10
10 μM Forward primers	0.8
10 μM Reverse primers	0.8
200 ng/μL of synthesized cDNA	1
Nuclease-free-H ₂ O	6.4
Total volume	20

After the preparation, the reactions were placed in the QuantStudio™ 3 Real-Time PCR Systems (Thermofisher, USA) and the qPCR was performed. The qPCR program was performed according to manufacturer's recommended protocols as described below.

Step 1	Pre-denaturation	95 °C for 2 minutes
Step 2	Denaturation	95 °C for 5 seconds
Step 3	Annealing	60 °C for 10 seconds
Step 4	Extension	72 °C for 15 seconds
Step 5	Repeat Step (3), (4) and (5) for 39 cycles	

Step 6 Melt curve stage

The relative expressions between gene of interests and internal control were calculated from difference between C_t of interested gene and reference gene (Delta C_t). The delta-delta C_t method was used to calculate relative fold-change of gene expression between control and infected samples (Livak & Schmittgen, 2001). Statistical differences between two groups were conducted using a simple student t-test. The results from qPCR were then compared with the results from RNAseq pipeline using heatmap and coefficient of determination (R^2).



CHAPTER 4

RESULTS

1. Molecular cloning and characterization of *Mr*TCTP cDNA

1.1 Molecular cloning and identification of partial *Mr*TCTP cDNA using degenerate primers

To identify partial sequence of *Mr*TCTP cDNA, two degenerate primers were designed based on conserved regions of the sequence alignment using TCTP proteins from related organisms. The PCR reaction was performed using a pair of degenerate primers and synthesized cDNA. The PCR reaction yielded a product of 423 bp which was an expected size. The product was then cloned into pCR™2.1-TOPO® vector for sequencing. The results showed high similarity to those of TCTP proteins from related organisms, according to BLASTx analysis (Figure 23).

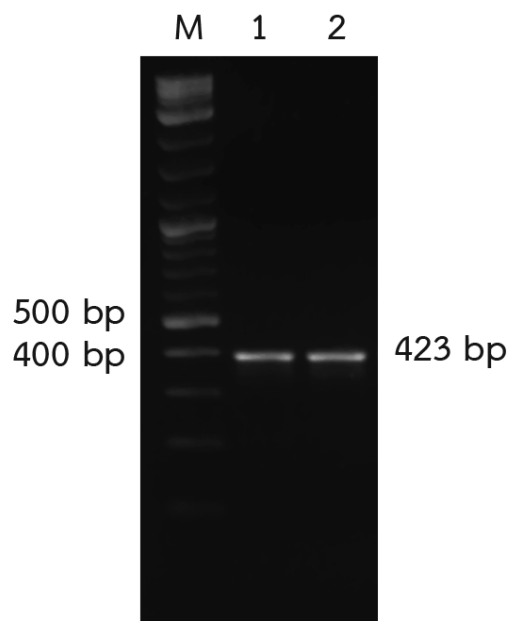


Figure 23 PCR product of partial *Mr*TCTP using degenerate primers

Lane 1 and 2 are PCR products of partial *Mr*TCTP which are 423 bp.

M is DNA marker (2-log DNA ladder).

1.2 Molecular cloning and identification of 5' and 3' ends of *MrTCTP* cDNA using Rapid amplification of cDNA ends (RACE)

To identify the remaining 3' and 5' end of *MrTCTP* cDNA, GSP001 and GSP002 oligonucleotide primers were designed based on the partial sequence. The RACE-PCR reactions were performed using GSP001 or GSP002 and synthesized RACE-ready cDNA. The 5'-RACE-PCR yield a product of 480 bp, whereas the 3'-RACE-PCR yield a product of 500 bp (Figure 24). Both of the RACE-PCR products were in expected product size. The products were then cloned into pCR™2.1-TOPO® vector for sequencing. The obtained sequences were aligned and combined with partial sequence to obtain full-length cDNA of *MrTCTP*. According to BLASTx analysis, the full-length cDNA of *MrTCTP* shared high similarity to other crustaceans.

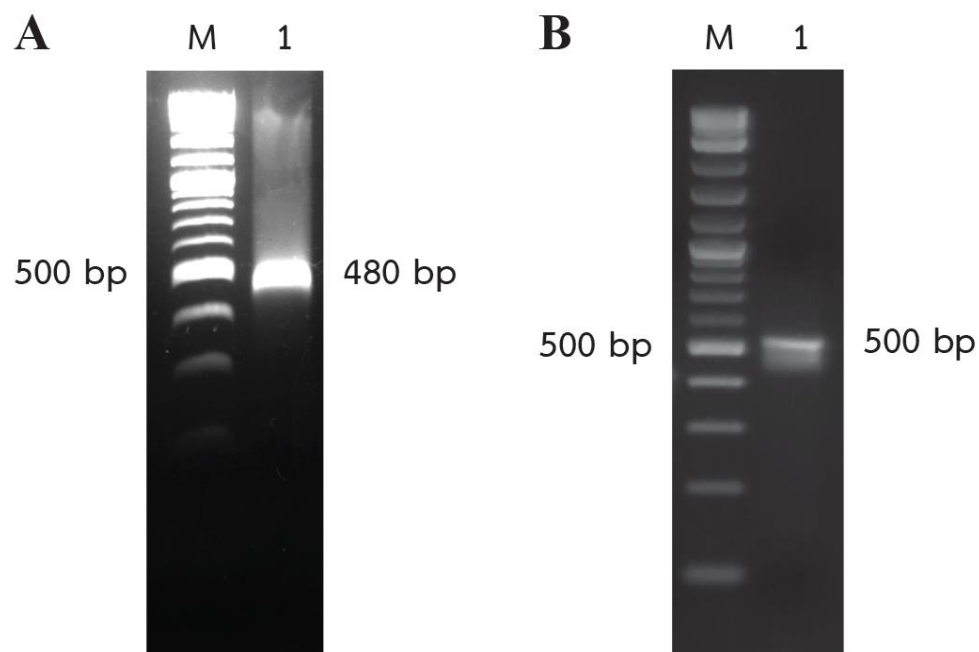


Figure 24 RACE-PCR products of *MrTCTP*

- (A) Lane 1 is 5'-RACE-PCR product *MrTCTP* with 480 bp in size.
 - (B) Lane 1 is 3'-RACE-PCR product *MrTCTP* with 500 bp in size.
- M is DNA marker (2-log DNA ladder).

1.3 Sequence confirmation of full-length *MrTCTP* cDNA

To verify the coding sequence of *MrTCTP* cDNA, PCR reaction was performed using prove reading polymerase and oligonucleotide primers that cover the coding sequence. The PCR reaction yielded an expected 598 bp PCR product (Figure 25A). The product was then cloned into pCR[®]-Blunt II-TOPO[®] vector for sequencing. The recombinant plasmid was verified the insertion using restriction enzyme digestion (Figure 25B). According to the sequence alignment, the obtained sequence was identical to the full-length cDNA. The full-length *MrTCTP* cDNA was then submitted into GenBank database under the accession number of KX809568.

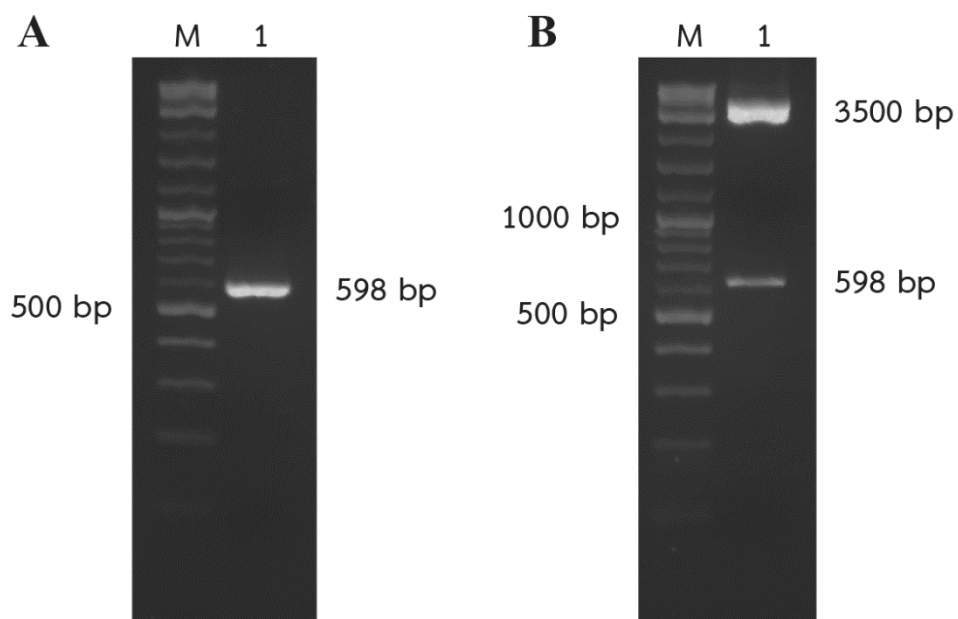


Figure 25 Cloning of *MrTCTP*-CDS PCR products

(A) Lane 1 is PCR product *MrTCTP*-CDS with 598 bp in size.

(B) Lane 1 is recombinant plasmid after the *EcoRI* digestion which consists of *MrTCTP*-CDS (598 bp) and pCR[®]-Blunt II vector (3.5 kb).

M is DNA marker (2-log DNA ladder).

1.4 Characterization of *MrTCTP* cDNA

The full-length *MrTCTP* cDNA was used to generate the deduced amino acid sequence. The deduced amino acid sequence of *MrTCTP* was characterized regarding molecular weight, domain and protein family, potential glycosylation sites, and ribbon diagram using web-based software.

```

-83                                     ATGGGGCCTTCCCTGGTCCGCCT
-60  CATCCCGGAGAGCAAGAACCAACCTAGGCCAATTTTCTACCGTCAATCATCCGTCATC

1    ATGAAGGTCCTCAAGGATCTGATCAGTGGGGATGAGATGTTCACCGACTCCTACAAGTAT
1    M K V F K D L I S G D E M F T D S Y K Y
61  GAGGTTGTCGACGATGCCTTCTACATGGTGATCGGAAAGACACCAAGTAACTCAGGGT
21  E V V D D A F Y M V I G K N T T V T Q G
121 GATATCCAGCTTGAAGGTGCCAATCCTTCAGCGGAAGAAGAAGATGAGGGCACAGAATCC
41  D I Q L E G A N P S A E E E D E G T E S
181 AACAGTGTCTCTGGTATTGACGTTGTCATATTTATGCGCCTCCAGGAGACTGGCTTTGGA
61  N S V S G I D V V I F M R L Q E T G F G
241 AACAAAGAAAGACTACCTTACCTACATGAAGGAATACATTAAGAATTTGAAGAGCAAGCTA
81  N K K D Y L T Y M K E Y I K N L K S K L
301 GAGGGAACCCAGCTGCTGACAAGCTTCTCTGCTATCCAGAAACCCCTAGCTGAATTGCTT
101 E G T P A A D K L P A I Q K P L A E L L
361 AAGAAATTC AAGGACCTTCAGTCTTCTCACTGGTGAATCCATGAACCCTGATGGTATGGTT
121 K K F K D L Q F F T G E S M N P D G M V
421 GCAATTGGCGATTACAAGGAGATTGATGGTGAAGAAAGACCTGTAATTTACTTCCCTAAG
141 A I G D Y K E I D G E E R P V I Y F P K
481 TTAGGCTAGAAAGAGGAAAACTTTAGGTACAATGTAATTTAAGATCCAGTATTCAGT
161 L G L E E E K L *

541  CATCCATTAACATCGGAACATCAATCTCATGTTGAATTAGCCTACGTTATTGGTGTCTTG
601  TTTTAATTTAATAAAATTCATCTAAAAAAAAAAAAAAAAAAAAAAAAAAAAAAAAAA

```

Figure 26 Full-length cDNA, deduced amino acid and sequence analysis of *MrTCTP*

The initiation codon (ATG) and the stop codon are shown in bold letters. Polyadenylation site (Poly-A) is underlined. Two CK2-phospho-sites (casein kinase II phosphorylation site) are in the box (LISGD and NPSAE) while protein kinase c site (PKC) is in the dashed box (TDSYK). Potential Asn-glycosylation sites are shown in rounded box (NTTV).

According to the nucleotide sequence analysis, the full-length *MrTCTP* cDNA consisted of 736 nucleotides, with an 83 nt of 5'-UTR (5'-untranslated region) and a 146 nt of 3'-UTR (3'-untranslated region). The putative polyadenylation signal (AATAAA) was located at 9 nucleotides upstream to the poly-A tail within the 3'-UTR. The open reading frame (ORF) comprised of 507 nucleotides, which encoding 168 amino acid polypeptides (Figure 26). The translation start site of *MrTCTP* (AAT**CA**TG) matched 6 out of 7 to *D.*

melanogaster (Arthropoda) consensus sequence (MAAMATG; M = A or C) (Cavener, 1987).

<i>L.vannamei</i>	M KVFKDMLT G E M F T D TYKYEEVDD-AFYM V IGK N ITVTE D NI--ELEGAN P S A E E A-DE 56
<i>P.monodon</i>	M KVFKDMLT G E M F T D TYKYEEVDD-AFYM V IGK N ITVTE D NI--ELEGAN P S A E E A-DE 56
<i>E.sinensis</i>	M KVFKDIIS G E M F T D TYK M EEI E D-AFYM V IGK N TTVTE G NI--ELAGAN P S A E E A-DE 56
<i>M.rosenbergii</i>	M KVFKDLIS G E M F T D SYKYEVVDD-AFYM V IGK N TTV T Q G DI--QLEGAN P S A E E E-DE 56
<i>D.melanogaster</i>	M KIYKDIIT G E M F A D TYK M KL V DD-VIYEVY G KLIT R Q G DDI--KLEGAN P S A E E A-DE 56
<i>S.pombe</i>	M LLYKDVIS G E LV S D A YDLKEVDD-IVYE A DC Q M V TV K Q G --GD V DI G AN P S A E D A E EN 57
<i>C.lupus familiaris</i>	M I I YRDLIS H E M F S D LYKIREI A D G L C LE V E G M V SR T E G N I DD S L I G G AN P S A E G P E G E 60
<i>H.sapiens</i>	M I I YRDLIS H E M F S D LYKIREI A D G L C LE V E G M V SR T E G N I DD S L I G G AN P S A E G P E G E 60
<i>D.rerio</i>	M I I YKDIIT G E M F S D LYKIK E SE N G M LE V E G K M IT R A E G D ID D AL I G G AN P S A E V A-DE 59
<i>L.rohita</i>	M I I YKDIIT G E M F S D LYKIK E SE N G M MI E VE G K M IS R A E GI D D A L I G G AN P S A E V Q-DE 59
	TCTP1
<i>L.vannamei</i>	GTDTTSQSGVD V LY M RL Q ET-GFQVKKDY L A M K E Y L K NVKAKLE G T P E A S-- * K L T S I 112
<i>P.monodon</i>	GTDTTSQSGVD V LY M RL Q ET-GFQVKKDY L A M K E Y L K NVKAKLE G T P E A S-- K L T S I 112
<i>E.sinensis</i>	GTESSSVSGID V LY M RL Q ET-GFGAKKDY L T M K NY L K S LK G KLE G T P K V E-- K L P A I 112
<i>M.rosenbergii</i>	GTESNSVSGID V LY M RL Q ET-GFGAKKDY L T M K E Y L K NL K S K LE G T P A A D-- K L P A I 112
<i>D.melanogaster</i>	GTDTITSESGVD V LN H RL Q ETCF A FGDKKSY T LY L K D Y M K K V LAKLE E K S P D Q V D I F K T N M 116
<i>S.pombe</i>	-A E E G T E T V N N I V S F HL S P T -S-FDKKSY S Y I K G Y M K A I K A R L Q E S N P E R V P V F E K N A 114
<i>C.lupus familiaris</i>	G T E S T V I T G V D I V M N H RL Q ET-S-FT K E A Y K K Y I K D Y M K S I K G K L E E Q R P E R V K H F M T G A 118
<i>H.sapiens</i>	G T E S T V I T G V D I V M N H RL Q ET-S-FT K E A Y K K Y I K D Y M K S I K G K L E E Q R P E R V K H F M T G A 118
<i>D.rerio</i>	G C D S T S V S G V D I V L N H RL Q ET-S-YDKKSY T A I K D Y M K A V K A K L Q E S A P N R V D E F M A N A 117
<i>L.rohita</i>	G C E S T T V S G V D I V L N H RL Q ET-S-YDKKSY T A I K D Y M K A V K A K L Q E V A P D R V D E F M A N A 117
	TCTP2
<i>L.vannamei</i>	QKPLTDL L K K F K D L Q F F T G E S M D P D G M V L M D Y K D I D G E E R P V L Y F P K Y G L T E E K L 168
<i>P.monodon</i>	QKPLTDL L K K F K D L Q F F T G E S M D P D G M V L M D Y K D I D G E E R P V L Y F P K Y G L T E E K L 168
<i>E.sinensis</i>	QKPLTE L L K N F K D LQ F F T G E S M N P D G M V L G D Y K E I D G E E R P V L Y F P K Y G L E E E K L 168
<i>M.rosenbergii</i>	QKPLA E L L K K F K D L Q F F T G E S M N P D G M V A I G D Y K E I D G E E R P V I Y F P K L G L E E E K L 168
<i>D.melanogaster</i>	NK A M K D I L G R F K E LQ F F T G E S M D C D G M V A L V E Y R E I N G D S V P V L M F F K H G L E E E K C 172
<i>S.pombe</i>	I G F V K K I L A N F K D Y D F Y I G E S M D P D A M V L M N Y R E D --G I T P Y M I F F K D G L V S E K F 168
<i>C.lupus familiaris</i>	A E Q I K H I L A N F K N Y Q F F I G E S M N P D G M V A L L D Y R E D--G V T P Y M I F F K D G L E M E K C 172
<i>H.sapiens</i>	A E Q I K H I L A N F K N Y Q F F I G E S M N P D G M V A L L D Y R E D--G V T P Y M I F F K D G L E M E K C 172
<i>D.rerio</i>	P A E V K I L G N I K N F Q F F T G E S M N P D G M I G L L D F R E D--G V T P Y M I S F K D G L E I E K C 171
<i>L.rohita</i>	P A E V K I L G N I K N F Q F F T G E S M N P D G M I G L L D F R E D--G V T P Y M L F F F K D G L E I E K C 171

Figure 27 Sequence alignment of *Mr*TCTP protein

Multiple sequence alignment of TCTP proteins from several organisms including *M. rosenbergii* was constructed by Clustal Omega. Conserved residues are in bold letters, the nine absolute conserved residues are in the box while the six conserved are in the round box with one mismatched indicated by a star. The TCTP signature 1 and 2 are indicated in blue and light-blue highlight, respectively (Bommer & Thiele, 2004).

According to domain and protein family analysis, the deduced *Mr*TCTP protein of 168 amino acid polypeptides, is highly homologous to the TCTP protein family in PFAM domains database (Figure 28B). In addition, using PROSITE database, the deduced *Mr*TCTP protein also carries two TCTP signatures including TCTP signature 1 and TCTP signature 2 at positions 45-55 and 123-145, respectively (Figure 27). The result from SignalP 4.1 Server revealed that the *Mr*TCTP protein showed the absence of signal

peptide. *Mr*TCTP protein contained one putative Asn-glycosylation site (N-glycosylation site) at positions 34-37 (NTTV), two putative casein kinase II phosphorylation sites (CK2-phospho sites) at positions 7-11 (LISGD) and 48-52 (NPSAE), and one protein kinase c site (PKC) at positions 15-19 (TDSYK) all of which located at β -stranded core (Figure 27). Sequence alignment of *Mr*TCTP protein revealed the characteristics of TCTP proteins which are 9 absolute conserved amino acid residues and 6 conserved amino acid residues with a mismatch in one sequence (Figure 27) (Bommer & Thiele, 2004). Moreover, predicted ribbon diagram of *Mr*TCTP demonstrated three major domains including β -stranded core domain, helical domain, and flexible loop which also are typical structure of TCTP protein (Figure 28A).

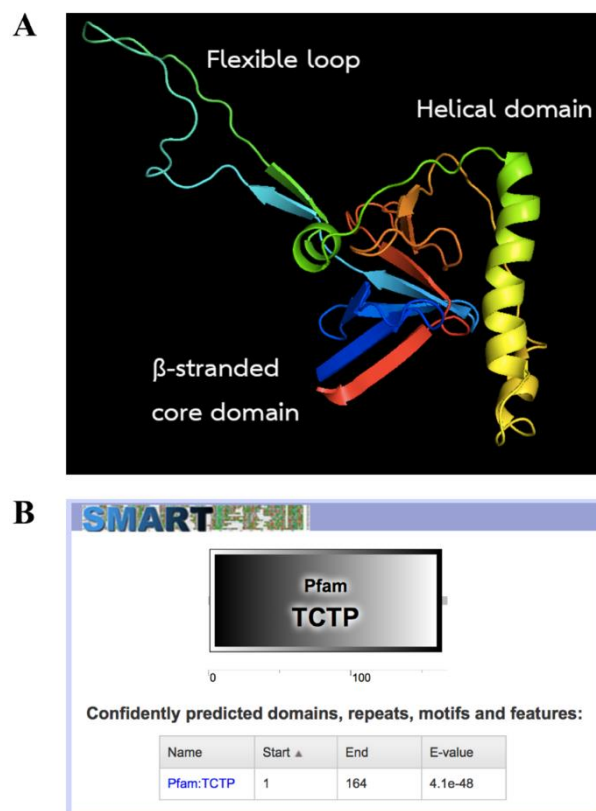


Figure 28 Ribbon diagram and protein family of *Mr*TCTP protein

(A) Ribbon diagram of *Mr*TCTP. Rainbow color demonstrates the first and the last amino acid residues (blue to red). (B) The results of domain and protein family analysis using SMART program.

To reveal conservation among TCTP proteins, amino acid sequences of TCTP from various organisms including fission yeast (*Schizosaccharomyces pombe*, Q10344), zebra fish (*Danio rerio*, NP937783.1), rohu (*Labeo rohita*, AAK27316.1), honey bee (*Apis mellifera*, XP395299.2), fruit fly (*Drosophila melanogaster*, AAF54603.1), Indian shrimp (*F. indicus*, FJ890311.1), whiteleg shrimp (*L. vannamei*, ABY55541.1), giant tiger prawn (*P. monodon*, AAO61938.1), Chinese white shrimp (*F. chinensis*, DQ205420.1), banana shrimp (*F. merguensis*, AY700595.1), Chinese mitten crab (*Eosimias sinensis*, AEF32710.1), and giant river prawn (*M. rosenbergii*, KX809568) were aligned. The identity and similarity matrix was generated from the sequence alignment. The results showed that MrTCTP shared highest identity to *E. sinensis* (Chinese mitten crab) with identity of 83.93 % and shared relatively high identity to those of penaeid shrimps including *F. merguensis*, *F. chinensis*, *P. monodon*, *L. vannamei*, and *F. indicus* (78.57, 78.57, 77.38, 77.98, and 76.79 %, respectively) In addition, the results also indicated that TCTP proteins are highly conserved among eukaryotes considering identity and similarity percentages in the matrix (38 % minimum identity, and 58 % minimum similarity) as shown in Figure 29.

Identity Similarity	Identity											
	1	2	3	4	5	6	7	8	9	10	11	12
1. <i>S. pombe</i>		50	49	46	43	40	41	38	39	40	40	40
2. <i>D. rerio</i>	73		94	54	57	47	47	46	45	47	48	44
3. <i>L. rohita</i>	73	98		53	55	45	45	44	44	45	47	44
4. <i>A. mellifera</i>	63	67	67		76	53	54	52	53	53	53	51
5. <i>D. melanogaster</i>	62	69	69	85		58	58	57	56	58	53	52
6. <i>L. vannamei</i>	59	62	63	67	71		99	98	98	99	81	78
7. <i>P. monodon</i>	59	62	63	67	71	100		98	98	99	80	77
8. <i>F. indicus</i>	58	61	61	66	70	99	99		98	98	80	77
9. <i>F. chinensis</i>	59	61	62	66	70	99	99	98		98	80	79
10. <i>F. merguensis</i>	59	62	63	67	71	100	100	99	99		82	79
11. <i>E. sinensis</i>	60	64	65	67	69	90	90	89	90	90		83
12. <i>M. rosenbergii</i>	58	61	63	67	69	89	89	88	89	89	89	

Figure 29 Identity and similarity of TCTP proteins

Pairwise matrix among TCTP proteins from various organisms including *M. rosenbergii* was generated using Iden and Sim Webserver. Upper right corner demonstrates pairwise identity, whereas the lower left demonstrates pairwise similarity

1.5 Phylogenetic relationship analysis of MrTCTP

Phylogenetic tree of TCTP proteins was constructed using maximum likelihood algorithm followed by bootstrap statistical analysis. Phylogenetic relationship analysis revealed that the deduced amino acid of MrTCTP was in the same clade with the arthropods including insects and crustaceans (Figure 30). The results also indicated that MrTCTP constitutes a distinct group within TCTP proteins from other crustaceans including *E. sinensis* (AEF32710.1), *F. merguensis* (AY700595.1), *F. chinensis* (DQ205420.1), *P. monodon* (AAO61938.1), *L. vannamei* (ABY55541.1), and *F. indicus* (FJ890311.1) with relatively high bootstrap values (Figure 30). In addition, MrTCTP was classified in subgroup with Chinese mitten crab (*E. sinensis*).

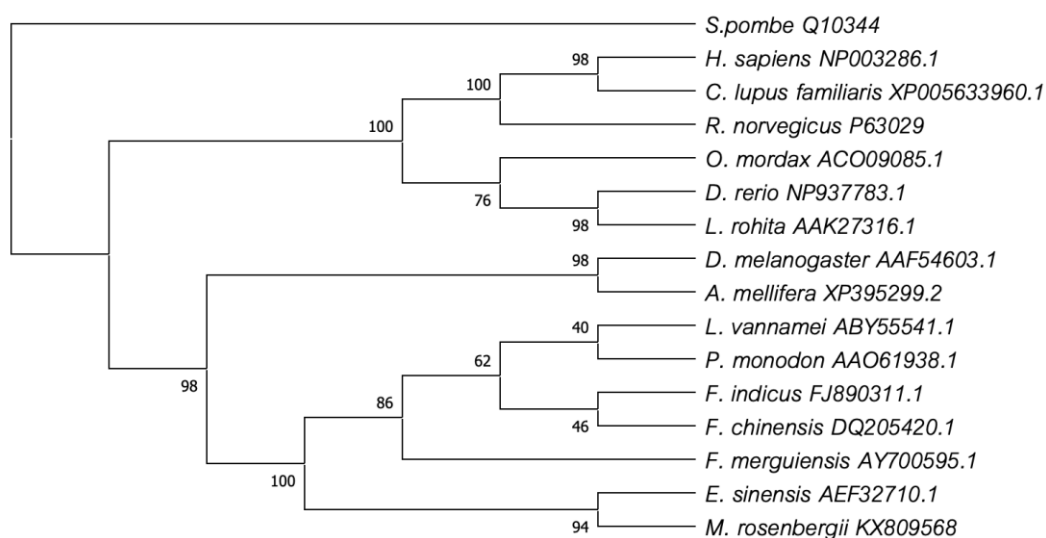


Figure 30 Phylogenetic relationship analysis of MrTCTP

The tree was constructed by the MEGA X program using maximum likelihood algorithm with 200 replicates of bootstrap analysis. The taxon name demonstrates organisms and GenBank accession number. Number on each branch represents bootstrap statistic.

1.6 Tissue distribution analysis of *MrTCTP*

The expression profile analysis of *MrTCTP* was performed using semi quantitative RT-PCR and *beta-actin* as an internal control gene. The results indicated that the *MrTCTP* expressed in every tissue examined including gill, hepatopancreas, heart, hemocyte, muscle, stomach, and intestine (Figure 31B). The predominant expression of *MrTCTP* transcript was found in hepatopancreas and muscle, while the expression was in the similar level in the other tissues (Figure 31A).

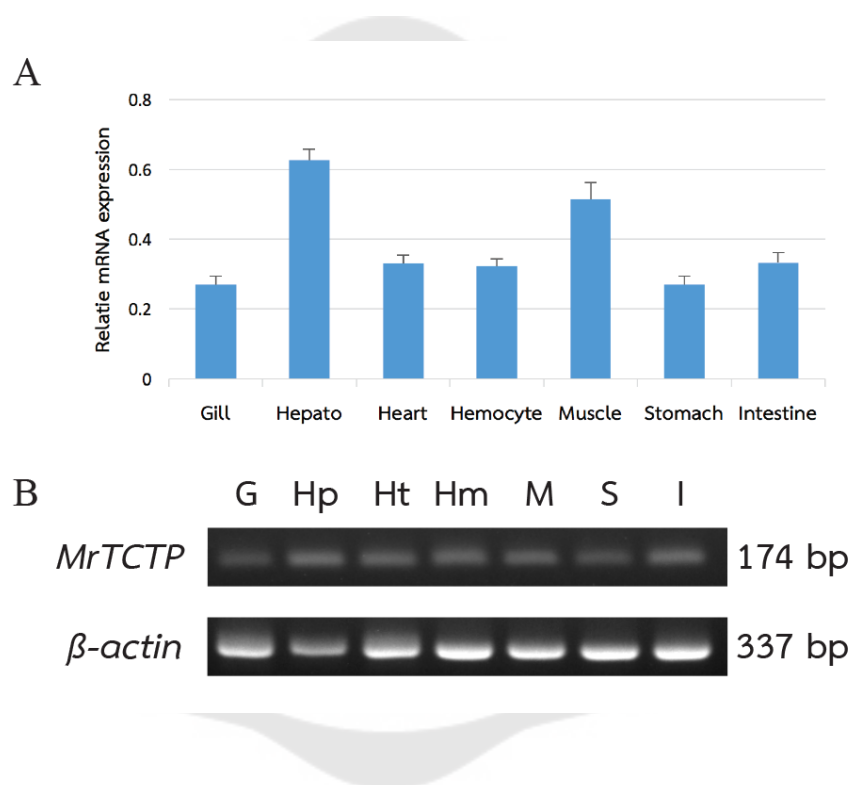


Figure 31 Tissue distribution analysis of *MrTCTP*

A) Relative expression of *MrTCTP* in various tissue determined by semi-quantitative RT-PCR. B) Expression profile of *MrTCTP* in various tissues using *beta-actin* as a reference gene. Total RNA was extracted from gill (G), hepatopancreas (Hp), heart (Ht), hemocyte (Hm), muscle (M), stomach (S), and intestine (I).

2. Response of *MrTCTP* after *MrNV* challenge

2.1 Preparation and RT-PCR for the detection of *MrNV*

For the preparation of *MrNV*-infected PL, the PL were used for the propagation of *MrNV* by the immersion method. The viral nucleic acid were extracted from the infected PL and then used in the RT-PCR for the detection of *MrNV*. The PCR reaction yielded a product of 729 bp which was an expected size (Figure 32A). The product was then cloned into pCR™2.1-TOPO® vector for sequencing (Figure 32B). The sequencing result showed that the PCR product has 99 % identity to the partial of *MrNV* segment RNA-1 under the accession number JQ418295.1 (Figure 32C).

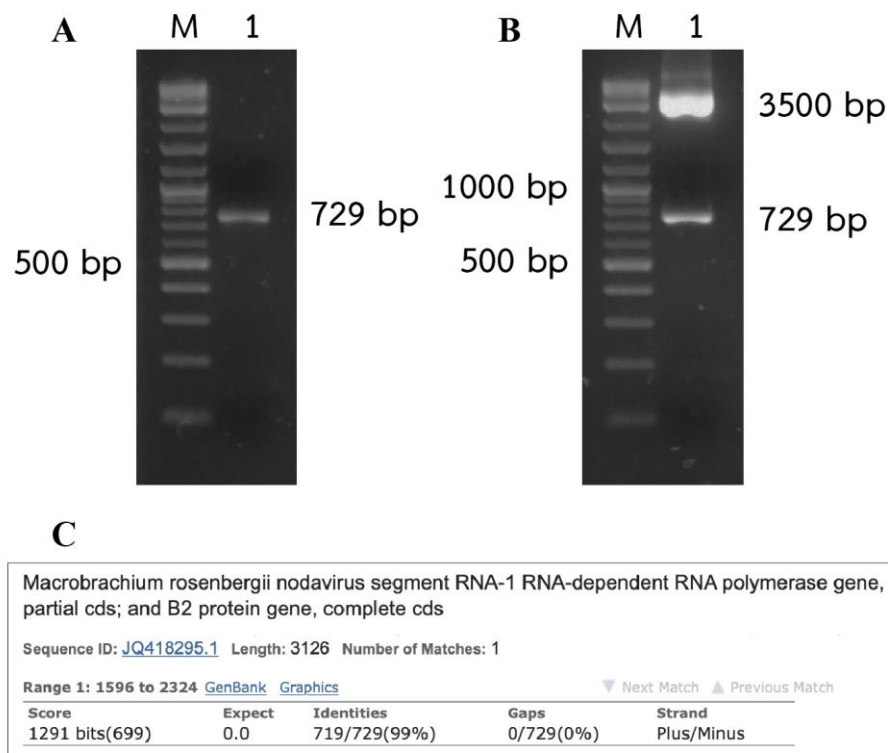


Figure 32 Cloning of *MrNV*729PCR products

- (A) Lane 1 is PCR product *MrNV*729 with 729 bp in size.
- (B) Lane 1 is recombinant plasmid after the *Eco*RI digestion which consists of *MrNV*729 (729 bp) and pCR™2.1-TOPO® (3.5 kb). M is DNA marker (2-log DNA ladder).
- (C) The results of pairwise alignment of *MrNV*729 using BLASTn.

2.2 Expression analysis of *MrTCTP* after *MrNV* challenge

To study the role of *MrTCTP* against the viral infection, time-course expression of *MrTCTP* in muscle samples after the injection of *MrNV* was determined. The prawn were injected with *MrNV* inoculum followed by time-course sampling in every 24 hours for the expression of *MrTCTP* and detection of *MrNV* (Figure 34A). The expression of *MrTCTP* was normalized using *beta-actin* as an internal control. The relative expressions of *MrTCTP* were then subtracted using means of relative expression of day 0 to obtain the basal expression (Figure 34B). The results demonstrated that *MrTCTP* expressions were significantly up-regulated at days 1 to 4 ranging from 1.3 to 2.2 fold after *MrNV* challenge and returned to basal level after 5 days of injection. In addition, *MrTCTP* expressions of the control group remained at basal level throughout the experiment. The infections of *MrNV* were also confirmed by RT-PCR using extracted viral nucleic acid from pleopod samples as shown in Figure 33 as the representative gel.

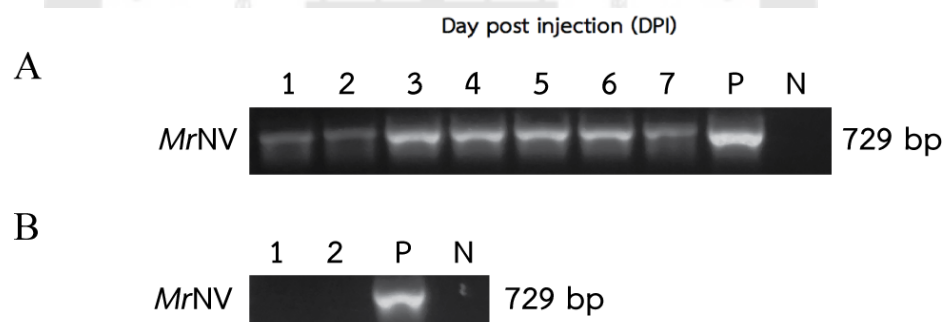


Figure 33 The RT-PCR detection of *MrNV* in immune challenge experiment

A) Confirmation of *MrNV* infection using RT-PCR and pleopod samples. Numbers indicate day after the injection of *MrNV*. The P and N letters indicate positive and negative control, respectively. B) The detection of *MrNV* in normal prawn using RT-PCR and pleopod samples. Numbers indicate random sampling

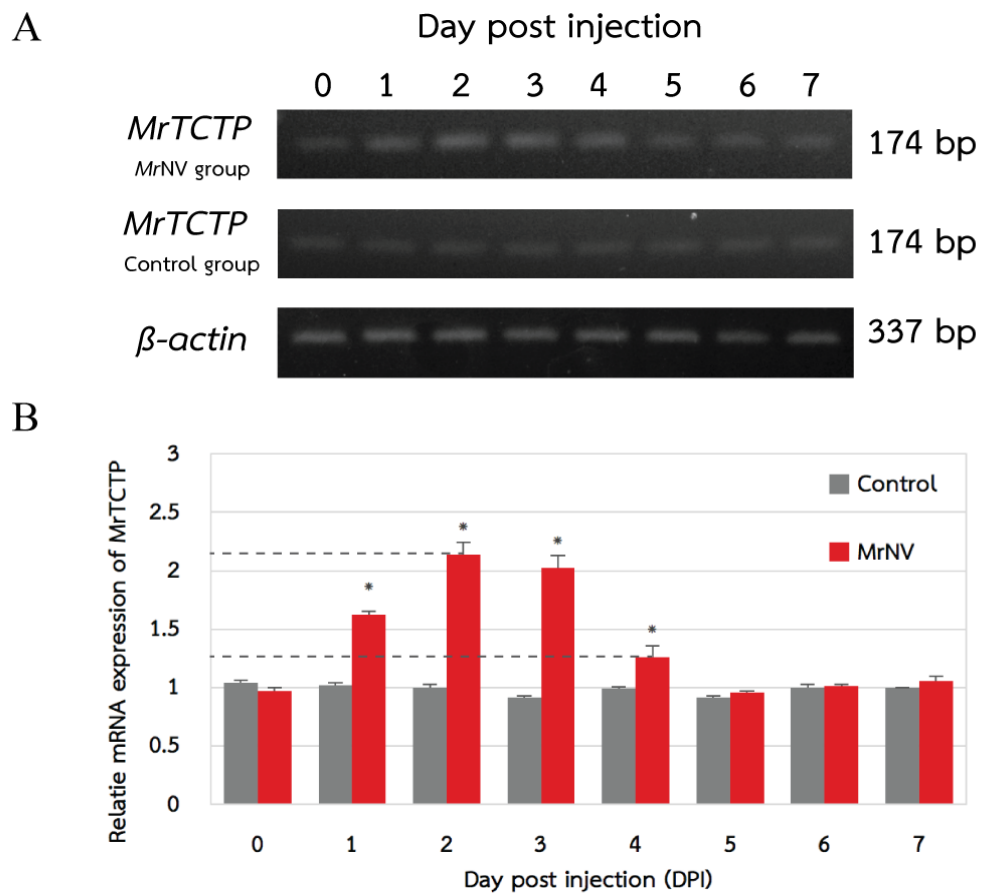


Figure 34 Expression of *MrTCTP* after *MrNV* challenge

A) Time-course expression of *MrTCTP* in muscle samples after the injection of *MrNV* using semi-quantitative RT-PCR. The *beta-actin* in this figure is the representative of an internal control. B) Relative expression of *MrTCTP* between *MrNV* group and TN buffer control group in each time point. Asterisks indicate statistical difference between *MrNV* and TN group ($p < 0.05$).

3. RNA interference experiment

3.1 Construction of DNA template for *in vitro* transcription

To construct DNA template for *in vitro* transcription, four oligonucleotide primers including the two with T7 promoter at the 5'-end were used. The PCR reactions of both sense and antisense template yielded products of 334 bp which were expected size as well as in the IMNV control (Figure 35). All of the products were excised from the gel and extracted for further *in vitro* transcription and dsRNA purification.

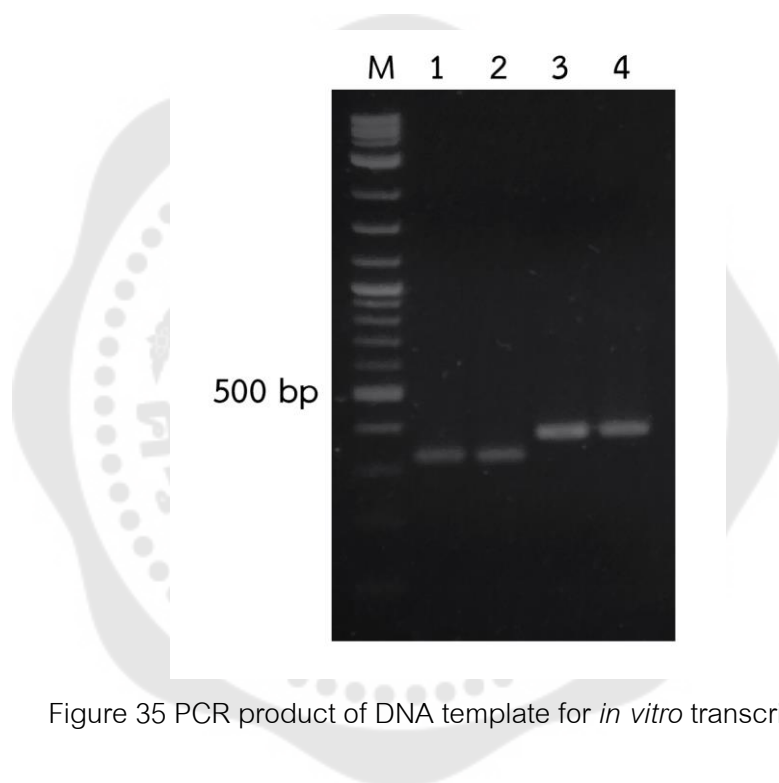


Figure 35 PCR product of DNA template for *in vitro* transcription

Lane 1 is sense strand of dsTCTP DNA template.

Lane 2 is antisense strand of dsTCTP DNA template.

Lane 3 is sense strand of dsIMNV DNA template.

Lane 4 is antisense strand of dsIMNV DNA template.

M is DNA marker (2-log DNA ladder).

3.2 Validation of dsRNA

The purified dsRNA were validated using three nuclease digestions using DNase I, RNase A, and RNase III which digest DNA, ssRNA, and dsRNA, respectively. The results demonstrated that the purified dsRNA in both dsTCTP and dsIMNV were completely digested by RNase III and were intact after DNase I, and RNase A digestion (Figure 36). The results suggested that the purified dsRNA had neither DNA nor single-stranded RNA contamination. The validated dsRNA were then used for the further knockdown experiment.

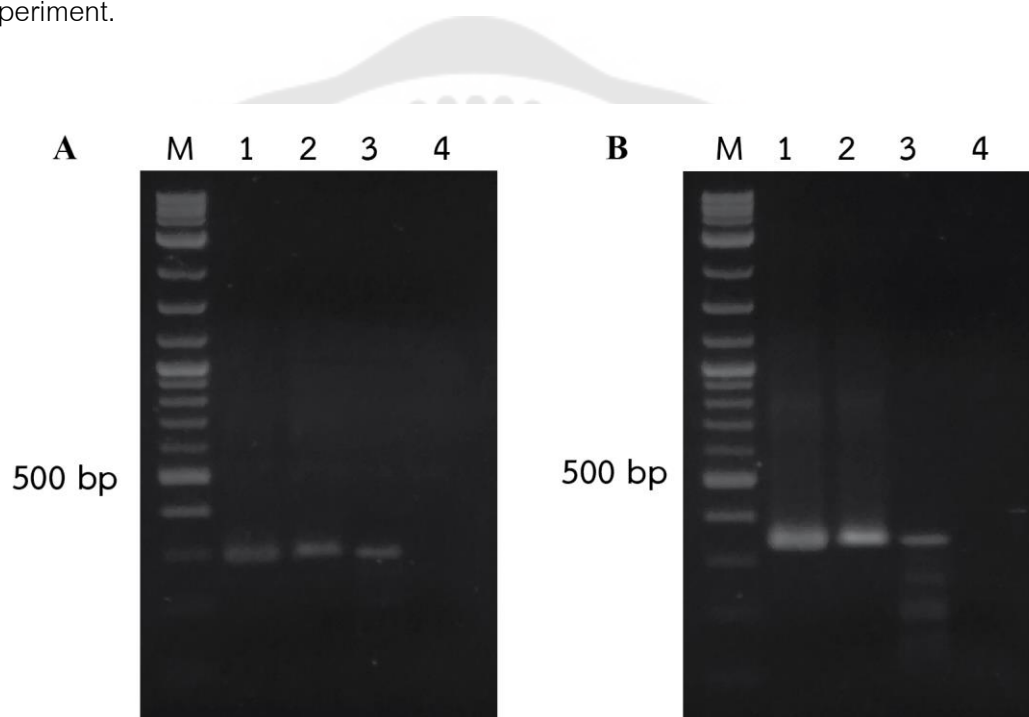


Figure 36 Validation of dsRNA using three different nucleases

A) Validation of dsTCTP. B) Validation of dsIMNV. Lane 1 are 1 µg of dsRNA. Lane 2 to 4 are different nuclease digestions including DNase I, RNase A, RNase III digestion, respectively. M is DNA marker (2-log DNA ladder).

3.3 *In vivo* knockdown of *MrTCTP* using dsRNA-mediated RNA interference

To knockdown the expression of *MrTCTP*, the prawn were injected intramuscularly with 5 µg of *MrTCTP* dsRNA (dsTCTP) dissolved in 50 µL of 2X PBS. The control experiments were 5 µg of dsIMNV and 2X PBS injection as exogenous gene control and negative control, respectively. The expression of *MrTCTP* was determined by RT-PCR using extracted RNA from muscle samples. The results demonstrated that *MrTCTP* expression was drastically decreased after 4 days of the injection of dsTCTP. There was no effect on *MrTCTP* expression after the injection of dsIMNV and 2X PBS (Figure 37). Therefore, day 4 post-injection of dsRNA was considered as the day in which *MrTCTP* is completely knockdown

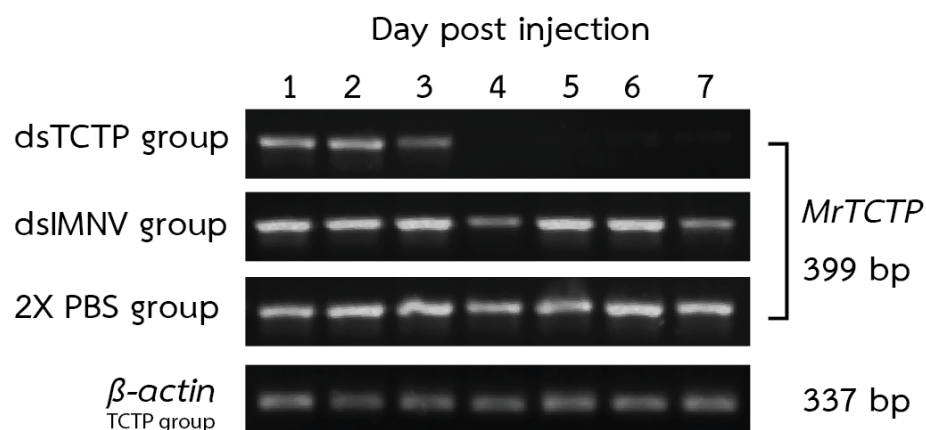


Figure 37 Expression of *MrTCTP* after *in vivo* knockdown

The expression of *MrTCTP* was determined by RT-PCR and 50 ng of extracted total RNA from muscle samples. Numbers indicate day after the injection of dsRNA. The dsIMNV and 2X PBS were used as exogenous gene control and negative control experiment, respectively. The *beta-actin* is the representative of an internal control.

3.4 Cumulative mortalities of *MrTCTP*-knockdown prawn after the viral injection

To further investigate the role *MrTCTP* in innate immune system against *MrNV* infection, the prawn were knock-downed the expression of *MrTCTP*. At day 4 post-injection of dsRNA, the prawn were then injected with *MrNV* inoculum. Time-course mortality rates were observed every 24 hours after the injection of *MrNV*.

The cumulative mortality results revealed that *MrTCTP*-knockdown prawns with *MrNV* infection showed 57% mortality rate within 10 days-post infection. Both of the control groups exhibited lower mortality rates of 30% (Figure 39A). According to post-hoc Tukey HSD analysis, there were significant differences between dsTCTP-*MrNV* group and both of the control groups since day 5 post infection (Tukey HSD, $p < 0.05$). However, there was significant differences between dsTCTP-*MrNV* group and 2X PBS-*MrNV* group at 4 days post infection (Tukey HSD, $p < 0.05$). The moribund prawns were tested for the infection of *MrNV* by RT-PCR using pleopod samples. The results indicated that moribund prawns from *MrNV* injection experiment were infected with *MrNV* (Figure 38).

In case of the TN buffer control experiment, all of experimental groups including dsTCTP-TN, dsIMNV-TN and 2X PBS-TN demonstrated low cumulative mortalities at 10%, 6.67%, and 10%, respectively. In addition, there was no statistically difference between each group (ANOVA, $p > 0.05$) (Figure 39B).



Figure 38 The RT-PCR detection of *MrNV* in RNAi experiment

A) The detection of *MrNV* by RT-PCR using pleopod samples of normal prawns (Day 0)
 B) Confirmation of *MrNV* infection by RT-PCR using pleopod samples from moribund prawns. Numbers indicate each sample. The P and N letters indicate positive and negative control, respectively.

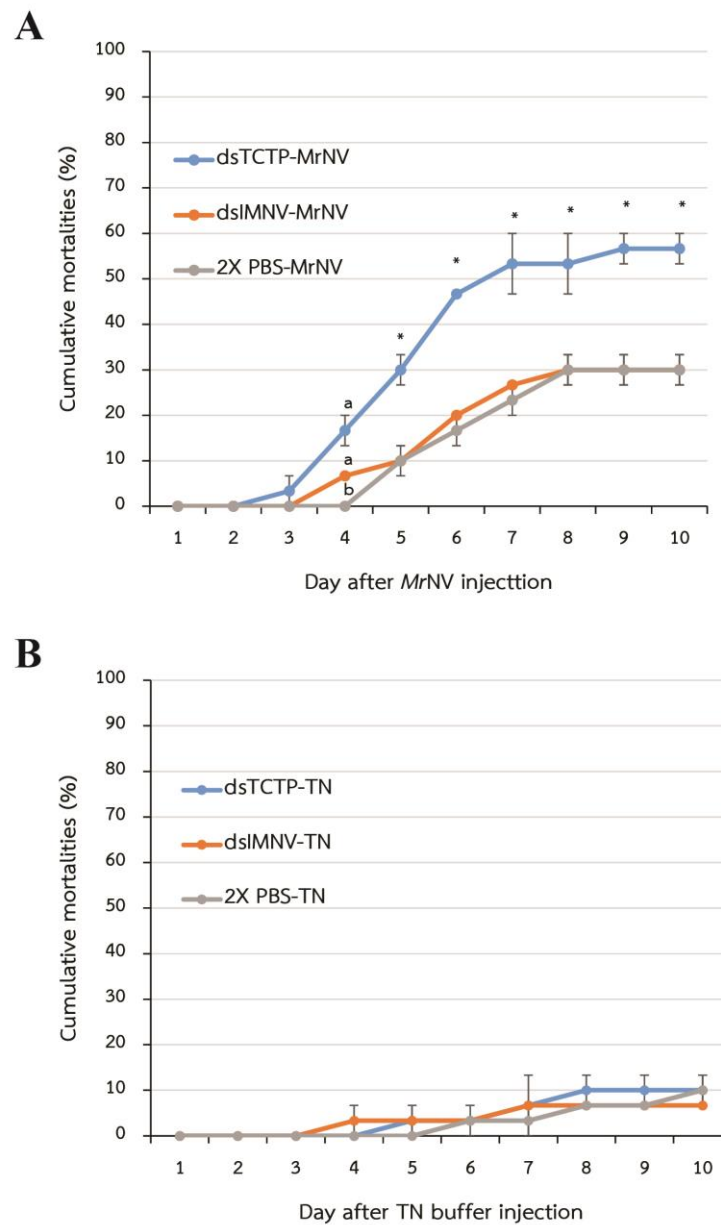


Figure 39 Cumulative mortalities of *MrTCTP*-silenced prawns after *MrNV* injection

A) Four days after the injection of dsTCTP, dsIMNV, and 2X PBS, prawns were intramuscularly injected with *MrNV* (n = 15). Mortality rates were observed for 10 days. B) Control groups were injected with TN buffer. The experiment was conducted in triplicates. The results were presented as mean of cumulative mortalities of three experiments \pm SD. Asterisks indicate difference among each experimental group using one-way ANOVA with post-hoc Tukey HSD ($p < 0.05$). The a and b letters indicate groups of means defined by post-hoc Tukey HSD.

4. Validation of the data analysis pipeline

To test validity of the pipeline, RNAseq sample data from *M. rosenbergii* in response to *V. parahaemolyticus* infection (Rao et al., 2015) were used. Total number of 54,708,014 and 54,295,342 from control and *Vibrio*-infected group were merged together and subjected to *de novo* assembly using Trinity software. In this study, the Trinity assembler produced 140,317 contigs which were then clustered into 104,514 unigenes (with N_{50} of 942 bp) by CD-HIT software. The assembled transcripts had 95.50% overall fragment mapping rate. Based on BUSCO, the assembled transcripts was highly complete with 74.4 % ortholog gene from Arthropoda database (C:74.4%[S:50.2%,D:24.2%],F:14.2%,M:11.4%,n:1066). The ExN50 plot showed that the peak of ExN50 value was on E80%. According to Rao and others, the Trinity assembler produced 95,645 and 123,141 contigs from control and *Vibrio*-infected groups, respectively (Rao et al., 2015). Both of the transcripts were then clustered together using TGICL software resulting in 64,411 unigenes (with N_{50} of 1,137 bp).

In this study, the unigenes were annotated using homology search by Blastx software against NCBI non-redundant Arthropods and UNIPROT database which produced 36,093 (45%), and 28,430 (27.2%) top hits. The top hit results from Blastx against UNIPROT database were then used to obtain KEGG, EggNOG, and GO annotation which produced 17,423 (16.6%), 17,464 (16.7%), and 20,631 (19.7%) hits, respectively. The annotation ratio were similar to those from Rao and others (Rao et al., 2015). According to differential expression analysis, total number of differentially expressed genes (DEG) were extremely different (1,803 with $FDR < 0.05$ compared to 14,569 with $FDR < 0.001$ from Rao and others). However, the DEGs from both analysis were compared using list of candidate genes that involved in *V. parahaemolyticus* infection provided by Rao and others (Rao et al., 2015). The results demonstrated that 58% were concurred with each other (46% with $FDR < 0.05$ and 12% with $FDR > 0.05$) whereas 9% were disagreed with each other (8% with $FDR < 0.05$ and 1% with $FDR > 0.05$). Total of 28% were reported non-DEG and 5% were unable to annotate using the pipeline (Figure 40). The summary

of the transcriptome assembly and post-processing comparisons are shown in Table 33 and the comparisons of DEG are demonstrated in Figure 40.

Table 33 Summary of the transcriptome assembly and post-processing comparisons between the results from the pipeline and from (Rao et al., 2015)

	Results from Rao and others		The pipeline
	Control	<i>Vibrio</i> -infected	
Total number of contigs	95,645	123,141	140,317
Total number of unigenes	59,050	73,946	104,514
		64,411	
NCBI Nr annotated	19,799 (30.73%)		36,093 (34.5%)
UNIPROT annotated	16,832 (26.13%)		28,430 (27.2%)
KEGG annotated	14,706 (22.83%)		17,423 (16.6%)
EggNOG annotated	7,856 (12.19%)		17,464 (16.7%)
GO annotated	6,007 (9.32%)		20,631 (19.7%)
Differentially expressed gene (total)	14,569 (FDR < 0.001)		1,803 (FDR < 0.05)
Up-regulated gene		11,446	1,124
Down-regulated gene		3,103	679

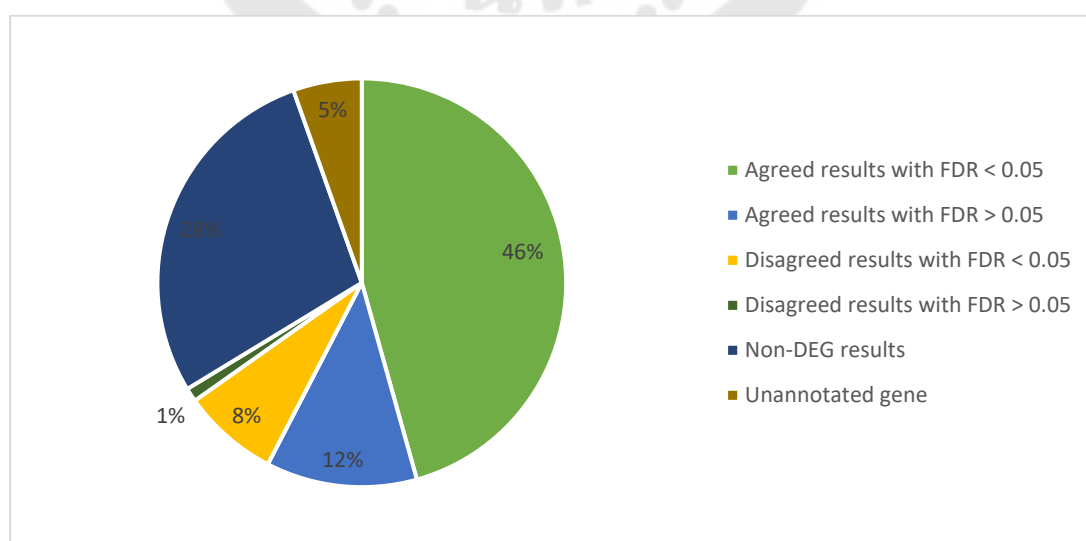


Figure 40 Summary of DEG comparisons between the results from the pipeline and (Rao et al., 2015)

5. Samples preparation, library preparation, and Illumina sequencing

5.1 Preparation of *MtNV* infected post-larvae prawn

All of PL samples including control and *MtNV* group were subjected to *MtNV* detection using RT-PCR. The viral nucleic acid were extracted from the PL and then used in the RT-PCR reaction. According to the RT-PCR results, the *MtNV* were negative in the control group (Figure 41A). Whereas, the PL in the *MtNV* group were infected with *MtNV* (Figure 41B).

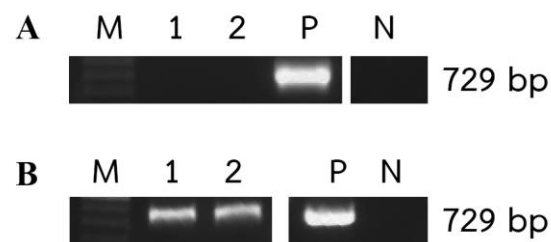


Figure 41 The RT-PCR detection of *MtNV* in NGS experiment

A) The detection of *MtNV* by RT-PCR using PL samples of the control group B) The detection of *MtNV* by RT-PCR using PL samples of the *MtNV* group. Numbers indicate each sampling. The P and N letters indicate positive and negative control, respectively.

5.2 Library preparation

After the library preparation, the prepared cDNA library was subjected to quality assessment before proceeding into denaturation and sequencing steps. The Qubit Fluorometer results showed that the concentrations of the library were ranging from 1.53 – 4.57 ng/ μ L. According to microfluidic nucleic acid analyzer, the average size were ranging from 339 – 379 bp as shown in Figure 42. The concentrations in nanomolar were calculated as demonstrated in Table 34.

Table 34 The library concentration and average size distribution

Library	Concentration (ng/uL)	Average size (bp)	Concentration (nM)*
Control 1	2.48	366	10.27
Control 2	2.22	357	9.42
Control 3	1.53	345	6.72
Control 4	2.06	339	9.21
Control 5	2.13	370	8.72
Control 6	1.92	337	8.63
Infected 1	2.79	358	11.81
Infected 2	3.87	365	16.06
Infected 3	3.61	360	15.19
Infected 4	3.05	344	13.43
Infected 5	3.57	379	14.27
Infected 6	4.57	352	19.67

*The concentrations (nM) were calculated by the following formula:

$$\text{Concentration (ng/uL)} \times 1,000,000 / \text{Average size (bp)} \times 660$$

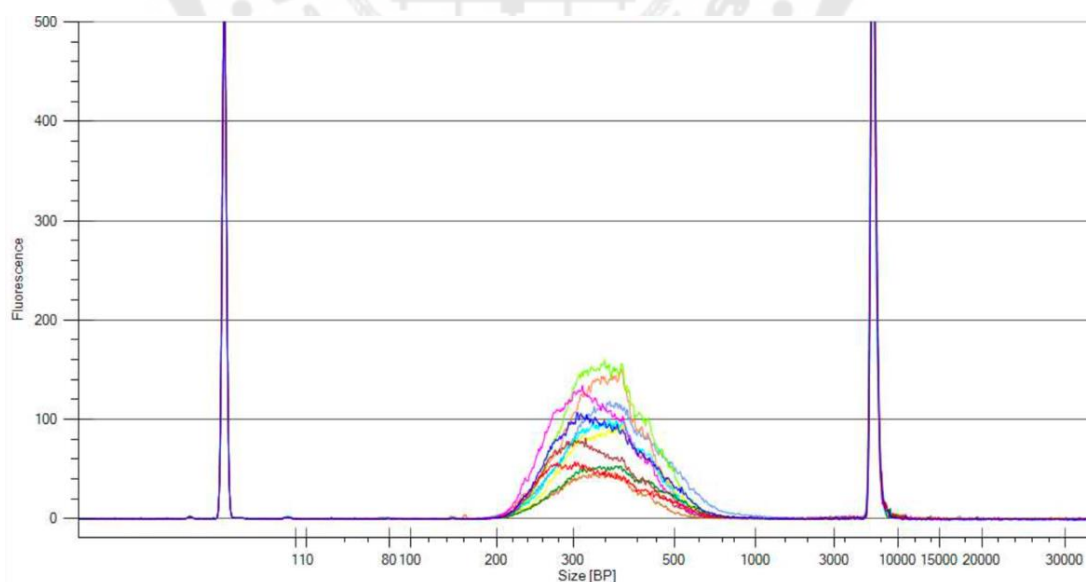


Figure 42 Electropherogram of the cDNA library

Each line represents each library. The first peak of the graph is lower marker, whereas the last peak of the graph is upper marker.

5.3 Library denaturation and sequencing

Prior to denaturation steps, the cDNA libraries (20 pmol each) were pooled together and then re-purified using magnetic beads. According to the quality assessment, the pooled library had the concentration of 2.01 ng/ μ L and the average size of 365 bp (Figure 43) which were calculated into 8.34 nM. After the denaturation steps, the denatured library was sequenced using NextSeq 550 sequencer.

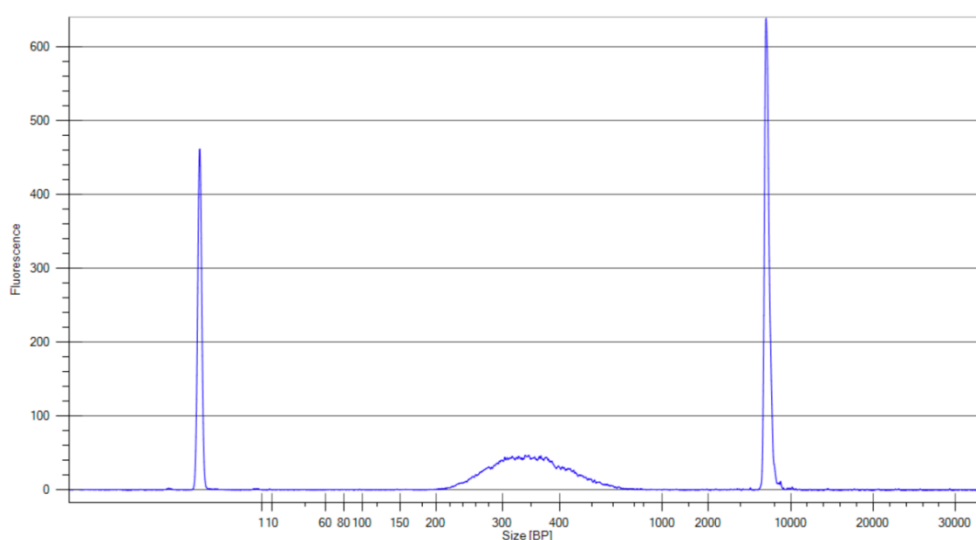


Figure 43 Electropherogram of the pooled cDNA library

The first peak of the graph is lower marker, whereas the last peak of the graph is upper marker. The average size of the pooled library was 365 bp.

Illumina RNA sequencing for two groups with six biological replicates ($n=12$) produced a total of 522,296,142 raw reads. The raw reads for each sample were ranging from 33,036,002 to 50,947,705 with an average of $43,524,769 \pm 5,068,124$ (mean \pm SD) (Table 35). According to reads quality assessment, the 75 bp raw reads had average Phred score of above 30 except the first nine bases of some of the reads which were then trimmed (Lexogen's recommendation). The last base of all reads are reported to be all guanine (data not shown). Therefore, the last base (75th base) of the both reads were also trimmed. After the quality trimming, the 65 bp trimmed reads had high average Phred score of above 30. The average Phred score of both raw and trimmed read are shown in Figure 44.

Table 35 Number of read pairs prior and after trimming

Sample	Raw paired-end reads	Trimmed paired-end reads
Control 1	46,497,004	44,697,960 (96.13 %)
Control 2	43,309,253	41,651,586 (96.17 %)
Control 3	40,571,354	38,896,140 (95.87 %)
Control 4	42,111,175	40,566,032 (96.33 %)
Control 5	47,098,377	45,404,272 (95.63 %)
Control 6	38,519,779	36,568,513 (94.93 %)
Infected 1	44,325,031	42,803,756 (96.57 %)
Infected 2	46,902,950	45,238,551 (96.45 %)
Infected 3	49,289,659	47,443,959 (96.26 %)
Infected 4	39,687,853	38,299,205 (96.50 %)
Infected 5	33,036,002	31,758,938 (96.13 %)
Infected 6	50,947,705	48,935,511 (96.05 %)



Figure 44 Average Phred score of both raw and trimmed read

Each line represents each read data. A) The average Phred score of the 75 bp raw reads. B) The average Phred score of the 65 bp trimmed reads.

6. *De novo* transcriptome assembly and annotation

Total of 501,900,423 (96.09 %) of the reads survived quality trimming. The trimmed reads were subjected to *de novo* transcriptome assembly using Trinity. The trimmed reads were further reduced into 51,971,920 reads (10.36 %) during *in silico* normalization prior to *de novo* assembly. The Trinity assembler produced 109,616 contigs with N_{50} of 1,522 bp, and mean length of 848.71 bp. Using 95 % similarity threshold, CD-HIT software clustered the contigs into 96,362 unigenes with N_{50} of 1,308 bp, and mean length of 776.73 bp. Bowtie2 aligner showed that the assembled transcripts had 96.85 % overall fragment mapping rate with 90.08 % that aligned concordantly ≥ 1 times (Figure 45A). Based on BUSCO, the assembled transcripts was highly complete with 889 (83.4 %) ortholog gene from Arthropoda database ($n = 1066$). Of those, total of 716 (67.2 %) were single-copy whereas 173 (16.2 %) were duplicated BUSCOs. In addition, only 142 (13.3 %) were fragmented and 35 (3.3 %) were missing BUSCOs (C:83.4%[S:67.2%,D:16.2%],F:13.3%, M:3.3%,n:1066). The ExN50 plot showed that the peak of ExN50 value was on E94% (Figure 45B). The summary of the transcriptome assembly and quality assessment are shown in Table 36.

Table 36 Summary of the transcriptome assembly and quality assessment

	Prior to <i>de novo</i> assembly
Length of raw reads (bp)	75
Total number of raw reads	522,296,142
Length of trimmed reads (bp)	65
Total number of trimmed reads	501,900,423 (96.09 %)
Total number of normalized reads	51,971,920 (10.36%)
	After <i>de novo</i> assembly
Total number of contigs	109,616
Total number of unigenes	96,362
Mean length of unigenes (bp)	776.73

Table 36 (Continued)

N50 length of unigenes (bp)	1,308
Highest ExN50 value (% Ex)	94
Fragment mapping rate (%)	96.85 %
BUSCO completeness (%)	83.4 %

A

```

501900423 reads; of these:
501900423 (100.00%) were paired; of these:
49819431 (9.93%) aligned concordantly 0 times
261683491 (52.14%) aligned concordantly exactly 1 time
190397501 (37.94%) aligned concordantly >1 times
-----
49819431 pairs aligned concordantly 0 times; of these:
7342288 (14.74%) aligned discordantly 1 time
-----
42477143 pairs aligned 0 times concordantly or discordantly; of these:
84954286 mates make up the pairs; of these:
31651457 (37.26%) aligned 0 times
10110360 (22.49%) aligned exactly 1 time
34192469 (40.25%) aligned >1 times
96.85% overall alignment rate

```

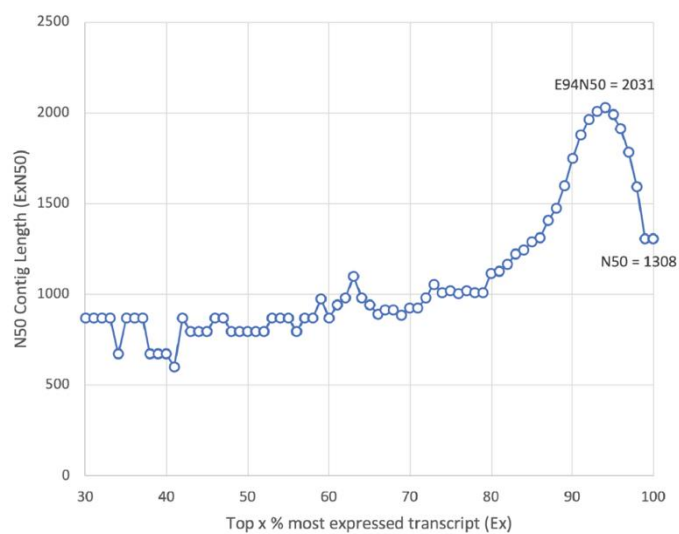
B

Figure 45 Transcriptome quality assessment results

- A) Bowtie2 alignment results using trimmed reads and transcriptome as reference.
- B) ExN50 statistics of the transcriptome with N_{50} of 1,308 bp and ExN50 peak at 94 % with 2,031 bp N_{50} length.

The assembled transcripts were subjected to the homology search by Blastx software using UniProt and non-redundant arthropod database. Blastx search against UniProt database yielded 25,761 (26.73 %) significant hits (E -value $< 1-e5$). Top-hit species distribution results demonstrated that majority of top-hit species were *Homo sapiens* with 5,587 (21.7 %) hits followed by *Mus musculus* and *Drosophila melanogaster* with 4,234 (16.4 %) and 4,043 (15.7 %) hits, respectively (Figure 46A). In case of non-redundant arthropod database, Blastx search yielded 32,523 (33.75 %) significant hits (E -value $< 1-e5$). Top-hit species distribution was mainly dominated by *Hyalomma azteca* with 11,197 (34.4 %) hits followed by *Cryptotermes secundus* with 1,841 (5.6 %) hits (Figure 46B). Shrimp species including *L. vannamei*, *M. nipponense*, *M. rosenbergii*, *P. monodon*, and *M. japonicus* were the eighth, eleventh, thirteenth, seventeenth, and eighteenth top-hits, respectively, as demonstrated in top-hit crustaceans species distribution (Figure 46C).

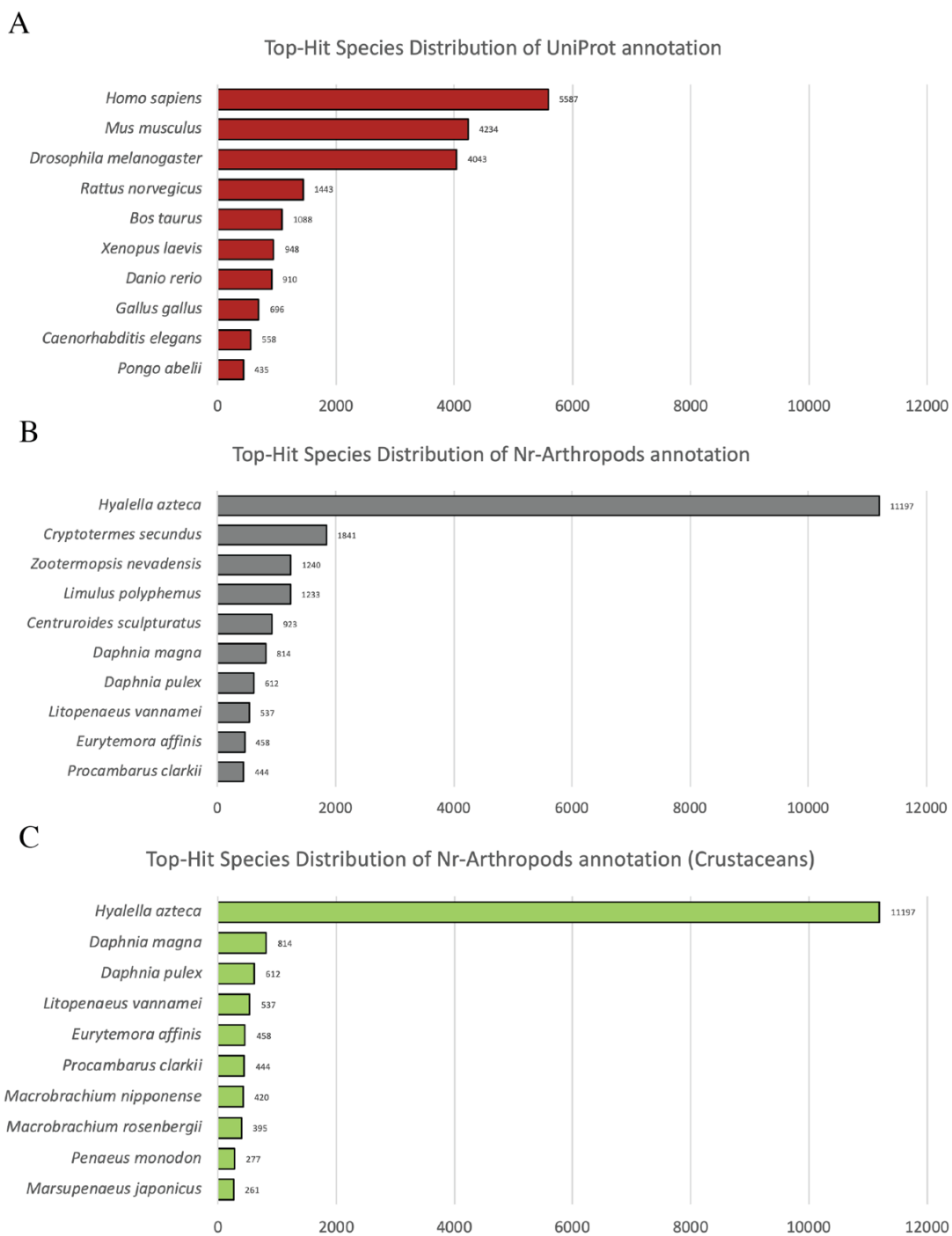


Figure 46 Top 10 species distribution of Blastx results from different databases

A) UniProt database B) Non-redundant arthropod database C) Non-redundant arthropod database with only crustacean species.

Functional annotations including EggNOG, KEGG, and GO were obtained from Blastx UniProt results using Trinotate suite. Total of 18,291 unigenes (18.98 % from total unigenes and 71 % from UniProt annotated) were GO mapped. Total of 187,582 GO assignments (level 2) were generated from GO annotations and divided into three GO domains including cellular component (75,535 or 40.27 %), molecular function (25,373 or 13.51 %), and biological process (86,674 or 46.20 %) (Figure 47). Among cellular component domain, annotated unigenes were mostly involved in “cell” (14,523) and “cell part” (14,499) followed by “organelle” (11,625). Molecular function domain was primarily dominated by “binding” (12,177) and “catalytic activity” (7,378). In biological process domain, annotated unigenes were mostly involved in “cellular process” (13,234) followed by “metabolic process” (10,855) (Figure 47).

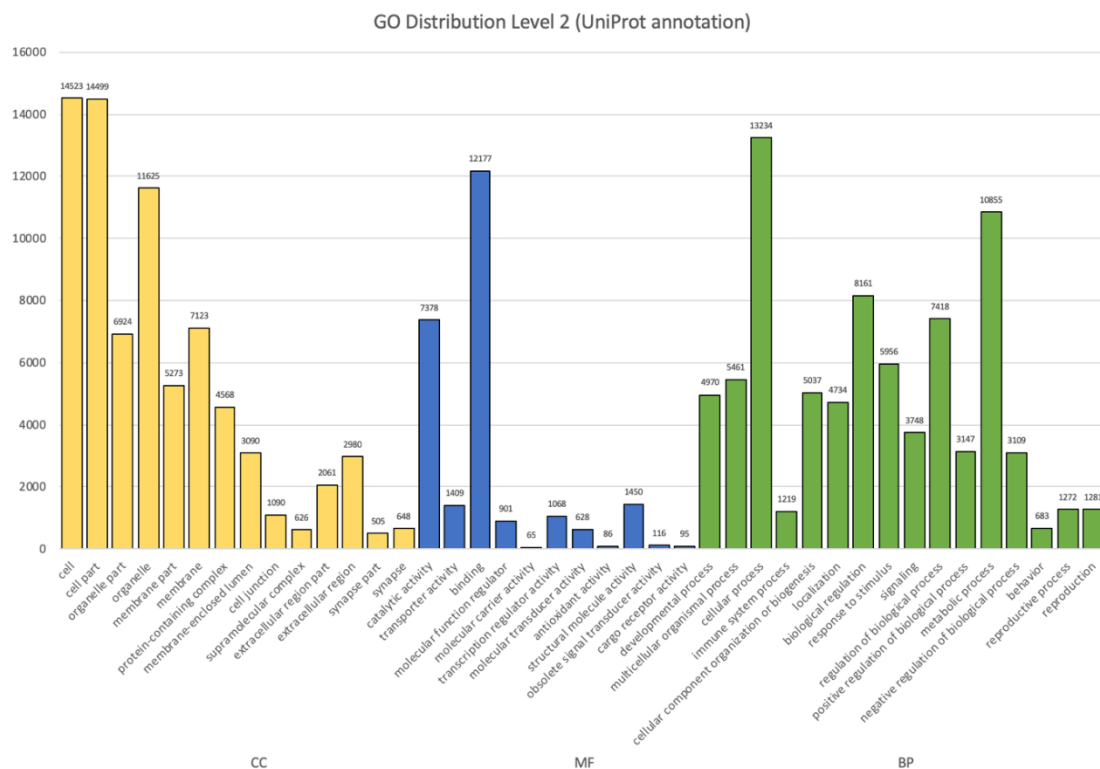


Figure 47 GO distribution (level 2) of annotated unigenes based on UniProt database GO assignments were divided into three categories including cellular process (CC, yellow), molecular function (MF, blue), and biological process (BP, green).

EggNOG classification showed that 20,130 unigenes (20.88 % from total unigenes and 78.14 % from UniProt annotated) were identified in the EggNOG database. Total of 20,704 EggNOG functional annotations were obtained and classified into 23 categories (Figure 48). The most abundance category was “Function unknown” (9,054 or 43.73 %) The second most abundance was “Post-translational modification, protein turnover, chaperones” (2,000 or 9.66 %) followed by “Intracellular trafficking, secretion, and vesicular transport” (1,614 or 7.79 %), and “Signal transduction mechanisms” (1,302 or 6.29 %), respectively. The least abundance category was “Nuclear structure” (2 or 0.01 %) followed by “Cell motility” (4 or 0.02 %) (Figure 48).

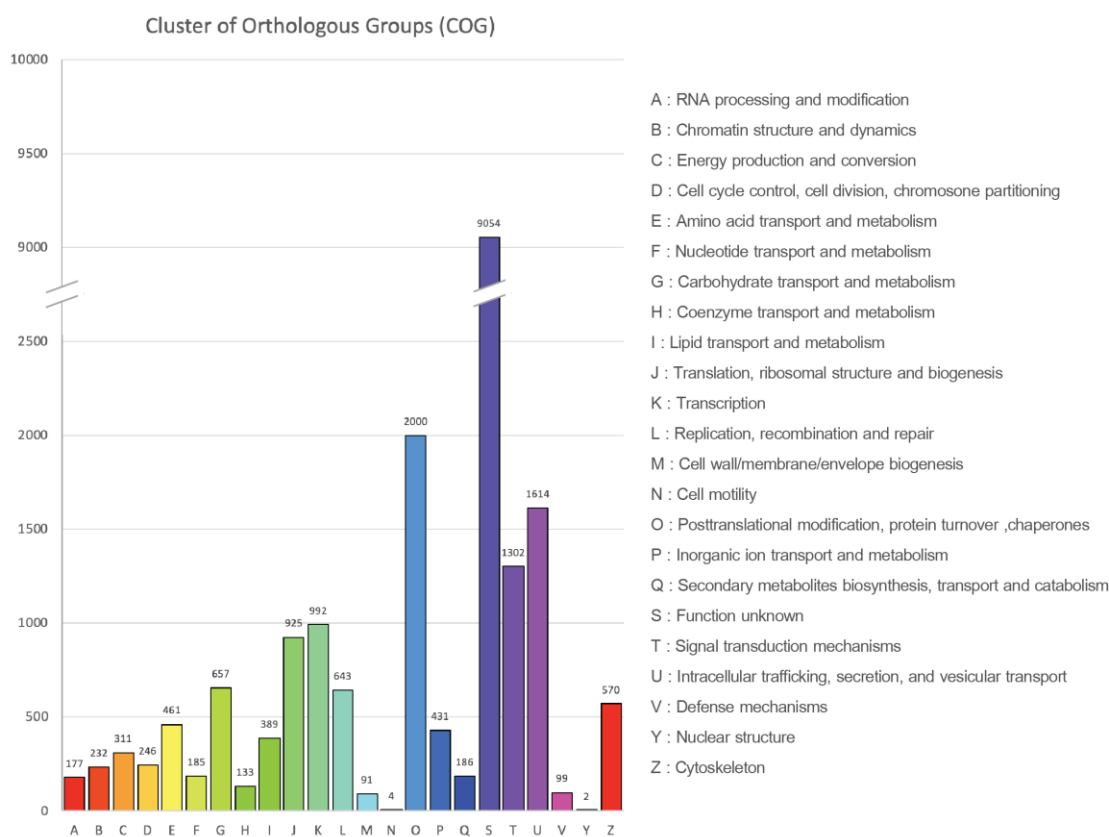


Figure 48 EggNOG classifications of annotated unigenes based on UniProt database

EggNOG functional annotations were divided into 23 categories. The EggNOG categories are shown on the horizontal axis as alphabets with category names on the right.

Total of 19,715 unigenes (20.46% from total unigenes and 76.53 % from UniProt annotated) were matched to the KEGG database. Of those, 7,917 unigenes had orthologs in the KEGG orthology database. Total of 14,289 KEGG orthology (KO) were obtained from those unigenes and then categorized into five major categories including “Metabolism” (3,171 or 22.19 %), “Genetic information processing” (2,351 or 16.45 %), “Environmental information processing” (3,203 or 22.42 %), “Cellular processes” (1,522 or 10.65 %), and “Organismal systems” (4,042 or 28.29 %) (Figure 49). KO distribution results showed that the most abundance orthology was signal transduction from “Environmental information processing” category with 1,779 unigenes. The second most abundance was translation from “Genetic information processing” category (1,078 unigenes) followed by transport and catabolism from “Environmental information processing” category (1,055 unigenes), respectively (Figure 49).

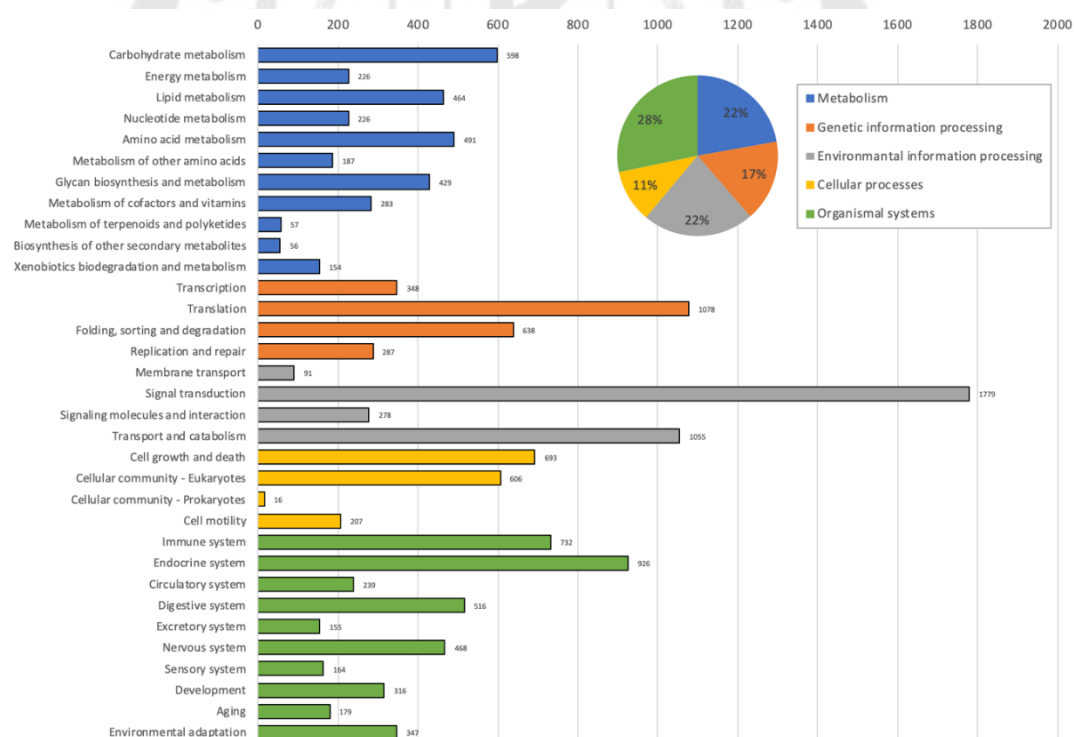


Figure 499 KEGG orthology of annotated unigenes based on UniProt database

KEGG orthology were categorized into five major categories. The names and distribution ratios of each category are shown in pie chart at the top right corner.

7. Differential expression analysis

To identify differentially expressed transcripts between two groups, transcripts that had count per millions (CPM) less than 1 in at least two samples were filtered out before the analysis. Total of 31,377 transcripts survived the cut-off and were subjected to TMM normalization. The differential expression analysis using EdgeR was performed followed by Benjamini-Hochberg method for multiple p -value correction. Total of 5,538 transcripts were reported to be differentially expressed (FDR < 0.05, LogFC < ± 1). Of those, 2,413 transcripts were significantly up-regulated and 3,125 transcripts were significantly down-regulated after the infection of *MrNV*. Summary of the transcriptome assembly, annotation and differential expression analysis were listed in Table 37.

Table 37 Summary of the transcriptome assembly, annotation and differential expression analysis

Total number of contigs	109,616
Total number of unigenes	96,362
NCBI Nr annotated	32,523 (33.75 %)
UniProt annotated	25,761 (26.73%)
GO annotated	18,291 (18.98%)
EggNOG annotated	20,130 (20.88%)
KEGG annotated	19,715 (20.46%)
Differentially expressed gene (total)	5,538 (FDR < 0.05, LogFC < ± 1)
Up-regulated gene	2,413
Down-regulated gene	3,125

Among those differentially expressed transcripts, various transcripts were reported to be involved in immune system regarding viral infection. These transcripts were categorized into 13 functional groups including antiviral protein (1 unigene), antimicrobial protein (9 unigenes), pattern recognition proteins (19 unigenes), toll-signaling pathway (3 unigenes), RNAi pathway (2 unigenes), prophenol oxidase system (4 unigenes), serine proteinase cascade (5 unigenes), ubiquitin proteasome pathway (4 unigenes), antioxidant

system (5 unigenes), blood coagulation (2 unigenes), apoptosis (3 unigenes), phagocytosis (7 unigenes), and other immune genes (10 unigenes) as listed in Table 38. From the list, total of 56 unigenes were reported to be significantly up-regulated, whereas 18 unigenes were significantly down-regulated.

Table 38 List of DEG transcripts involved in immune system

Unigene	Functional annotation	Organisms	FC
Antiviral protein			
DN14192_c1_g1_i2	antiviral protein	<i>Litopenaeus vannamei</i>	2.48
Antimicrobial protein			
DN46855_c0_g1_i1	anti-lipopolysaccharide factor	<i>Macrobrachium rosenbergii</i>	2.25
DN3291_c0_g1_i1	anti-lipopolysaccharide factor 1	<i>Macrobrachium rosenbergii</i>	2.73
DN34234_c0_g1_i1	anti-lipopolysaccharide factor 3	<i>Macrobrachium rosenbergii</i>	4.20
DN9599_c0_g1_i3	crustin 7, partial	<i>Macrobrachium rosenbergii</i>	6.59
DN584_c0_g1_i2	crustin 6, partial	<i>Macrobrachium rosenbergii</i>	3.48
DN2919_c0_g1_i1	crustin 5	<i>Macrobrachium rosenbergii</i>	3.05
DN13113_c0_g1_i1	i-type lysozyme-like protein 2	<i>Penaeus monodon</i>	-2.45
DN5315_c0_g1_i1	crustin A	<i>Litopenaeus vannamei</i>	-8.94
DN25544_c0_g1_i1	crustin 4	<i>Panulirus japonicus</i>	-2.25
Pattern recognition proteins (PRPs)			
DN27838_c0_g1_i1	C-type lectin	<i>Procambarus clarkii</i>	3.29
DN3149_c0_g1_i3	C-type lectin 1	<i>Palaemon modestus</i>	3.46
DN25495_c0_g1_i4	C-type lectin 2	<i>Marsupenaeus japonicus</i>	4.32
DN39427_c0_g1_i1	C-type lectin 4	<i>Fenneropenaeus merguensis</i>	-2.91
DN8487_c0_g1_i1	C-type lectin H	<i>Eriocheir sinensis</i>	-3.05
DN79_c0_g1_i9	C-type lectin-like domain-containing protein	<i>Portunus trituberculatus</i>	2.58
PtLP			
DN9664_c0_g1_i1	C-type lectin-like protein	<i>Fenneropenaeus chinensis</i>	-4.08
DN1597_c0_g1_i2	down syndrome cell adhesion molecule	<i>Cherax quadricarinatus</i>	-2.03
DN1969_c0_g1_i2	ficolin	<i>Macrobrachium nipponense</i>	2.55
DN458_c0_g1_i6	ficolin-like protein 2	<i>Pacifastacus leniusculus</i>	3.32
DN2732_c0_g1_i1	lectin	<i>Macrobrachium rosenbergii</i>	2.41
DN22168_c0_g1_i1	lectin 1	<i>Macrobrachium rosenbergii</i>	2.36
DN1016_c0_g1_i2	lectin 2	<i>Macrobrachium rosenbergii</i>	3.56
DN2249_c0_g1_i2	lectin 3	<i>Macrobrachium rosenbergii</i>	2.28

Table 38 (Continued)

DN248_c1_g1_i2	lectin B isoform 2, partial	<i>Marsupenaeus japonicus</i>	2.13
DN59056_c0_g1_i1	lectin D, partial	<i>Marsupenaeus japonicus</i>	2.45
DN11184_c0_g1_i1	lectin E	<i>Marsupenaeus japonicus</i>	2.68
DN15806_c0_g1_i1	mannose-binding protein	<i>Procambarus clarkii</i>	-6.02
DN51_c0_g1_i3	tachylectin	<i>Macrobrachium rosenbergii</i>	2.17
	Toll-signaling pathway		
DN1501_c0_g4_i1	spatzle protein, partial	<i>Fenneropenaeus chinensis</i>	-17.88
DN6896_c0_g2_i1	toll-receptor 9	<i>Penaeus monodon</i>	3.81
DN48150_c0_g1_i1	Nuclear factor NF-kappa-B p110 subunit	<i>Nicrophorus vespilloides</i>	4.69
	RNAi pathway		
DN14942_c0_g1_i2	dicer-2	<i>Macrobrachium rosenbergii</i>	3.66
DN13890_c0_g1_i2	argonaute-3	<i>Macrobrachium rosenbergii</i>	2.16
	Prophenol oxidase system (ProPO)		
DN24054_c0_g1_i2	prophenoloxidase, partial	<i>Macrobrachium rosenbergii</i>	2.01
DN9200_c0_g1_i1	prophenoloxidase-activating enzyme 2a	<i>Penaeus monodon</i>	2.99
DN27498_c0_g1_i2	prophenoloxidase activating factor 1	<i>Scylla paramamosain</i>	2.31
DN6266_c0_g1_i1	prophenoloxidase activating enzyme III	<i>Macrobrachium rosenbergii</i>	2.23
	Serine proteinase cascade		
DN449_c1_g1_i1	serine proteinase	<i>Scylla paramamosain</i>	2.51
DN11492_c0_g1_i8	serine proteinase stubble	<i>Lucilia cuprina</i>	-6.73
DN833_c0_g1_i2	serine proteinase inhibitor 6	<i>Penaeus monodon</i>	-2.48
DN2466_c0_g1_i2	alpha-2-macroglobulin	<i>Macrobrachium rosenbergii</i>	-2.68
DN17466_c0_g1_i2	pacifastin heavy chain	<i>Macrobrachium rosenbergii</i>	2.14
	Ubiquitin proteasome pathway		
DN49814_c0_g5_i1	E3 ubiquitin-protein ligase Ubr3	<i>Copidosoma floridanum</i>	2.22
DN8249_c1_g1_i1	E3 ubiquitin-protein ligase RNF216-like, partial	<i>Hyalella azteca</i>	3.89
DN10760_c0_g1_i3	ubiquitin	<i>Papilio xuthus</i>	-4.89
DN1685_c0_g1_i9	RING finger protein nhl-1-like	<i>Limulus polyphemus</i>	3.63
	Antioxidant system		
DN6006_c0_g2_i1	Microsomal glutathione S-transferase 1	<i>Penaeus monodon</i>	2.01
DN19734_c0_g1_i1	glutathione peroxidase 3	<i>Penaeus monodon</i>	4.08
DN8125_c0_g1_i2	selenium independent glutathione peroxidase	<i>Penaeus monodon</i>	-2.20
DN27870_c0_g2_i3	copper/zinc superoxide dismutase isoform 3	<i>Marsupenaeus japonicus</i>	-13.45
DN29677_c0_g1_i1	thioredoxin	<i>Macrobrachium nipponense</i>	-2.16

Table 38 (Continued)

Blood coagulation			
DN49188_c0_g1_i1	transglutaminase	<i>Macrobrachium rosenbergii</i>	2.08
DN2823_c0_g1_i2	hemicentin-1-like isoform X2	<i>Pieris rapae</i>	5.31
Apoptosis			
DN370_c0_g1_i2	caspase	<i>Eriocheir sinensis</i>	2.64
DN12951_c0_g1_i2	caspase 4	<i>Portunus trituberculatus</i>	3.76
DN21090_c0_g1_i2	inhibitor of apoptosis protein	<i>Scylla paramamosain</i>	2.79
Phagocytosis			
DN57596_c0_g2_i1	Ras-related protein Rab-37	<i>Zootermopsis nevadensis</i>	2.66
DN13418_c0_g1_i1	Rab32	<i>Macrobrachium rosenbergii</i>	2.46
DN19755_c0_g3_i1	rac GTPase-activating protein 1-like	<i>Centruroides sculpturatus</i>	2.95
DN13060_c0_g1_i1	VLIG2	<i>Macrobrachium rosenbergii</i>	3.92
DN147_c0_g2_i3	VLIG1	<i>Macrobrachium rosenbergii</i>	2.89
DN18093_c0_g1_i3	ADP-ribosylation factor	<i>Marsupenaeus japonicus</i>	2.19
DN27087_c0_g1_i2	interferon regulatory factor	<i>Litopenaeus vannamei</i>	3.32
Other immune genes			
DN8990_c0_g1_i3	Ferritin	<i>Macrobrachium rosenbergii</i>	2.93
DN39999_c0_g1_i6	calcium/calmodulin-dependent protein kinase type II alpha chain isoform X6	<i>Zootermopsis nevadensis</i>	2.19
DN47919_c0_g1_i9	integrin, partial	<i>Procambarus clarkii</i>	2.53
DN17544_c0_g2_i1	integrin alpha 8	<i>Fenneropenaeus chinensis</i>	2.55
DN11203_c0_g4_i1	integrin alpha 4, partial	<i>Fenneropenaeus chinensis</i>	2.04
DN2727_c0_g1_i3	Cathepsin B	<i>Macrobrachium rosenbergii</i>	2.69
DN928_c0_g1_i2	cathepsin C	<i>Fenneropenaeus chinensis</i>	2.50
DN12284_c0_g1_i1	cathepsin L	<i>Marsupenaeus japonicus</i>	2.66
DN1236_c0_g1_i6	crustacyanin-like lipocalin	<i>Macrobrachium rosenbergii</i>	-2.10
DN18816_c0_g2_i1	crustacyanin A, partial	<i>Penaeus monodon</i>	-2.48

To examine the homogeneity across biological replicates, principle component analysis (PCA) was performed. Transcripts with extremely low expression (sum of read count < 10) were filtered out. Total of 84,092 transcripts survived the cut-off and were subjected to the PCA. The PCA results showed strong clustering within each group. The both groups formed distinct clusters within principle component 1 (PC1) which responsible for 42.62 % of the variance in the expression (Figure 50). In addition, the top 100 most differentially expressed transcripts were clustered using Pearson's correlation and displayed in heatmap (Figure 51). The biological replicates were clustered within the same group and demonstrate clear distinction between control and infected group.

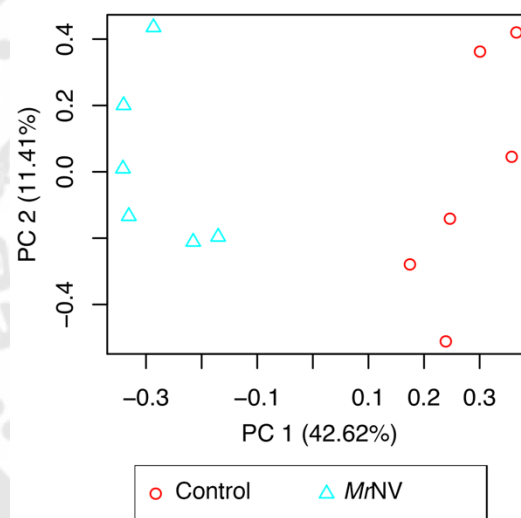


Figure 50 Principle component analysis of twelve samples (84,092 transcripts)

PC 1 and 2 are principle component 1 and 2, respectively. Blue triangles are *MrNV*-infected group (n = 6), whereas red circles are control group (n = 6).

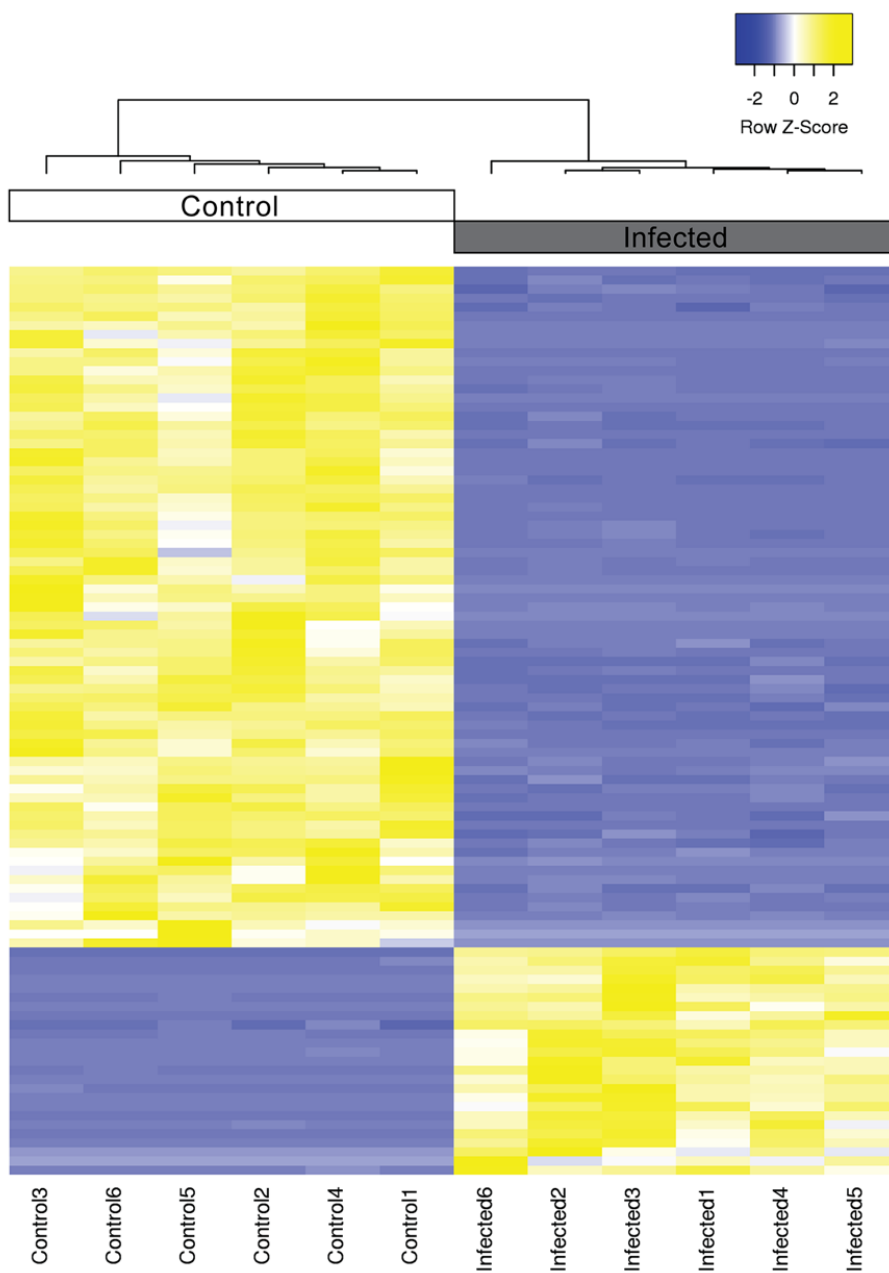


Figure 51 Heatmap of top 100 differentially expressed transcripts

The heatmap was generated using trimmed mean of M-values (TMM). Sample clustering was done using Pearson's correlation. The Z-score scale is shown in the top-right corner ranging from -2 (blue) to 2 (yellow).

8. Quantitative RT-PCR validation of selected genes

To validate differential expression results from RNAseq pipeline, qRT-PCR was performed using nine selected genes from list of DEG involved in immune system and *elongation factor1-alpha* (EF1-alpha) as an internal reference gene. Four separate biological replicates from each group were used in two-step qRT-PCR. The expression levels were calculated using the delta-delta C_t method. Table 39 summarizes the qRT-PCR results compared with RNAseq results. All of the selected genes had the same expression pattern between the two methods. The qRT-PCR results showed that all up-regulated genes had greater differences in expression levels than those of RNAseq, whereas all down-regulated genes had smaller differences. According to the qRT-PCR results, all of the selected genes were differentially expressed after the infection of *MtNV* ($p > 0.05$) except *Spz* which had p -value of 0.053 (Figure 52C).

To examine the gene expression after the infection of *MtNV* between the two methods, heatmaps were generated using relative expression (qRT-PCR) and transcript per millions (TPM) for RNAseq results (Figure 52A). Expression patterns of all selected genes were comparable between qRT-PCR and RNAseq. Furthermore, the Pearson's correlation coefficients were calculated using the average log-fold change ratio between the two methods and demonstrated highly significant correlation as shown in Figure 52B ($R^2 = 0.9531$).

Table 39 Comparison of fold change in gene expression between qRT-PCR and RNAseq

Gene symbol	qRT-PCR		RNAseq	
	Fold change \pm SD	P	Fold change	Corrected P
<i>ALF1</i>	5.86 \pm 0.72	0.001	2.25	0.011
<i>CuZnSOD3</i>	-5.72 \pm 1.09	0.003	-13.45	0.001
<i>Anv</i>	8.97 \pm 1.19	0.001	2.48	0.007
<i>Spz</i>	-3.26 \pm 1.08	0.053	-17.88	2.90E-09
<i>CASP</i>	12.05 \pm 0.91	7.04E-05	2.64	1.03E-06

Table 39 (Continued)

<i>DICER</i>	6.81 ± 1.32	0.006	3.66	4.31E-11
<i>HMCN1</i>	16.07 ± 3.91	0.005	5.31	0.003
<i>ARF</i>	5.45 ± 0.90	0.004	2.19	0.008
<i>ProPO</i>	9.38 ± 1.43	0.002	2.01	8.65E-06

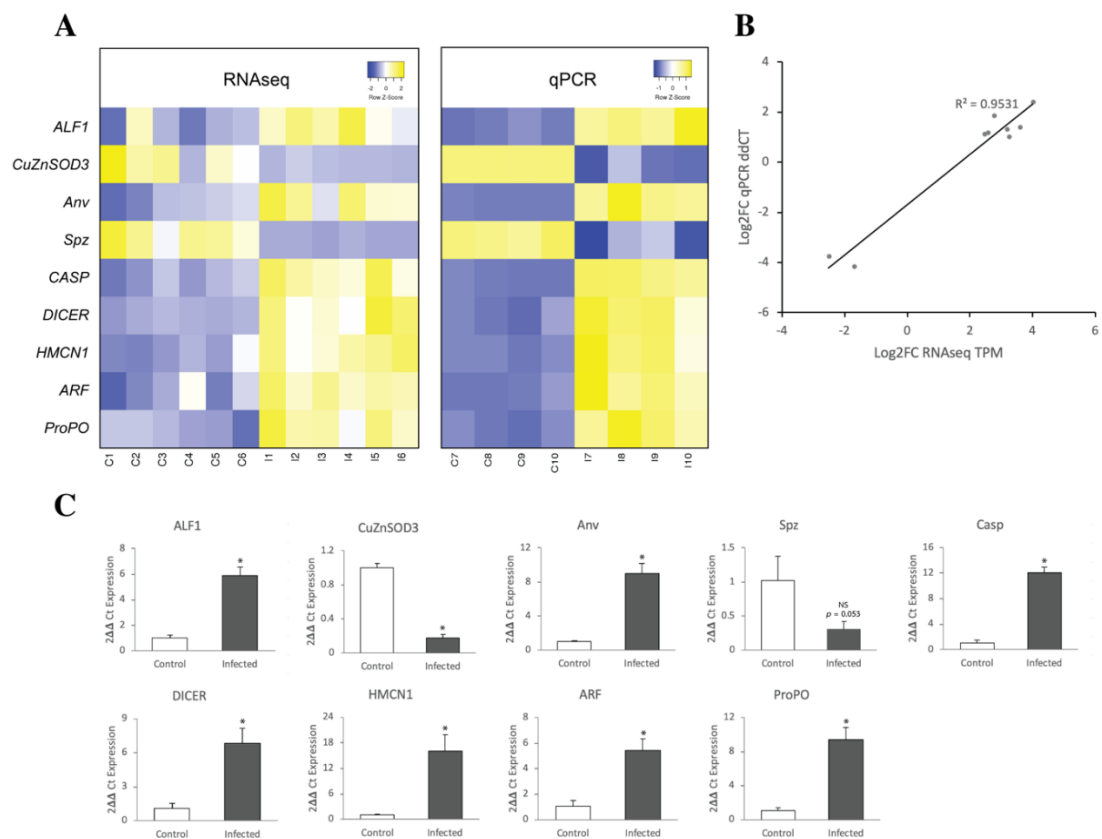


Figure 52 Comparison of fold change in gene expression between qRT-PCR and RNAseq

A) Heatmap representing transcript per million (TPM) expression from RNAseq and relative expression from qRT-PCR. The Z-score scales are shown in the top-right corner ranging from blue to yellow. B) Regression plot demonstrating the direct correlation between the average log₂ FC expression values from both RNAseq and qRT-PCR. C) The qRT-PCR validation results of nine selected genes including *anti-lipopolysaccharide factor 1 (ALF1)*, *Spatzle (Spz)*, *copper/zinc superoxide dismutase 3 (CuZnSOD3)*,

caspase (CASP), antiviral protein (Anv), dicer (DICER), hemicentin-1-like (HMCN1), ADP ribosylation factors (ARF), and prophenoloxidase (ProPO) with elongation factor1-alpha (EF1-alpha) as an internal reference.



CHAPTER 5

DISCUSSION

White tail disease (WTD) caused by *Macrobrachium rosenbergii* nodavirus (*MrNV*) is the most serious threat to *M. rosenbergii* post-larvae culture (Sahul Hameed et al., 2004). WTD has caused up to 100% mortalities and severe economic losses to *M. rosenbergii* post-larvae culture in Taiwan (Tung et al., 1999), China (Qian et al., 2003), India (Sahul Hameed et al., 2004), Thailand (Yoganandhan et al., 2005), and Australia (Owens et al., 2009). Providing more information about effects of *MrNV* infection would be valuable in order to contain and restrict the disease outbreak. Apoptosis is considered as an important cellular response that limit viral replication and eliminate viral-infected cells in multicellular organisms (Everett & McFadden, 1999; Koyama et al., 2000). However, there is limited information regarding apoptosis mechanism regulator in *M. rosenbergii* such as TCTP, one of the apoptosis regulators. Therefore, in this study, TCTP from *M. rosenbergii* (*MrTCTP*) was characterized and examined its role in innate immunity against viral infection.

Recently, NGS technology has been widely used in both genomic and transcriptome research as rapid and efficient tool to generate high-throughput sequencing data (Morozova & Marra, 2008). NGS technology combined with *de novo* transcriptome assembler such as Trinity allows researcher to discover novel genes and study the gene expression in non-model organisms which lack of genome or transcriptome database (Grabherr et al., 2011). In this study, highly complete transcriptome for *M. rosenbergii* post-larvae was reported. Additionally, immune-related genes in response to *MrNV* infection were identified using NGS platform and the gene expression of selected genes were verified using qRT-PCR.

Molecular cloning and characterization of *MrTCTP*

TCTP was originally discovered as P21, Q23, and P23 by three research groups in 1980s (Gachet et al., 1999). This protein was identified in human tumor and regulated at translational level, therefore, the name “translationally controlled tumor protein” has been used since the late 1980s (Gross et al., 1989). Later on, many functional analyses of this protein were conducted. TCTP has been reported to be involved in various biological processes including cell growth and cell cycle control (Cans et al., 2003; Gachet et al., 1999), microtubule stabilization (Yarm, 2002), inflammation (MacDonald et al., 1995), chemo-resistance (Sinha et al., 2000), and anti-apoptotic mechanisms (H. Liu et al., 2005). Five TCTP have been identified in shrimp including *PmTCTP* (Bangrak et al., 2004), *PmerTCTP* (Wiriya, Amornrat, & Wilaiwan, 2007), *FcTCTP* (S. Wang et al., 2009), *PtTCTP* (Rajesh, Kiruthiga, Rashika, Priya, & Narayanan, 2010), and *LvTCTP* (W. Wu et al., 2013). These reported also suggested that TCTP might play crucial roles in shrimp antiviral immunity (Bangrak et al., 2004; Rajesh et al., 2010; S. Wang et al., 2009; W. Wu et al., 2013).

In this study, *MrTCTP* was cloned through RACEs and re-identified using specific primers. The re-identification of the gene by performing independent PCR reaction was to mitigate sequencing error from DNA polymerase which lacks of proof reading capability. Deduced amino acid sequence of *MrTCTP* was analyzed by various bioinformatics software. *MrTCTP*, 168 amino acid polypeptide, had all major characteristics of TCTP as follow; exhibited high homology to TCTP protein family (Thomas et al., 1981), carried two TCTP signature regions, and contained highly conserved amino acid sequences (Bommer & Thiele, 2004). The two TCTP signature includes TCTP signature 1 and 2, whereas highly conserved amino acid sequences include nine absolute conserved and six conserved with one mismatch (Bommer & Thiele, 2004). *MrTCTP* also contained four putative sites, according to prediction software, including one putative N-glycosylation site, two putative CK2 phosphorylation sites, and one predicted PKC site. The positions of these putative sites were similar to those of *LvTCTP* (W. Wu et al., 2013). Amino acid sequence analysis showed that *MrTCTP* is lack of the signal peptide sequence. However, TCTP is believed

to be secreted through exosome with an assistance of H,K-ATPase which is one of non-classical pathway (Amzallag et al., 2004). This hypothesis was supported by *in vivo* proton pump inhibitors (PPIs) treatment inhibited the secretion of TCTP (Choi et al., 2009).

Predicted ribbon diagram of *MrTCTP* had a typical features of TCTP protein. The ribbon diagram of *MrTCTP* consisted of three major domains which include beta-stranded core domain, helical domain, and flexible loop. It was known that beta-stranded core of TCTP is highly conserved and plays a major role interacting with other molecules (Bommer & Thiele, 2004). Predicted ribbon diagram demonstrated that beta-stranded core domain of *MrTCTP* contained most of the highly conserved amino acid sequence, putative N-glycosylation site and most of the putative phosphorylation sites. The flexible loop of *MrTCTP* ribbon diagram contained one putative phosphorylation site, TCTP signature 1 and 2 which are unique and highly conserved regions listed in PROSITE database. In addition, it has been reported that the tubulin binding region and Ca^{2+} binding area are located at the helical loop of TCTP (Gachet et al., 1999; Kim et al., 2000).

Identity/similarity matrix showed that *MrTCTP* had the highest identity to *E. sinensis* and high identity to those of other crustacean species, despite that *MrTCTP* showed relatively low identity to those of other invertebrates, vertebrates, and fission yeast. In addition, similarity percentages among TCTP proteins were considerably high indicating that TCTP proteins have highly conserved biological functions and structure. According to phylogenetic analysis, *MrTCTP* was in the same clade with crustaceans, additionally in the subgroup with *E. sinensis*. Despite that *MrTCTP* was in the subgroup with *E. sinensis*, identity percentages between *MrTCTP* and *E. sinensis* and TCTP proteins of penaeid shrimp species including *F. merguensis*, *F. chinensis*, *F. indicus*, *P. monodon*, and *L. vannamei* were very comparable. In addition, Lavy and others reported closer phylogenetic relationship of *M. rosenbergii* insulin-like androgenic gland hormone (IAG) to crabs including chesapeake blue crab (*Callinectes sapidus*), and mud crab (*Scylla paramamosain*) (Levy, Rosen, Simons, Savaya Alkalay, & Sagi, 2017).

To understand the function of *MrTCTP*, the expressions of *MrTCTP* in various tissue were examined using semi-quantitative RT-PCR. In this study, *Beta-actin* was used

as an internal reference to normalize the gene expression among samples. As the results, *MrTCTP* was constitutively expressed in every tissue examined. The highest expression of *MrTCTP* was found in hepatopancreas followed by muscle as the second highest. The expressions were in the same level in other tissues. This expression pattern in which *TCTP* expression was the highest in hepatopancreas followed by muscle was similarly found in *LvTCTP* (W. Wu et al., 2013) and *EsTCTP* (Q. Wang, Fang, Li, Wang, & Jiang, 2011). In crustacean, hepatopancreas is a crucial organ responsible for food absorption and storage, producing digestive enzymes and essential hormones in many pathways during growth and reproductive stages (W. Wang, Wu, Liu, Zheng, & Cheng, 2014). Therefore, the highest expression of *MrTCTP* in hepatopancreas may be because the expression of *TCTP* is mainly regulated by cytokines and growth signals (Bommer et al., 2002; Teshima et al., 1998). *TCTP* has been reported to play important roles in cell growth and cell cycle control (Cans et al., 2003; Thiele et al., 2000). Moreover, in mouse cell line, *TCTP* was involved in muscle fiber hypertrophy induction and inhibition of protein degradation in muscle (Goodman et al., 2017). Since muscle had high expression of *MrTCTP* and is the primary target to *MrNV* infection, therefore, muscle tissue was selected for RT-PCR in *MrNV* challenge experiment.

To investigate the role of *MrTCTP* against *MrNV* infection, *MrNV* challenge experiment was conducted using *MrNV* inoculum. The control group was used to eliminate the response caused by stress or injury. Before conducting the challenge experiment, recombinant plasmid containing *MrNV* PCR product was constructed. This recombinant plasmid was validated by sequencing and was then used as positive control in further RT-PCR reaction for the detection of *MrNV*. As the results, *MrTCTP* expression was up-regulated after 1, 2, 3, and 4 days of the injection of *MrNV*. The expression was returned to normal level at 5 days post injection. The infection of *MrNV* was confirmed using pleopod samples by RT-PCR. Up-regulations of *TCTP* in response to viral infection were also found in other shrimps. *PmTCTP* was up-regulated in haemocyte after 24 h of the injection with white spot syndrome virus (WSSV) (Bangrak et al., 2004). *FcTCTP* was up-regulated in hepatopancreas 6, 12, and 24 h after the WSSV exposure at both

transcriptional and translational levels (S. Wang et al., 2009), and *LvTCTP* transcripts and protein levels in gills were up-regulated at 8 to 48 h after the injection of WSSV (W. Wu et al., 2013). These suggested that *MrTCTP* might play an important role in shrimp immune response.

To further examine *MrTCTP* role against *MrNV* infection, dsRNA-mediated RNAi was used to knockdown the expression of *MrTCTP* before the *MrNV* exposure. The dsRNAs were synthesized using *in vitro* transcription with T7 promoter and validated using three different types of nucleases. The dsRNAs were not digested by DNase I and RNase A at high salt concentration, whereas being digested by RNase III. The results confirmed that the purified dsRNA had no DNA and single-stranded RNA contamination. Before the knockdown combined with *MrNV* challenge experiment, time-course knockdown experiment was performed. Two control groups including dsIMNV and 2X PBS were used. The results showed that neither non-target dsRNA nor 2X PBS control affected the expression of *MrTCTP*. *MrTCTP* expression was drastically reduced at day 4 post dsTCTP injection, therefore, this day was used as the time point for *MrNV* challenge.

The experiment was divided into 2 group, *MrNV* and TN group, in which each was sub-divided into 3 subgroup, dsTCTP, dsIMNV, and 2X PBS group. The results revealed that all 3 subgroups without *MrNV* challenge (TN group) exhibited no statistically difference between each group. The results indicated that knocking down the expression of *MrTCTP* has no effect on prawn survival in typical environment. On the other hand, *MrTCTP*-knock-down prawns followed by *MrNV* challenge demonstrated significantly increased cumulative mortality compared to the two control groups. The infection of *MrNV* was also confirmed using pleopod samples from moribund shrimp by RT-PCR. These results indicated that *MrTCTP* was involved in shrimp immune response against *MrNV* infection. In addition, these results were comparable to those experimented in *PmTCTP*-knock-down-shrimp in which the increased mortality rate after WSSV challenge was observed (100% within 7 days compared to the *LacZ*-dsRNA control group with 37.5% within 12 days) (Sinthujaroen et al., 2015). It was worth noticing that *MrNV* caused mortalities in the two control group (dsIMNV and 2X PBS). Although it is known that *MrNV*

does not cause mortality in adult prawns (Sahul Hameed et al., 2004), however, higher mortality rates of per os and intramuscular injection of *MrNV* compared to the control group were reported (83% and 77%, respectively, compared to 90% after 30 days of experiment) (Owens et al., 2009).

TCTP has been shown to be involved in anti-apoptotic mechanisms by interaction of apoptotic-related proteins including MCL1 (D. Zhang et al., 2002), Bcl-xL (Y. Yang et al., 2005), and caspase-3 (Sirois et al., 2011). In cell line, TCTP was a critical survival factor that preventing oxidative stress-induced cell death caused by reactive oxygen species (ROS) (Nagano-Ito et al., 2009). Moreover, shrimp TCTP has been reported to bind to Ca^{2+} which involved in Ca^{2+} -dependent apoptosis pathway. They also reported TCTP might keep viral-infected hemocyte from dying and make the infected shrimp less ill (Bangrak et al., 2004). Taken together, the up-regulation of *MrTCTP* might help minimizing the oxidative stress caused by *MrNV* infection and reduce intracellular-induced apoptosis, therefore, increasing prawn survivability.

It is believed that viruses can utilize host small GTPase-mediated signaling pathway to trigger viral-induced membrane remodeling in which this mechanism contributes to viral replication (Belov et al., 2007). In shrimp, the small GTPases are reported to have precipitated in anti-viral immunity by regulating phagocytosis (W. Liu, Han, & Zhang, 2009; W. Wu, Zong, Xu, & Zhang, 2008). In previous studies, TCTP is reported to be a modulator of GTPase activity including Rab GTPase. Rab GTPase functioned as intracellular virus recognition particle and triggered downstream phagocytosis against viral infection in shrimp (Thaw et al., 2001; W. Wu et al., 2008). It is possible that *MrTCTP* might involve in phagocytosis by interacting with Rab GTPase. ProPO is considered a crucial first line of innate immune response of shrimp which trigger melanization and involved in many immune responses (Cerenius & Soderhall, 2004; Soderhall & Cerenius, 1998; Soderhall et al., 1994). In addition, it has been reported that the expression of prophenoloxidase (proPO) was decreased after the *PmTCTP*-dsRNA injection (Sinthujaroen et al., 2015). They also reported that decreasing opsonization, and

phagocytosis were found in TCTP silenced shrimp causing increased mortality in viral infected shrimp (Sinthujaroen et al., 2015).

Conclusion

This study was the first to identify and characterize TCTP from *M. rosenbergii*. *MrTCTP* demonstrated major characteristics of TCTP and showed high similarity to those of crustacean species. Up-regulation of *MrTCTP* in response to *MrNV* infection and increased mortality rates in *MrTCTP*-knock-down prawns demonstrated potential role of *MrTCTP* in antiviral immunity. This information provided better understanding of TCTP roles in *M. rosenbergii* and could be useful for containing the disease outbreak in *M. rosenbergii* culture.

Transcriptomic analysis of *M. rosenbergii* post-larvae in response to *MrNV* infection

Data analysis pipeline

The data analysis pipeline was written using Snakemake which can be easily reproduced and rescaled by changing the input data in the config file (Koster & Rahmann, 2012). In addition, user can also change the parameters for each software in this pipeline within the config file without altering the workflow. Using RNAseq sample data from *M. rosenbergii* in response to *V. parahaemolyticus* infection (in total of 109M reads), Trinity assembler produced 140,317 contigs which were then clustered into 104,514 unigenes by CD-HIT software which more than the results from Rao and others (Rao et al., 2015). The pipeline merged all read data together before the assembly whereas Rao and others' method assembled first and then clustered the contigs into unigenes. The advantage of merging read data together before the assembly is increasing the abundance of lowly expressed transcripts which allows the assembler to generate full transcript from them instead of fragmented data, therefore, increasing depth/coverage of the assembled transcripts (Haas et al., 2013). According to transcriptome quality assessment, the assembled transcripts had high fragment mapping rate (95.5%). In addition, the assembled transcripts showed considerably high sequencing depth judging by ExN50

peak which near 90% (80%) and good BUSCO statistic (74.7% complete orthologs). These results indicated that RNAseq data in this study (expected 400M reads) would provide very high sequencing depth.

Differential expression analysis demonstrated that, using EdgeR, total of 1,803 genes were differentially expressed (FDR < 0.05). The results were drastically different from Rao and others (14,569 DEGs with FDR < 0.001) in which FPKM method was used (Rao et al., 2015). However, majority of the list provided by Rao and others had the same expression pattern. EdgeR requires biological replicates to calculate dispersion value. Therefore, synthetic dispersion value (0.1) was used in order to perform DEG analysis using this sample data. It was worth noticing that FPKM is calculated by dividing counts by total reads (library size) and gene length, and multiplying by 1,000,000 (Mortazavi, Williams, McCue, Schaeffer, & Wold, 2008). Differences in library size between each sample affect the results, since comparing FPKM does not taken the differences in library size into account. FPKM method also doesn't have normalization regarding library composition. For example, comparing five genes (A,B,C,D, and E) between sample 1 and 2, if gene A is only and highly expressed in sample 1 whereas the other genes have the same expression, the FPKM of the other genes (B,C,D, and E) from sample 1 are lower than those of sample 2 despite the expressions are the same. TMM normalization method (within EdgeR) aims to make non-DEG's counts similar between samples based on assumption that most genes are non-DEG (Robinson & Oshlack, 2010). Therefore, EdgeR was selected as DEG analysis software in this pipeline.

De novo assembly and annotation

In this study, total of 12 cDNA libraries were synthesized from 6 replicates of each normal and *M/r*NV-infected post-larvae which were indexed by 6 nt index-specific sequence allowing all libraries to be sequenced on one Illumina's flow cell. According to the Qubit fluorometer and microfluidic nucleic acid analyzer, average size of all 12 libraries were within suitable range for PE75 sequencing (339-379 bp with insert size of 217-257 bp) and showed no contamination of undesired DNA nor RNA. The Libraries were

then pooled, diluted, and proceeded into sequencing. Illumina sequencing produced generous amount of 522 M raw reads (with average of 44 M per sample) which exceeded expectation (400 M). The 75 bp PE raw reads were trimmed the first 9 bases, according to Lexogen's recommendation and judging by low Phred score, and the last base, which reported to be all guanine, to obtain 65 bp quality trimmed reads. The trimmed reads were then subjected to *de novo* assembly using Trinity.

Transcriptome of the giant river prawn (*M. rosenbergii*) was assembled and annotated from six libraries of each control and infected samples. The aim of this study was to expand the transcriptomic recourses for further differential expression analysis. The ultimate goal was to generate the highest quality and coverage transcriptome as possible while minimizing the redundancy. The assembled transcripts showed considerably high sequencing depth and low redundancy, and were good representative of raw reads. The assembled transcriptome showed high complete BUSCO score at C:83.4% with low fragmentation, missing, and duplication (F:13%, M:3.3%, D:16.2%). These results were comparable to the assembled transcriptome reported for *P. monodon* (C:98.2%, F:0.8%, M:1.0%, D:51.3%) (Huerlimann et al., 2018) and from *L. vannamei* (C:98.0%, F:0.7%, M:1.3%, D:25.5%) (Ghaffari et al., 2014). Highest ExN50 value at 94% indicated that the assembled transcripts had high coverage and was assembled from sufficient read data (Bryant et al., 2017). In addition, the assembled transcripts were good representative of the raw reads with fragment mapping rate of 96.85 %. Both BUSCO and ExN50 statistics exceeded those of *M. rosenbergii* assembly using 109 M read data by the same pipeline as described earlier (highest ExN50 value of 80 % and 74 % complete BUSCO).

Using the UniProt database, 26.73 % of transcripts were successfully annotated. These annotated transcripts were then generated GO assignment, EggNOG, and KEGG annotation. On the other hand, using the Nr-Arthropod database, 33.75 % of the transcripts were successfully annotated. Relatively low annotation ratios might be because *M. rosenbergii* is a non-model organism which not yet well studied in terms of genomics/transcriptomics and has no complete genome published. Despite that, these

annotation ratios were comparable to those previous *M. rosenbergii* transcriptomes reported (Cao et al., 2017; Z. F. Ding et al., 2015; Rao et al., 2016; Rao et al., 2015). UniProt database is a comprehensive protein sequence and annotation database which manually reviewed and annotated by the experts. Most of UniProt entries were derived from well published and annotated genome projects (UniProt, 2019). This explains why top-3 species distribution of Blastx results against UniProt database were *H. sapiens*, *M. musculus*, and *D. melanogaster*. Most of Blastx annotations against Nr-Arthropod database was matched to *Hyalella azteca* (34.4%). It was because this species of amphipod crustacean, *H. Azteca*, is widely used in aquatic toxicology assays and molecular ecotoxicology. The genome of *H. Azteca* has been sequenced and annotated, additionally, *H. Azteca* genome project is now running under the i5K Initiative (i, 2013; Poynton et al., 2018).

Raw read data generated in this study has been uploaded into the National Centre for Biotechnology Information Sequence Read Archive (SRA) under the BioProject number: PRJNA550272. The data analysis pipeline including additional information about the analysis is publicly available on GitHub at "https://github.com/prawnseq/Mrosenbergii_MrNV_RNAseq".

Differential expression analysis

Six replicates of each normal post-larvae and *MrNV* infected post-larvae were used to identify differentially expressed transcripts during the *MrNV* infection. RNA sequencing was performed on a total of twelve samples. Differential expression analysis was performed using TMM normalization method by EdgeR software followed by Benjamini-Hochberg method for multiple p correction. Total of 5,538 differentially expressed transcripts were reported with 2,413 up-regulated transcripts and 3,125 down-regulated transcripts. Among those, some were involved in the innate immune system of shrimp regarding the antiviral mechanisms. Those involved in innate immune system were categorized by function and listed as candidate genes involved in the infection of *MrNV*.

In this study, qPCR was used to validate differential expression results and transcriptome assembly. Total of 9 gene were selected as targets for qPCR validation. These genes were selected according to functional groups including pattern recognition proteins (PRPs) and antiviral protein, prophenol oxidase (ProPO) system, the Toll-IMD signaling pathways, antimicrobial peptides (AMPs) and blood clotting system, phagocytosis and apoptosis, antioxidant system, and RNA interference (RNAi). Validation of RNAseq results using qPCR has demonstrated high correlation between RNAseq and qPCR (Asmann et al., 2009; Griffith et al., 2010; A. R. Wu et al., 2014). In addition, high correlations between RNAseq and qPCR results were previously reported in *M. rosenbergii* regarding bacterial and viral infection (Cao et al., 2017; Rao et al., 2016; Rao et al., 2015). Therefore, in this study, separate biological samples were used in the qPCR validation to enhance the confidence.

Pattern recognition proteins (PRPs) are crucial components for triggering the immune responses in innate immune system of shrimp (Medzhitov & Janeway, 2000). PRPs, germ-line encoded proteins, activate cellular and humoral immune response through immune signaling pathway (X. W. Wang & Wang, 2013). Several shrimp PRPs have been identified and examined the role in innate immune system against viral infection. Up-regulation of C-type lectin of *M. rosenbergii* (*MrCTL*) expression in hepatopancreas was found after *Vibrio parahaemolyticus* or white spot syndrome virus (WSSV) challenge (X. Huang, Huang, Shi, Ren, & Wang, 2015). *M. rosenbergii* ficolin expression in hepatopancreas was up-regulated after the infection of *V. anguillarum* and WSSV (X. W. Zhang et al., 2014). In addition, expression of *M. rosenbergii* mannose-binding lectin (MBL) also found to be up-regulated during *MrNV* or WSSV infection (Arockiaraj et al., 2015). In this study, C-type lectin family, members of PRPs, including C-type lectin, ficolin, and antiviral protein were differentially expressed during *MrNV* infection. This suggested that these members of PRPs are involved in innate immune system against *MrNV* infection. In addition, validation of one of these genes, antiviral protein, using qPCR showed up-regulation by 8.97-fold compared to 2.48-fold in the RNAseq. However, in this report, down-regulation of MBL was contradicted to the

previous report (Arockiaraj et al., 2015). It is possible that MBL does not play role in antiviral response of *M. rosenbergii* post-larvae or MBL expression is being suppressed in *M. rosenbergii* post-larvae during *MtNV* infection. Further investigation is required to understand the role of MBL in *M. rosenbergii* post-larvae during the infection of *MtNV*.

First line of crustacean immunity involve prophenol oxidase (ProPO) activating system which triggers melanization and other responses such as encapsulation, nodule formation, and hemocyte induction (Cerenius & Soderhall, 2004; Soderhall & Cerenius, 1998; Soderhall et al., 1994). Recognition of PAMPs by PRPs activates serine proteinases cascade which leads to the production of active PO enzyme. As a result, melanization occurred from production of polymeric melanin around invading pathogens by the active PO enzyme (Cerenius & Soderhall, 2004). According to RNAseq results, Up-regulation of ProPO expression by 2.01-fold was found during the infection of *MtNV* in which the up-regulation was validated by qPCR (9.38-fold up-regulation). Moreover, up-regulations of three types of prophenoloxidase activating enzyme were found by RNAseq. These indicate involvement of ProPO-activating system in *MtNV* infection.

The Toll and IMD pathways are known to be the most important immune signaling pathways in invertebrates (De Gregorio et al., 2002). Activation of the Toll receptor caused by cytokine-like ligand Spätzle, whereas in vertebrate, Toll-like receptors (TLRs) are triggered directly by pathogens (Lemaitre & Hoffmann, 2007; P. H. Wang et al., 2012). Activation of NF-kappa-B family protein Dif/Dorsal by the activated Toll receptor positively regulates the expression of immune-related genes such as antimicrobial peptide (AMPs) (Lemaitre & Hoffmann, 2007). Previous studies have identified Toll receptor from *M. rosenbergii* (Feng et al., 2016; Srisuk, Longyant, Senapin, Sithigorngul, & Chaivisuthangkura, 2014) and demonstrated that the expression was gradually up-regulated in gills during the WSSV challenge (Feng et al., 2016). The expression of spätzle protein of *M. rosenbergii* in hemocytes was up-regulated after the bacteria infection (Vaniksampanna, Longyant, Charoensapsri, Sithigorngul, & Chaivisuthangkura, 2019). Moreover, *F. chinensis* challenged with *V. anguillarum* and WSSV showed up-regulation of spätzle protein (X. Z. Shi et al., 2009). Relish, known as nuclear factor NF-kappa-B

p110, is an important transcription factor in the IMD pathway which has parallel function to the Toll signaling pathway (Hedengren et al., 1999; Lemaitre & Hoffmann, 2007). Previous study showed that *M. rosenbergii* relish involved in the infection of bacteria and up-regulations of various AMPs were caused by overexpression of relish (Y. R. Shi et al., 2015). In this study, RNAseq results showed up-regulations of the Toll receptor and NF-kappa-B p110 in response to *MrNV*, whereas spätzle was found to be down-regulated. The expression of spätzle was validated using qPCR which showed 3.26-fold down-regulation compared to 17.88-fold down-regulation in RNAseq. The results suggested that these Toll/IMD signaling pathway genes are involved in antiviral mechanisms against *MrNV*. Down-regulation of spätzle may be caused by negative feedback as a result of the activation of the Toll pathway (Misra, Hecht, Maeda, & Anderson, 1998; Towb, Bergmann, & Wasserman, 2001).

Antimicrobial peptides (AMPs) plays an important role in crustacean first line of innate immunity. Generally, AMPs are small amphipathic, cationic, germ-line encoded polypeptides with efficient broad spectrum of antimicrobial capabilities against various types of pathogens including virus, bacteria, and fungi. Different types of AMPs vary in protein structure, amphipathicity, and ionic charge (Bulet et al., 1991; Yount et al., 2006). AMPs destroy pathogen by acting as specific membrane-integrity disruptor resulting in membrane destabilization or pore formation of the microbe (Brogden, 2005; Yount et al., 2006). There have been reported that the expression of lysozymes and anti-lipopolysaccharide factors (ALFs) were up-regulated in response to WSSV in *M. rosenbergii*, *L. vannamei*, and *F. chinensis* (Ren et al., 2012; B. Wang et al., 2006; P. H. Wang, Wan, Gu, et al., 2013). In *M. rosenbergii* hemocytes, crustin expression was up-regulated after the infections of WSSV, *Aeromonas hydrophila*, infectious hypodermal and hematopoietic necrosis virus (IHHNV) (Arockiaraj et al., 2013). However, in *P. monodon*, the expression of crustin 3 was up-regulated in response to WSSV infection, whereas down-regulation of crustin 1 and 2 expressions were reported (Swapna, Rosamma, Valsamma, & BrightSingh, 2011). In this study, various AMPs including crustin members, ALFs, and i-type lysozyme-like protein 2 (LYZL2) were aberrantly expressed after the

MrNV infection. The expression ALFs and LYZL2 were up-regulated, whereas the expression of crustin members were both up- and down-regulated. The qPCR validation of ALF1 showed 5.86-fold up-regulation compared to 2.25-fold up-regulation from RNAseq results. These results indicated that ALFs and LYZL2 play roles in antiviral response against *MrNV*, whereas only specific isoforms of crustin are involved.

Blood clotting minimizes microbial spread and hemolymph loss during injury, as part of a humoral response (Maningas et al., 2013). Blood clotting mechanisms in crustacean requires calcium-dependent transglutaminase (TGase) which produced from the hemocyte to catalyze cross-linking aggregation of clotting proteins (CPs) (Hall et al., 1999). Previous study reported a link between blood clotting and AMPs in *M. japonicus* by demonstrating that TGase depleted prawn had down-regulation of both lysozyme and crustin (Fagutao et al., 2012). In this study, the expression of hemicentin-1-like isoform X2 (HMCN1) and transglutaminase were up-regulated. The qPCR validation of HMCN1 showed 16.07-fold up-regulation compared to 5.31-fold up-regulation in the RNAseq. These indicated involvement of these two blood coagulation components during the infection of *MrNV*. In addition, up-regulation of members of AMPs including lysozyme, and crustin isoforms along with up-regulation of two blood coagulation components could indicate a link between blood clotting and AMPs in *M. rosenbergii*.

Apoptosis, known as programmed cell death, is one of the important cellular immune responses in which this process limits replication of virus and eliminates virus infected cells in multicellular organisms (Everett & McFadden, 1999; Koyama et al., 2000). Caspases, highly conserved cysteine proteases, are the hallmark of apoptosis mechanisms in which activated caspases are involved in execution of apoptosis (Menze et al., 2010). Previous study identified *M. rosenbergii* caspase (*MrCasp*) and showed that *MrNV* capsid protein could inhibit apoptotic activities of *MrCasp* in Sf9 cells (Youngcharoen et al., 2015). Moreover, the expression of caspase 3c in *M. rosenbergii* hemocyte was up-regulated during the IHNV infection (Arockiaraj et al., 2012a). IAP or inhibitor of apoptosis protein is an apoptosis regulator which binds and inhibit caspase activity (Roy, Deveraux, Takahashi, Salvesen, & Reed, 1997). IAP of *M. rosenbergii* has

been identified and *MrIAP* expression in hepatopancreas was up-regulated after the infection of IHHNV (Arockiaraj et al., 2011). In addition, up-regulation of WSSV genes and significantly lower expression of AMP genes were found in *L. vannamei* IAPs-silenced using RNA interference (P. H. Wang, Wan, Gu, et al., 2013). In this study, the expression of caspase, caspase 4 and IAP were up-regulated in response to *MrNV* infection. The qPCR validation of caspase showed 12.05-fold up-regulation compared to 2.64-fold up-regulation in RNAseq suggesting that these genes are involved in apoptotic responses to *MrNV* infection.

Cellular responses include phagocytosis in which this process ingests microparticles including cellular debris from apoptosis and necrosis and microbial pathogens (Stuart & Ezekowitz, 2008). It has been reported that the small GTPases control cellular trafficking and regulate phagocytosis as a part of cellular immune responses. (W. Liu et al., 2009; Myers & Casanova, 2008; W. Wu et al., 2008). ADP ribosylation factors (Arfs), a small-ubiquitously-expressed GTPases, have been identified in *M. rosenbergii* and *M. japonicus*. The expression of Arfs was reported to be up-regulated in both *M. rosenbergii* and *M. japonicas* during WSSV infection (Z. F. Ding et al., 2015; Ma, Zhang, Ruan, Shi, & Xu, 2010; M. Zhang, Ma, Lei, & Xu, 2010). Additionally, Rab GTPases, known as Ras-like GTPase superfamily members, expression in *M. rosenbergii* was up-regulated after WSSV infection (Y. Huang & Ren, 2015) and *MrNV* infection (from RNAseq results). Validation of ADP ribosylation factor (Arf) using qPCR showed up-regulation of 5.45 fold compared to 2.19-fold up-regulation by RNAseq. These results indicated that these small GTPases may involve in innate immunity regarding *MrNV* infection.

During immune responses, reactive oxygen species (ROS) are eliminated by antioxidant enzymes (De la Fuente & Victor, 2000). Previous studies have identified several of *M. rosenbergii* antioxidant enzymes including thiol-dependent peroxiredoxin (Prdx) (Arockiaraj et al., 2012b), glutathione S-transferase (GST) (Arockiaraj et al., 2014), copper/zinc superoxide dismutase (CuZnSOD) (Cheng, Tung, Liu, & Chen, 2006), and selenium dependent glutathione peroxidase (Yeh et al., 2009). It also reported that these genes were aberrantly expression in response to different types of pathogens (Arockiaraj

et al., 2012b; Arockiaraj et al., 2014; Cheng et al., 2006; Yeh et al., 2009). In this study, RNAseq results showed five differentially-expressed antioxidant enzyme genes after the infection of *MtNV*. The qPCR validation of CuZnSOD3, one of those five genes, showed 5.72-fold down regulation compared to 13.46-fold down regulation by RNAseq.

RNA interference (RNAi) is considered to have an essential role in shrimp antiviral responses. Dicer is an RNase III-like enzyme which initiates RNA interference by cleavage of long dsRNA into siRNA (21-30 bp dsRNA) (S. M. Elbashir, W. Lendeckel, & T. Tuschl, 2001; Hannon, 2002). Genome derived silencing RNAs, are unwound and bound with argonaute protein within the RNA-induced silencing complex (RISC) (Dykxhoorn, Novina, & Sharp, 2003). Specific mRNA degradation occurs when RISC recognizes and binds to the target, therefore the target gene is knockdowned (Bernstein et al., 2001). Essential components of RNAi mechanism including dicer and argonaute has been identified in various shrimp species including *M. rosenbergii* (Shpak et al., 2017), *P. monodon* (Su et al., 2008; Unajak, Boonsaeng, & Jitrapakdee, 2006), and *L. vannamei* (Y. H. Chen et al., 2011; Labreuche et al., 2010; Yao et al., 2010). In shrimp antiviral immunity, both miRNAs and siRNAs have been reported to participate in the response. It has been reported that 31 miRNAs were differentially expressed in response to WSSV infection indicating involvement in antiviral immunity (T. Huang & Zhang, 2012). In *M. japonicas*, 24 miRNAs have been identified and found that these miRNAs involved in regulating immune processes such as apoptosis, proPO system, and phagocytosis (G. Yang et al., 2012). Previous studies reported specific inhibition in viral replication after the administration of synthetic dsRNA/siRNA specific to yellow head virus (YHV) genes (Tirasophon et al., 2005; Yodmuang et al., 2006), or WSSV genes (J. Xu et al., 2007). Additionally, during the replication of both DNA (WSSV) and RNA viruses (including YHV and taura syndrome virus (TSV)), formation of dsRNA occurred which can lead to antiviral responses via RNAi mechanisms (T. Huang & Zhang, 2013b). In this study, RNAseq results showed significant up-regulation of dicer-2 and argonaute-3 during the *MtNV* infection. The qPCR validation of dicer-2 showed 6.81-fold up-regulation compared to 3.66-fold up-regulation by

RNAseq suggesting that RNAi mechanism of *M.rosenbergii* may involve in antiviral responses against *MrNV* infection.

Conclusion

This study reported a highly complete *de novo* assembled transcriptome of giant river prawn, *M. rosenbergii*, post-larvae stage. This transcriptome can be used as reference transcriptome for transcriptomic profiling in response to pathogen infection, stress, or certain conditions and for gene functional analysis. This study is also the first to report transcriptomic profile of *M. rosenbergii* post-larvae in response to *MrNV* infection. Differential expression analysis revealed significant differences in the expression of numerous immune-related genes. These include numerous genes in many immune responses such as immune signaling pathway, antimicrobial peptides, prophenol oxidase system, phagocytosis and apoptosis, blood clotting system, and RNA interference. This study provides preliminary information on how *M. rosenbergii* post-larvae response to the infection of *MrNV* on the molecular levels and may provide biorational targets to restrain the disease.

REFERENCES

- A. Barki, A., Karplus, I., & Goren, M. (1991). Morphotype related dominance hierarchies in males of *Macrobrachium rosenbergii* (Crustacea, Palaemonidae). *Behaviour*, 117(3/4), 145-160.
- Agrawal, N., Dasaradhi, P. V., Mohmmmed, A., Malhotra, P., Bhatnagar, R. K., & Mukherjee, S. K. (2003). RNA interference: biology, mechanism, and applications. *Microbiol Mol Biol Rev*, 67(4), 657-685.
- Alberts, B., Johnson, A., Lewis, J., Raff, M., Roberts, K., & Walter, P. (2008). Apoptosis: Programmed Cell Death Eliminates Unwanted Cells. In *Molecular Biology of the Cell* (5 ed., pp. 1115): Garland Science.
- Amparyup, P., Sutthangkul, J., Charoensapsri, W., & Tassanakajon, A. (2012). Pattern recognition protein binds to lipopolysaccharide and beta-1,3-glucan and activates shrimp prophenoloxidase system. *J Biol Chem*, 287(13), 10060-10069. doi:10.1074/jbc.M111.294744
- Amzallag, N., Passer, B. J., Allanic, D., Segura, E., They, C., Goud, B., . . . Telerman, A. (2004). TSAP6 facilitates the secretion of translationally controlled tumor protein/histamine-releasing factor via a nonclassical pathway. *J Biol Chem*, 279(44), 46104-46112. doi:10.1074/jbc.M404850200
- Andrew, S. (2010). FastQC: a quality control tool for high throughput sequence data. Retrieved from <http://www.bioinformatics.babraham.ac.uk/projects/fastqc>
- Arcier, J. M., Herman, F., Lightner, D. V., Redman, R. M., Mari, J., & Bonami, J. R. (1999). A viral disease associated with mortalities in hatchery-reared postlarvae of the giant freshwater prawn *Macrobrachium rosenbergii*. *Diseases of Aquatic Organisms* 38, 177-181.
- Arockiaraj, J., Chaurasia, M. K., Kumaresan, V., Palanisamy, R., Harikrishnan, R., Pasupuleti, M., & Kasi, M. (2015). *Macrobrachium rosenbergii* mannose binding lectin: synthesis of MrMBL-N20 and MrMBL-C16 peptides and their antimicrobial

- characterization, bioinformatics and relative gene expression analysis. *Fish Shellfish Immunol*, 43(2), 364-374. doi:10.1016/j.fsi.2014.12.036
- Arockiaraj, J., Easwaran, S., Vanaraja, P., Singh, A., Othman, R. Y., & Bhassu, S. (2012a). Effect of infectious hypodermal and haematopoietic necrosis virus (IHHNV) infection on caspase 3c expression and activity in freshwater prawn *Macrobrachium rosenbergii*. *Fish Shellfish Immunol*, 32(1), 161-169. doi:10.1016/j.fsi.2011.11.006
- Arockiaraj, J., Easwaran, S., Vanaraja, P., Singh, A., Othman, R. Y., & Bhassu, S. (2012b). Immunological role of thiol-dependent peroxiredoxin gene in *Macrobrachium rosenbergii*. *Fish Shellfish Immunol*, 33(1), 121-129. doi:10.1016/j.fsi.2012.04.010
- Arockiaraj, J., Gnanam, A. J., Muthukrishnan, D., Gudimella, R., Milton, J., Singh, A., . . . Bhassu, S. (2013). Crustin, a WAP domain containing antimicrobial peptide from freshwater prawn *Macrobrachium rosenbergii*: immune characterization. *Fish Shellfish Immunol*, 34(1), 109-118. doi:10.1016/j.fsi.2012.10.009
- Arockiaraj, J., Gnanam, A. J., Palanisamy, R., Bhatt, P., Kumaresan, V., Chaurasia, M. K., . . . Sathyamoorthi, A. (2014). A cytosolic glutathione s-transferase, GST-theta from freshwater prawn *Macrobrachium rosenbergii*: molecular and biochemical properties. *Gene*, 546(2), 437-442. doi:10.1016/j.gene.2014.05.063
- Arockiaraj, J., Vanaraja, P., Easwaran, S., Singh, A., Othman, R. Y., & Bhassu, S. (2011). Bioinformatic characterization and gene expression pattern of apoptosis inhibitor from *Macrobrachium rosenbergii* challenged with infectious hypodermal and hematopoietic necrosis virus. *Fish Shellfish Immunol*, 31(6), 1259-1267. doi:10.1016/j.fsi.2011.09.008
- Asmann, Y. W., Klee, E. W., Thompson, E. A., Perez, E. A., Middha, S., Oberg, A. L., . . . Kocher, J. P. (2009). 3' tag digital gene expression profiling of human brain and universal reference RNA using Illumina Genome Analyzer. *BMC Genomics*, 10, 531. doi:10.1186/1471-2164-10-531
- Bangrak, P., Graidist, P., Chotigeat, W., & Phongdara, A. (2004). Molecular cloning and expression of a mammalian homologue of a translationally controlled tumor protein

- (TCTP) gene from *Penaeus monodon* shrimp. *J Biotechnol*, 108(3), 219-226.
doi:10.1016/j.jbiotec.2003.12.007
- Belov, G. A., Altan-Bonnet, N., Kovtunovych, G., Jackson, C. L., Lippincott-Schwartz, J., & Ehrenfeld, E. (2007). Hijacking components of the cellular secretory pathway for replication of poliovirus RNA. *J Virol*, 81(2), 558-567. doi:10.1128/JVI.01820-06
- Benjamini, Y., & Hochberg, Y. (1995). Controlling the False Discovery Rate: A Practical and Powerful Approach to Multiple Testing. *Journal of the Royal Statistical Society. Series B (Methodological)*, 57(1), 289-300.
- Bentley, D. R., Balasubramanian, S., Swerdlow, H. P., Smith, G. P., Milton, J., Brown, C. G., . . . Smith, A. J. (2008). Accurate whole human genome sequencing using reversible terminator chemistry. *Nature*, 456(7218), 53-59.
doi:10.1038/nature07517
- Bernstein, E., Caudy, A. A., Hammond, S. M., & Hannon, G. J. (2001). Role for a bidentate ribonuclease in the initiation step of RNA interference. *Nature*, 409(6818), 363-366.
doi:10.1038/35053110
- Bheekha-Escura, R., MacGlashan, D. W., Langdon, J. M., & MacDonald, S. M. (2000). Human recombinant histamine-releasing factor activates human eosinophils and the eosinophilic cell line, AML14-3D10. *Blood*, 96(6), 2191-2198.
- Blaszczyk, J., Tropea, J. E., Bubunenko, M., Routzahn, K. M., Waugh, D. S., Court, D. L., & Ji, X. (2001). Crystallographic and modeling studies of RNase III suggest a mechanism for double-stranded RNA cleavage. *Structure*, 9(12), 1225-1236.
- Bolger, A. M., Lohse, M., & Usadel, B. (2014). Trimmomatic: a flexible trimmer for Illumina sequence data. *Bioinformatics*, 30(15), 2114-2120.
doi:10.1093/bioinformatics/btu170
- Bommer, U. A., Borovjagin, A. V., Greagg, M. A., Jeffrey, I. W., Russell, P., Laing, K. G., . . . Clemens, M. J. (2002). The mRNA of the translationally controlled tumour protein P23/TCTP is a highly structured RNA, which activates the dsRNA-dependent protein kinase PKR. *RNA*, 8, 478-496.

- Bommer, U. A., & Thiele, B. J. (2004). The translationally controlled tumour protein (TCTP). *Int J Biochem Cell Biol*, 36(3), 379-385.
- Bonami, J. R., Shi, Z., Qian, D., & Sri Widada, J. (2005). White tail disease of the giant freshwater prawn, *Macrobrachium rosenbergii*: separation of the associated virions and characterization of MrNV as a new type of nodavirus. *J Fish Dis*, 28(1), 23-31. doi:10.1111/j.1365-2761.2004.00595.x
- Bonnet, C., Perret, E., Dumont, X., Picard, A., Caput, D., & Lenaers, G. (2000). Identification and transcription control of fission yeast genes repressed by an ammonium starvation growth arrest. *Yeast*, 16(1), 23-33. doi:10.1002/(SICI)1097-0061(20000115)16:1<23::AID-YEA503>3.0.CO;2-A
- Borregaard, N., Elsbach, P., Ganz, T., Garred, P., & Svejgaard, A. (2000). Innate immunity: from plants to humans. *Immunol Today*, 21(2), 68-70.
- Brogden, K. A. (2005). Antimicrobial peptides: pore formers or metabolic inhibitors in bacteria? *Nat Rev Microbiol*, 3(3), 238-250. doi:10.1038/nrmicro1098
- Bryant, D. M., Johnson, K., DiTommaso, T., Tickle, T., Couger, M. B., Payzin-Dogru, D., . . . Whited, J. L. (2017). A Tissue-Mapped Axolotl De Novo Transcriptome Enables Identification of Limb Regeneration Factors. *Cell Rep*, 18(3), 762-776. doi:10.1016/j.celrep.2016.12.063
- Bulet, P., Cociancich, S., Dimarcq, J. L., Lambert, J., Reichhart, J. M., Hoffmann, D., . . . Hoffmann, J. A. (1991). Insect immunity. Isolation from a coleopteran insect of a novel inducible antibacterial peptide and of new members of the insect defensin family. *J Biol Chem*, 266(36), 24520-24525.
- Cans, C., Passer, B. J., Shalak, V., Nancy-Portebois, V., Crible, V., Amzallag, N., . . . Telerman, A. (2003). Translationally controlled tumor protein acts as a guanine nucleotide dissociation inhibitor on the translation elongation factor eEF1A. *Proc Natl Acad Sci U S A*, 100(24), 13892-13897. doi:10.1073/pnas.2335950100
- Cao, J., Wu, L., Jin, M., Li, T., Hui, K., & Ren, Q. (2017). Transcriptome profiling of the *Macrobrachium rosenbergii* lymphoid organ under the white spot syndrome virus challenge. *Fish Shellfish Immunol*, 67, 27-39. doi:10.1016/j.fsi.2017.05.059

- Cavener, D. R. (1987). Comparison of the consensus sequence flanking translational start sites in *Drosophila* and vertebrates. *Nucleic Acids Res*, *15*(4), 1353-1361.
doi:10.1093/nar/15.4.1353
- Cerenius, L., & Soderhall, K. (2004). The prophenoloxidase-activating system in invertebrates. *Immunol Rev*, *198*, 116-126.
- Chen, K., Li, E., Li, T., Xu, C., Wang, X., Lin, H., . . . Chen, L. (2015). Transcriptome and Molecular Pathway Analysis of the Hepatopancreas in the Pacific White Shrimp *Litopenaeus vannamei* under Chronic Low-Salinity Stress. *PLoS One*, *10*(7), e0131503. doi:10.1371/journal.pone.0131503
- Chen, Y. H., Jia, X. T., Zhao, L., Li, C. Z., Zhang, S., Chen, Y. G., . . . He, J. G. (2011). Identification and functional characterization of Dicer2 and five single VWC domain proteins of *Litopenaeus vannamei*. *Dev Comp Immunol*, *35*(6), 661-671.
doi:10.1016/j.dci.2011.01.010
- Cheng, W., Tung, Y. H., Liu, C. H., & Chen, J. C. (2006). Molecular cloning and characterisation of copper/zinc superoxide dismutase (Cu,Zn-SOD) from the giant freshwater prawn *Macrobrachium rosenbergii*. *Fish Shellfish Immunol*, *21*(1), 102-112. doi:10.1016/j.fsi.2005.10.009
- Choi, S., Min, H. J., Kim, M., Hwang, E. S., & Lee, K. (2009). Proton pump inhibitors exert anti-allergic effects by reducing TCTP secretion. *PLoS One*, *4*(6), e5732.
doi:10.1371/journal.pone.0005732
- Christophides, G. K., Vlachou, D., & Kafatos, F. C. (2004). Comparative and functional genomics of the innate immune system in the malaria vector *Anopheles gambiae*. *Immunol Rev*, *198*, 127-148.
- De Gregorio, E., Spellman, P. T., Tzou, P., Rubin, G. M., & Lemaitre, B. (2002). The Toll and Imd pathways are the major regulators of the immune response in *Drosophila*. *EMBO J*, *21*(11), 2568-2579. doi:10.1093/emboj/21.11.2568
- De la Fuente, M., & Victor, V. M. (2000). Anti-oxidants as modulators of immune function. *Immunol Cell Biol*, *78*(1), 49-54. doi:10.1046/j.1440-1711.2000.00884.x

- de Veer, M. J., Holko, M., Frevel, M., Walker, E., Der, S., Paranjape, J. M., . . . Williams, B. R. (2001). Functional classification of interferon-stimulated genes identified using microarrays. *J Leukoc Biol*, *69*(6), 912-920.
- Destoumieux-Garzon, D., Saulnier, D., Garnier, J., Jouffrey, C., Bulet, P., & Bachere, E. (2001). Crustacean immunity. Antifungal peptides are generated from the C terminus of shrimp hemocyanin in response to microbial challenge. *J Biol Chem*, *276*(50), 47070-47077. doi:10.1074/jbc.M103817200
- Dhar, A. K., Bowers, R. M., Licon, K. S., Veazey, G., & Read, B. (2009). Validation of reference genes for quantitative measurement of immune gene expression in shrimp. *Mol Immunol*, *46*(8-9), 1688-1695. doi:10.1016/j.molimm.2009.02.020
- Ding, Z., Jin, M., & Ren, Q. (2018). Transcriptome analysis of *Macrobrachium rosenbergii* intestines under the white spot syndrome virus and poly (I:C) challenges. *PLoS One*, *13*(9), e0204626. doi:10.1371/journal.pone.0204626
- Ding, Z. F., Ren, J., Tan, J. M., Wang, Z., Yin, S. W., Huang, Y., . . . Ren, Q. (2015). Characterization of two novel ADP ribosylation factors from giant freshwater prawn *Macrobrachium rosenbergii* and their responses to WSSV challenge. *Dev Comp Immunol*, *48*(1), 204-209. doi:10.1016/j.dci.2014.10.006
- Dykxhoorn, D. M., Novina, C. D., & Sharp, P. A. (2003). Killing the messenger: short RNAs that silence gene expression. *Nat Rev Mol Cell Biol*, *4*(6), 457-467. doi:10.1038/nrm1129
- Elbashir, S. M., Lendeckel, W., & Tuschl, T. (2001). RNA interference is mediated by 21- and 22-nucleotide RNAs. *Genes Dev*, *15*(2), 188-200. doi:10.1101/gad.862301
- Elbashir, S. M., Lendeckel, W., & Tuschl, T. (2001). RNA interference is mediated by 21- and 22-nucleotide RNAs. *Genes Dev*, *15*(2), 188-200.
- Everett, H., & McFadden, G. (1999). Apoptosis: an innate immune response to virus infection. *Trends Microbiol*, *7*(4), 160-165.
- Ewels, P., Magnusson, M., Lundin, S., & Kaller, M. (2016). MultiQC: summarize analysis results for multiple tools and samples in a single report. *Bioinformatics*, *32*(19), 3047-3048. doi:10.1093/bioinformatics/btw354

- Fagard, M., Boutet, S., Morel, J. B., Bellini, C., & Vaucheret, H. (2000). AGO1, QDE-2, and RDE-1 are related proteins required for post-transcriptional gene silencing in plants, quelling in fungi, and RNA interference in animals. *Proc Natl Acad Sci U S A*, 97(21), 11650-11654. doi:10.1073/pnas.200217597
- Fagutao, F. F., Maningas, M. B., Kondo, H., Aoki, T., & Hirono, I. (2012). Transglutaminase regulates immune-related genes in shrimp. *Fish Shellfish Immunol*, 32(5), 711-715. doi:10.1016/j.fsi.2012.01.018
- Feng, J., Zhao, L., Jin, M., Li, T., Wu, L., Chen, Y., & Ren, Q. (2016). Toll receptor response to white spot syndrome virus challenge in giant freshwater prawns (*Macrobrachium rosenbergii*). *Fish Shellfish Immunol*, 57, 148-159. doi:10.1016/j.fsi.2016.08.017
- Ferri, K. F., & Kroemer, G. (2001). Organelle-specific initiation of cell death pathways. *Nat Cell Biol*, 3(11), E255-263. doi:10.1038/ncb1101-e255
- Flegel, T. W., Lightner, D. V., Lo, C., & Owens, L. (2008). Shrimp disease control: past, present and future. *Diseases in Asian Aquaculture VI Fish Health Section*, 355-378.
- Frohman, M. A. (1994). On beyond classic RACE (rapid amplification of cDNA ends). *PCR Methods Appl*, 4(1), S40-58.
- Gachet, Y., Tournier, S., Lee, M., Lazaris-Karatzas, A., Poulton, T., & Bommer, U. A. (1999). The growth-related, translationally controlled protein P23 has properties of a tubulin binding protein and associates transiently with microtubules during the cell cycle. *J Cell Sci*, 112 (Pt 8), 1257-1271.
- Gene Ontology, C. (2008). The Gene Ontology project in 2008. *Nucleic Acids Res*, 36(Database issue), D440-444. doi:10.1093/nar/gkm883
- Ghaffari, N., Sanchez-Flores, A., Doan, R., Garcia-Orozco, K. D., Chen, P. L., Ochoa-Leyva, A., . . . Criscitiello, M. F. (2014). Novel transcriptome assembly and improved annotation of the whiteleg shrimp (*Litopenaeus vannamei*), a dominant crustacean in global seafood mariculture. *Sci Rep*, 4, 7081. doi:10.1038/srep07081

- GmbH, L. (2018). SENSE mRNA-Seq Library Prep Kit V2 - User Guide. Retrieved from https://www.lexogen.com/wp-content/uploads/2019/03/001UG004V0322_SENSE-mRNA-Seq.pdf
- Goodman, C. A., Coenen, A. M., Frey, J. W., You, J. S., Barker, R. G., Frankish, B. P., . . . Hornberger, T. A. (2017). Insights into the role and regulation of TCTP in skeletal muscle. *Oncotarget*, *8*(12), 18754-18772. doi:10.18632/oncotarget.13009
- Grabherr, M. G., Haas, B. J., Yassour, M., Levin, J. Z., Thompson, D. A., Amit, I., . . . Regev, A. (2011). Full-length transcriptome assembly from RNA-Seq data without a reference genome. *Nat Biotechnol*, *29*(7), 644-652. doi:10.1038/nbt.1883
- Gregory, J. H. (2002). RNA interference. *Nature*, *418*, 244-251.
- Griffith, M., Griffith, O. L., Mwenifumbo, J., Goya, R., Morrissy, A. S., Morin, R. D., . . . Marra, M. A. (2010). Alternative expression analysis by RNA sequencing. *Nat Methods*, *7*(10), 843-847. doi:10.1038/nmeth.1503
- Gross, B., Gaestel, M., Boehm, H., & Bielka, H. (1989). cDNA sequence coding for a translationally controlled human tumour protein. *Nucleic Acids Research*, *17*, 8367.
- Haas, B. J., Papanicolaou, A., Yassour, M., Grabherr, M., Blood, P. D., Bowden, J., . . . Regev, A. (2013). De novo transcript sequence reconstruction from RNA-seq using the Trinity platform for reference generation and analysis. *Nat Protoc*, *8*(8), 1494-1512. doi:10.1038/nprot.2013.084
- Hall, M., Wang, R., van Antwerpen, R., Sottrup-Jensen, L., & Soderhall, K. (1999). The crayfish plasma clotting protein: a vitellogenin-related protein responsible for clot formation in crustacean blood. *Proc Natl Acad Sci U S A*, *96*(5), 1965-1970.
- Hand, S. C., & Menze, M. A. (2008). Mitochondria in energy-limited states: mechanisms that blunt the signaling of cell death. *J Exp Biol*, *211*, 1829-1840.
- Hannon, G. J. (2002). RNA interference. *Nature*, *418*(6894), 244-251. doi:10.1038/418244a
- Hedengren, M., Asling, B., Dushay, M. S., Ando, I., Ekengren, S., Wihlborg, M., & Hultmark, D. (1999). Relish, a central factor in the control of humoral but not cellular immunity in *Drosophila*. *Mol Cell*, *4*(5), 827-837.

- Holthuis, L. B. (2000). Nomenclature and taxonomy. In M. B. New & W. C. Valenti (Eds.), *Freshwater Prawn Culture. The Farming of Macrobrachium rosenbergii* (pp. 18-40): Blackwell Science.
- Huang, T., & Zhang, X. (2012). Functional analysis of a crustacean microRNA in host-virus interactions. *J Virol*, *86*(23), 12997-13004. doi:10.1128/JVI.01702-12
- Huang, T., & Zhang, X. (2013a). Host defense against DNA virus infection in shrimp is mediated by the siRNA pathway. *Eur. J. Immunol*, *43*, 137-146.
- Huang, T., & Zhang, X. (2013b). Host defense against DNA virus infection in shrimp is mediated by the siRNA pathway. *Eur J Immunol*, *43*(1), 137-146. doi:10.1002/eji.201242806
- Huang, X., Huang, Y., Shi, Y. R., Ren, Q., & Wang, W. (2015). Function of a novel C-type lectin with two CRD domains from *Macrobrachium rosenbergii* in innate immunity. *Dev Comp Immunol*, *49*(1), 121-126. doi:10.1016/j.dci.2014.11.015
- Huang, Y., & Ren, Q. (2015). Identification and function of 11 Rab GTPases in giant freshwater prawn *Macrobrachium rosenbergii*. *Fish Shellfish Immunol*, *43*(1), 120-130. doi:10.1016/j.fsi.2014.12.021
- Huerlimann, R., Wade, N. M., Gordon, L., Montenegro, J. D., Goodall, J., McWilliam, S., . . . Jerry, D. R. (2018). De novo assembly, characterization, functional annotation and expression patterns of the black tiger shrimp (*Penaeus monodon*) transcriptome. *Sci Rep*, *8*(1), 13553. doi:10.1038/s41598-018-31148-4
- Huerta-Cepas, J., Szklarczyk, D., Forslund, K., Cook, H., Heller, D., Walter, M. C., . . . Bork, P. (2016). eggNOG 4.5: a hierarchical orthology framework with improved functional annotations for eukaryotic, prokaryotic and viral sequences. *Nucleic Acids Res*, *44*(D1), D286-293. doi:10.1093/nar/gkv1248
- i, K. C. (2013). The i5K Initiative: advancing arthropod genomics for knowledge, human health, agriculture, and the environment. *J Hered*, *104*(5), 595-600. doi:10.1093/jhered/est050

- Illumina, I. (2016). Nextera DNA Library Prep Kit. Retrieved from https://www.illumina.com/documents/products/datasheets/datasheet_nextera_dna_sample_prep.pdf
- Illumina, I. (2017). An introduction to Next-Generation Sequencing Technology. Retrieved from https://www.illumina.com/content/dam/illumina-marketing/documents/products/illumina_sequencing_introduction.pdf
- Jariyapong, P., Pudgerd, A., Cheloh, N., Hirono, I., Kondo, H., Vanichviriyakit, R., . . . Chotwiwatthanakun, C. (2019). Hematopoietic tissue of *Macrobrachium rosenbergii* plays dual roles as a source of hemocyte hematopoiesis and as a defensive mechanism against *Macrobrachium rosenbergii* nodavirus infection. *Fish Shellfish Immunol*, 86, 756-763. doi:10.1016/j.fsi.2018.12.021
- Jensen, S., & Thomsen, A. R. (2012). Sensing of RNA viruses: a review of innate immune receptors involved in recognizing RNA virus invasion. *J Virol*, 86(6), 2900-2910. doi:10.1128/JVI.05738-11
- Jiravanichpaisal, P., Lee, B. L., & Soderhall, K. (2006). Cell-mediated immunity in arthropods: hematopoiesis, coagulation, melanization and opsonization. *Immunobiology*, 211(4), 213-236. doi:10.1016/j.imbio.2005.10.015
- Johansson, M. W., Keyser, P., & Sritunyalucksana, K. (2000). Crustacean haemocytes and haematopoiesis. *Aquaculture*, 191, 45-52.
- Kamath, R. S., Fraser, A. G., Dong, Y., Poulin, G., Durbin, R., Gotta, M., . . . Ahringer, J. (2003). Systematic functional analysis of the *Caenorhabditis elegans* genome using RNAi. *Nature*, 421(6920), 231-237. doi:10.1038/nature01278
- Kanehisa, M., & Goto, S. (2000). KEGG: kyoto encyclopedia of genes and genomes. *Nucleic Acids Res*, 28(1), 27-30. doi:10.1093/nar/28.1.27
- Kang, H. S., Lee, M. J., Song, H., Han, S. H., Kim, Y. M., Im, J. Y., & Choi, I. (2001). Molecular identification of IgE-dependent histamine-releasing factor as a B cell growth factor. *J Immunol*, 166(11), 6545-6554.
- Karam, J. A. (2009). *Apoptosis in Carcinogenesis and Chemotherapy*. Netherlands: Springer.

- Kim, M., Jung, Y., Lee, K., & Kim, C. (2000). Identification of the calcium binding sites in translationally controlled tumour protein. *Archives of Pharmacological Research*, 22, 633-636.
- Koster, J., & Rahmann, S. (2012). Snakemake--a scalable bioinformatics workflow engine. *Bioinformatics*, 28(19), 2520-2522. doi:10.1093/bioinformatics/bts480
- Koyama, A. H., Fukumori, T., Fujita, M., Irie, H., & Adachi, A. (2000). Physiological significance of apoptosis in animal virus infection. *Microbes Infect*, 2(9), 1111-1117.
- Kumar, S. (2007). Caspase function in programmed cell death. *Cell Death Differ*, 14(1), 32-43. doi:10.1038/sj.cdd.4402060
- Kupferschmidt, K. (2013). A lethal dose of RNA. *Science*, 341(6147), 732-733. doi:10.1126/science.341.6147.732
- Labreuche, Y., Veloso, A., de la Vega, E., Gross, P. S., Chapman, R. W., Browdy, C. L., & Warr, G. W. (2010). Non-specific activation of antiviral immunity and induction of RNA interference may engage the same pathway in the Pacific white leg shrimp *Litopenaeus vannamei*. *Dev Comp Immunol*, 34(11), 1209-1218. doi:10.1016/j.dci.2010.06.017
- Langmead, B., & Salzberg, S. L. (2012). Fast gapped-read alignment with Bowtie 2. *Nat Methods*, 9(4), 357-359. doi:10.1038/nmeth.1923
- Lemaitre, B., & Hoffmann, J. (2007). The host defense of *Drosophila melanogaster*. *Annu Rev Immunol*, 25, 697-743. doi:10.1146/annurev.immunol.25.022106.141615
- Leu, J. H., Kuo, Y. C., Kou, G. H., & Lo, C. F. (2008). Molecular cloning and characterization of an inhibitor of apoptosis protein (IAP) from the tiger shrimp, *Penaeus monodon*. *Dev Comp Immunol*, 32(2), 121-133. doi:10.1016/j.dci.2007.05.005
- Leu, J. H., Lin, S. J., Huang, J. Y., Chen, T. C., & Lo, C. F. (2013). A model for apoptotic interaction between white spot syndrome virus and shrimp. *Fish Shellfish Immunol*, 34, 1011-1017.

- Levy, T., Rosen, O., Simons, O., Savaya Alkalay, A., & Sagi, A. (2017). The gene encoding the insulin-like androgenic gland hormone in an all-female parthenogenetic crayfish. *PLoS One*, *12*(12), e0189982. doi:10.1371/journal.pone.0189982
- Li, B., & Dewey, C. N. (2011). RSEM: accurate transcript quantification from RNA-Seq data with or without a reference genome. *BMC Bioinformatics*, *12*, 323. doi:10.1186/1471-2105-12-323
- Li, C., Weng, S., Chen, Y., Yu, X., Lu, L., Zhang, H., . . . Xu, X. (2012). Analysis of *Litopenaeus vannamei* Transcriptome Using the Next-Generation DNA Sequencing Technique. *PLoS One*, *7*(10), 1-12.
- Li, F., & Xiang, J. (2013). Recent advances in researches on the innate immunity of shrimp in China. *Dev Comp Immunol*, *39*(1-2), 11-26. doi:10.1016/j.dci.2012.03.016
- Li, F., Zhang, D., & Fujise, K. (2001). Characterization of fortilin, a novel antiapoptotic protein. *J Biol Chem*, *276*(50), 47542-47549. doi:10.1074/jbc.M108954200
- Li, H., Li, W. X., & Ding, S. W. (2002). Induction and suppression of RNA silencing by an animal virus. *Science*, *296*(5571), 1319-1321. doi:10.1126/science.1070948
- Li, S., Zhang, X., Sun, Z., Li, F., & Xiang, J. (2013). Transcriptome analysis on Chinese shrimp *Fenneropenaeus chinensis* during WSSV acute infection. *PLoS One*, *8*(3), e58627. doi:10.1371/journal.pone.0058627
- Li, W., & Godzik, A. (2006). Cd-hit: a fast program for clustering and comparing large sets of protein or nucleotide sequences. *Bioinformatics*, *22*(13), 1658-1659. doi:10.1093/bioinformatics/btl158
- Lightner, D. V., & Redman, R. M. (1998). Shrimp diseases and current diagnostic methods. *Aquaculture*, *164*(1-4), 201-220.
- Lipardi, C., Wei, Q., & Paterson, B. M. (2001). RNAi as random degradative PCR: siRNA primers convert mRNA into dsRNAs that are degraded to generate new siRNAs. *Cell*, *107*(3), 297-307.
- Liu, H., Peng, H. W., Cheng, Y. S., Yuan, H. S., & Yang-Yen, H. F. (2005). Stabilization and enhancement of the antiapoptotic activity of mcl-1 by TCTP. *Mol Cell Biol*, *25*(8), 3117-3126. doi:10.1128/MCB.25.8.3117-3126.2005

- Liu, W., Han, F., & Zhang, X. (2009). Ran GTPase regulates hemocytic phagocytosis of shrimp by interaction with myosin. *J Proteome Res*, 8(3), 1198-1206. doi:10.1021/pr800840x
- Livak, K. J., & Schmittgen, T. D. (2001). Analysis of relative gene expression data using real-time quantitative PCR and the 2(-Delta Delta C(T)) Method. *Methods*, 25(4), 402-408. doi:10.1006/meth.2001.1262
- Lu, K. Y., Huang, Y. T., Lee, H. H., & Sung, H. H. (2006). Cloning the prophenoloxidase cDNA and monitoring the expression of proPO mRNA in prawns (*Macrobrachium rosenbergii*) stimulated in vivo by CpG oligodeoxynucleotides. *Fish Shellfish Immunol*, 20(3), 274-284. doi:10.1016/j.fsi.2005.05.001
- Ma, J., Zhang, M., Ruan, L., Shi, H., & Xu, X. (2010). Characterization of two novel ADP ribosylation factors from the shrimp *Marsupenaeus japonicus*. *Fish Shellfish Immunol*, 29(6), 956-962. doi:10.1016/j.fsi.2010.08.003
- MacDonald, S. M., Bhisutthibhan, J., Shapiro, T. A., Rogerson, S. J., Taylor, T. E., Tembo, M., . . . Meshnick, S. R. (2001). Immune mimicry in malaria: *Plasmodium falciparum* secretes a functional histamine-releasing factor homolog in vitro and in vivo. *Proc Natl Acad Sci U S A*, 98(19), 10829-10832. doi:10.1073/pnas.201191498
- MacDonald, S. M., Rafnar, T., Langdon, J., & Lichtenstein, L. M. (1995). Molecular identification of an IgE-dependent histamine-releasing factor. *Science*, 269(5224), 688-690.
- Maningas, M. B., Kondo, H., & Hirono, I. (2013). Molecular mechanisms of the shrimp clotting system. *Fish Shellfish Immunol*, 34(4), 968-972. doi:10.1016/j.fsi.2012.09.018
- Mardis, E. R. (2008). Next-generation DNA sequencing methods. *Annu Rev Genomics Hum Genet*, 9, 387-402. doi:10.1146/annurev.genom.9.081307.164359
- Mardis, E. R. (2013). Next-generation sequencing platforms. *Annu Rev Anal Chem (Palo Alto Calif)*, 6, 287-303. doi:10.1146/annurev-anchem-062012-092628
- Medzhitov, R., & Janeway, C., Jr. (2000). Innate immunity. *N Engl J Med*, 343(5), 338-344. doi:10.1056/NEJM200008033430506

- Menze, M. A., Fortner, G., Nag, S., & Hand, S. C. (2010). Mechanisms of apoptosis in Crustacea: What conditions induce versus suppress cell death? *Apoptosis*, *15*(3), 293-312. doi:10.1007/s10495-009-0443-6
- Misra, S., Hecht, P., Maeda, R., & Anderson, K. V. (1998). Positive and negative regulation of Easter, a member of the serine protease family that controls dorsal-ventral patterning in the *Drosophila* embryo. *Development*, *125*(7), 1261-1267.
- Morozova, O., & Marra, M. A. (2008). Applications of next-generation sequencing technologies in functional genomics. *Genomics*, *92*(5), 255-264. doi:10.1016/j.ygeno.2008.07.001
- Mortazavi, A., Williams, B. A., McCue, K., Schaeffer, L., & Wold, B. (2008). Mapping and quantifying mammalian transcriptomes by RNA-Seq. *Nat Methods*, *5*(7), 621-628. doi:10.1038/nmeth.1226
- Motoh, H., & Kuronuma, K. (1980). *Field guide for the edible crustacea of the Philippines* (S. A. F. D. C. Aquaculture Department Ed.). Iloilo, Philippines.
- Murphy, F. A., Fauquet, C. M., Bishop, D. H. L., Ghabrial, S. A., Jarvis, A., Martelli, G. P., . . . Summers, M. D. (1995). *Virus Taxonomy: Classification and Nomenclature of Viruses*: Springer-Verlag Wien.
- Myers, K. R., & Casanova, J. E. (2008). Regulation of actin cytoskeleton dynamics by Arp-family GTPases. *Trends Cell Biol*, *18*(4), 184-192. doi:10.1016/j.tcb.2008.02.002
- Nagano-Ito, M., Banba, A., & Ichikawa, S. (2009). Functional cloning of genes that suppress oxidative stress-induced cell death: TCTP prevents hydrogen peroxide-induced cell death. *FEBS Lett*, *583*(8), 1363-1367. doi:10.1016/j.febslet.2009.03.045
- Nakamoto, M., Moy, R. H., Xu, J., Bambina, S., Yasunaga, A., Shelly, S. S., . . . Cherry, S. (2012). Virus recognition by Toll-7 activates antiviral autophagy in *Drosophila*. *Immunity*, *36*(4), 658-667. doi:10.1016/j.immuni.2012.03.003
- New, M. B. (2000). Commercial freshwater prawn farming around the World. In M. B. New & W. C. Valenti (Eds.), *Freshwater Prawn Culture. The Farming of Macrobrachium rosenbergii* (pp. 290-325): Blackwell Science.

- Nguyen, C., Nguyen, T. G., Nguyen, L. V., Pham, H. Q., Nguyen, T. H., Pham, H. T., . . . Dinh, K. D. (2016). De novo assembly and transcriptome characterization of major growth-related genes in various tissues of *Penaeus monodon*. *Aquaculture*, *464*, 545-553.
- Nielsen, H. V., Johnsen, A. H., Sanchez, J. C., Hochstrasser, D. F., & Schiotz, P. O. (1998). Identification of a basophil leukocyte interleukin-3-regulated protein that is identical to IgE-dependent histamine-releasing factor. *Allergy*, *53*(7), 642-652.
- Nykanen, A., Haley, B., & Zamore, P. D. (2001). ATP requirements and small interfering RNA structure in the RNA interference pathway. *Cell*, *107*(3), 309-321.
- OIE. (2009). WHITE TAIL DISEASE In *Manual of Diagnostic Tests for Aquatic Animals* (pp. 132-143).
- Oikawa, K., Ohbayashi, T., Mimura, J., Fujii-Kuriyama, Y., Teshima, S., Rokutan, K., . . . Kuroda, M. (2002). Dioxin stimulates synthesis and secretion of IgE-dependent histamine-releasing factor. *Biochem Biophys Res Commun*, *290*(3), 984-987. doi:10.1006/bbrc.2001.6302
- Oladapo, Y., & Michael, A. F. (2011). Rapid Amplification of cDNA Ends (RACE). In H. Nielsen (Ed.), *RNA: Methods and Protocols (Methods in Molecular Biology, 703)* (pp. 107-122): Springer Science+Business Media.
- Owens, L., La Fauce, K., Juntunen, K., Hayakijkosol, O., & Zeng, C. (2009). Macrobrachium rosenbergii nodavirus disease (white tail disease) in Australia. *Dis Aquat Organ*, *85*(3), 175-180. doi:10.3354/dao02086
- Powell, D., Knibb, W., Remilton, C., & Elizur, A. (2015). De-novo transcriptome analysis of the banana shrimp (*Fenneropenaeus merguensis*) and identification of genes associated with reproduction and development. *Mar Genomics*, *22*, 71-78. doi:10.1016/j.margen.2015.04.006
- Poynton, H. C., Hasenbein, S., Benoit, J. B., Sepulveda, M. S., Poelchau, M. F., Hughes, D. S. T., . . . Richards, S. (2018). The Toxicogenome of *Hyalella azteca*: A Model for Sediment Ecotoxicology and Evolutionary Toxicology. *Environ Sci Technol*, *52*(10), 6009-6022. doi:10.1021/acs.est.8b00837

- Qian, D., Shi, Z., Zhang, S., Cao, Z., Liu, W., Li, L., . . . Bonami, J. R. (2003). Extra small virus-like particle (XSV) and nodavirus associated with whitish muscle disease in the giant freshwater prawn, *Macrobrachium rosenbergii*. *J. Fish Dis.* , 26, 521-527.
- Rajesh, S., Kamalakannan, V., & Narayanan, R. B. (2014). Immune modulations and protection by translationally controlled tumor protein (TCTP) in *Fenneropenaeus indicus* harboring white spot syndrome virus infection. *J Invertebr Pathol*, 120, 33-39. doi:10.1016/j.jip.2014.05.003
- Rajesh, S., Kiruthiga, C., Rashika, V., Priya, R., & Narayanan, R. B. (2010). Molecular cloning, sequence analysis and tissue expression of translationally controlled tumour protein from the WSSV-infected Indian shrimp *Penaeus indicus*. *Aquaculture research*, 41(4), 545-551.
- Rao, R., Bhassu, S., Bing, R. Z., Alinejad, T., Hassan, S. S., & Wang, J. (2016). A transcriptome study on *Macrobrachium rosenbergii* hepatopancreas experimentally challenged with white spot syndrome virus (WSSV). *J Invertebr Pathol*, 136, 10-22. doi:10.1016/j.jip.2016.01.002
- Rao, R., Bing Zhu, Y., Alinejad, T., Tiruvayipati, S., Lin Thong, K., Wang, J., & Bhassu, S. (2015). RNA-seq analysis of *Macrobrachium rosenbergii* hepatopancreas in response to *Vibrio parahaemolyticus* infection. *Gut Pathog*, 7, 6. doi:10.1186/s13099-015-0052-6
- Ravi, M., Nazeer Basha, A., Taju, G., Ram Kumar, R., & Sahul Hameed, A. S. (2010). Clearance of *Macrobrachium rosenbergii* nodavirus (MrNV) and extra small virus (XSV) and immunological changes in experimentally injected *Macrobrachium rosenbergii*. *Fish Shellfish Immunol*, 28(3), 428-433. doi:10.1016/j.fsi.2009.11.022
- Ren, Q., Zhang, Z., Li, X. C., Jie, D., Hui, K. M., Zhang, C. Y., & Wang, W. (2012). Three different anti-lipopolysaccharide factors identified from giant freshwater prawn, *Macrobrachium rosenbergii*. *Fish Shellfish Immunol*, 33(4), 766-774. doi:10.1016/j.fsi.2012.06.032

- Rho, S. B., Lee, J. H., Park, M. S., Byun, H. J., Kang, S., Seo, S. S., . . . Park, S. Y. (2011). Anti-apoptotic protein TCTP controls the stability of the tumor suppressor p53. *FEBS Lett*, *585*(1), 29-35. doi:10.1016/j.febslet.2010.11.014
- Robinson, M. D., McCarthy, D. J., & Smyth, G. K. (2010). edgeR: a Bioconductor package for differential expression analysis of digital gene expression data. *Bioinformatics*, *26*(1), 139-140. doi:10.1093/bioinformatics/btp616
- Robinson, M. D., & Oshlack, A. (2010). A scaling normalization method for differential expression analysis of RNA-seq data. *Genome Biol*, *11*(3), R25. doi:10.1186/gb-2010-11-3-r25
- Roch, P. (1999). Defense mechanisms and disease prevention in farmed marine invertebrates. *Aquaculture*, *172*, 125-145.
- Rosa, R. D., & Barracco, M. A. (2010). Antimicrobial peptides in crustaceans. *Invertebrate Survival Journal*, *7*, 262-284.
- Roy, N., Deveraux, Q. L., Takahashi, R., Salvesen, G. S., & Reed, J. C. (1997). The c-IAP-1 and c-IAP-2 proteins are direct inhibitors of specific caspases. *EMBO J*, *16*(23), 6914-6925. doi:10.1093/emboj/16.23.6914
- Sadler, A. J., & Williams, B. R. (2008). Interferon-inducible antiviral effectors. *Nat Rev Immunol*, *8*(7), 559-568. doi:10.1038/nri2314
- Sahoo, P. K., Shekhar, M. S., Das, A., Kumar, M. D., Pillai, B. R., & Sahul Hameed, A. (2012). Immunomodulatory effect of recombinant RNA-dependent RNA polymerase protein of *Macrobrachium rosenbergii* nodavirus in giant freshwater prawn *M. rosenbergii*. *Aquaculture research*, *43*(8), 1096-1106.
- Sahul Hameed, A. S., Yoganandhan, K., Sri Widada, J., & Bonami, J. R. (2004). Experimental transmission and tissue tropism of *Macrobrachium rosenbergii* nodavirus (MrNV) and its associated extra small virus (XSV). *Dis Aquat Organ*, *62*(3), 191-196. doi:10.3354/dao062191
- Saurabh, S., Vidyarthi, A. S., & Prasad, D. (2014). RNA interference: concept to reality in crop improvement. *Planta*, *239*(3), 543-564. doi:10.1007/s00425-013-2019-5

- Sellars, M. J., Trewin, C., McWilliam, S. M., Graves, R. S., & Hertzler, P. L. (2015). Transcriptome profiles of *Penaeus (Marsupenaeus) japonicus* animal and vegetal half-embryos: identification of sex determination, germ line, mesoderm, and other developmental genes. *Mar Biotechnol (NY)*, *17*(3), 252-265. doi:10.1007/s10126-015-9613-4
- Senapin, S., Phewsaiya, K., Briggs, M., & Flegel, T. W. (2007). Outbreaks of infectious myonecrosis virus (IMNV) in Indonesia confirmed by genome sequencing and use of an alternative RT-PCR detection method. *Aquaculture*, *266*(1-4), 32-38.
- Senapin, S., Phiwsaiya, K., Gangnonngiw, W., Briggs, M., Sithigorngul, P., & Flegel, T. W. (2012). Infections of MrNV (*Macrobrachium rosenbergii* nodavirus) in cultivated whiteleg shrimp *Penaeus vannamei* in Asia. *Aquaculture*, *338-341*, 41-46. doi:10.1016/j.aquaculture.2012.01.019
- Shi, X., Meng, X., Kong, J., Luan, S., Luo, K., Cao, B., . . . Cao, J. (2018). Transcriptome analysis of 'Huanghai No. 2' *Fenneropenaeus chinensis* response to WSSV using RNA-seq. *Fish Shellfish Immunol*, *75*, 132-138. doi:10.1016/j.fsi.2018.01.045
- Shi, X. Z., Zhang, R. R., Jia, Y. P., Zhao, X. F., Yu, X. Q., & Wang, J. X. (2009). Identification and molecular characterization of a Spatzle-like protein from Chinese shrimp (*Fenneropenaeus chinensis*). *Fish Shellfish Immunol*, *27*(5), 610-617. doi:10.1016/j.fsi.2009.07.005
- Shi, Y. R., Jin, M., Ma, F. T., Huang, Y., Huang, X., Feng, J. L., . . . Ren, Q. (2015). Involvement of Relish gene from *Macrobrachium rosenbergii* in the expression of anti-microbial peptides. *Dev Comp Immunol*, *52*(2), 236-244. doi:10.1016/j.dci.2015.05.008
- Shoshan-Barmatz, V., & Ben-Hail, D. (2012). VDAC, a multi-functional mitochondrial protein as a pharmacological target. *Mitochondrion* *12*, 24-34.
- Shpak, N., Manor, R., Aibilevich, L. K., Mantal, O., Shavit, K., Aflalo, E. D., . . . Sagi, A. (2017). Short versus long double-stranded RNA activation of a post-transcriptional gene knockdown pathway. *RNA Biol*, *14*(12), 1766-1775. doi:10.1080/15476286.2017.1356567

- Sijen, T., Fleenor, J., Simmer, F., Thijssen, K. L., Parrish, S., Timmons, L., . . . Fire, A. (2001). On the role of RNA amplification in dsRNA-triggered gene silencing. *Cell*, *107*(4), 465-476.
- Simao, F. A., Waterhouse, R. M., Ioannidis, P., Kriventseva, E. V., & Zdobnov, E. M. (2015). BUSCO: assessing genome assembly and annotation completeness with single-copy orthologs. *Bioinformatics*, *31*(19), 3210-3212. doi:10.1093/bioinformatics/btv351
- Sinha, P., Kohl, S., Fischer, J., Hutter, G., Kern, M., Kottgen, E., . . . Schadendorf, D. (2000). Identification of novel proteins associated with the development of chemoresistance in malignant melanoma using two-dimensional electrophoresis. *Electrophoresis*, *21*(14), 3048-3057. doi:10.1002/1522-2683(20000801)21:14<3048::AID-ELPS3048>3.0.CO;2-W
- Sinthujaroen, P., Tonganunt, M., Eurwilaichitr, L., & Phongdara, A. (2015). Protection of *Litopenaeus vannamei* against the white spot syndrome virus using recombinant Pm-fortilin expressed in *Pichia pastoris*. *Aquaculture*, *435*, 450–457.
- Sirois, I., Raymond, M. A., Brassard, N., Cailhier, J. F., Fedjaev, M., Hamelin, K., . . . Hebert, M. J. (2011). Caspase-3-dependent export of TCTP: a novel pathway for antiapoptotic intercellular communication. *Cell Death Differ*, *18*(3), 549-562. doi:10.1038/cdd.2010.126
- Soderhall, K., & Cerenius, L. (1998). Role of the prophenoloxidase-activating system in invertebrate immunity. *Curr Opin Immunol*, *10*(1), 23-28.
- Soderhall, K., Cerenius, L., & Johansson, M. W. (1994). The prophenoloxidase activating system and its role in invertebrate defence. *Ann N Y Acad Sci*, *712*, 155-161.
- Song, Y. L., & Hsieh, Y. T. (1994). Immunostimulation of tiger shrimp (*Penaeus monodon*) hemocytes for generation of microbicidal substances: analysis of reactive oxygen species. *Dev Comp Immunol*, *18*(3), 201-209.
- Soonthornchai, W., Chaiyapechara, S., Klinbunga, S., Thongda, W., Tangphatsornruang, S., Yoocha, T., . . . Jiravanichpaisal, P. (2016). Differentially expressed transcripts

- in stomach of *Penaeus monodon* in response to AHPND infection. *Dev Comp Immunol*, 65, 53-63. doi:10.1016/j.dci.2016.06.013
- Sricharoen, S., Kim, J. J., Tunkijjanukij, S., & Soderhall, I. (2005). Exocytosis and proteomic analysis of the vesicle content of granular hemocytes from a crayfish. *Dev Comp Immunol*, 29(12), 1017-1031. doi:10.1016/j.dci.2005.03.010
- Srisuk, C., Longyant, S., Senapin, S., Sithigorngul, P., & Chaivisuthangkura, P. (2014). Molecular cloning and characterization of a Toll receptor gene from *Macrobrachium rosenbergii*. *Fish Shellfish Immunol*, 36(2), 552-562. doi:10.1016/j.fsi.2013.12.025
- Stuart, L. M., & Ezekowitz, R. A. (2008). Phagocytosis and comparative innate immunity: learning on the fly. *Nat Rev Immunol*, 8(2), 131-141. doi:10.1038/nri2240
- Su, J., Oanh, D. T., Lyons, R. E., Leeton, L., van Hulten, M. C., Tan, S. H., . . . Walker, P. J. (2008). A key gene of the RNA interference pathway in the black tiger shrimp, *Penaeus monodon*: identification and functional characterisation of Dicer-1. *Fish Shellfish Immunol*, 24(2), 223-233. doi:10.1016/j.fsi.2007.11.006
- Sudhakaran, R., Ishaq Ahmed, V. P., Haribabu, P., Mukherjee, S. C., Sri Widada, J., Bonami, J. R., & Sahul Hameed, A. S. (2007). Experimental vertical transmission of *Macrobrachium rosenbergii* nodavirus (MrNV) and extra small virus (XSV) from brooders to progeny in *Macrobrachium rosenbergii* and *Artemia*. *J Fish Dis*, 30(1), 27-35. doi:10.1111/j.1365-2761.2007.00774.x
- Swapna, P. A., Rosamma, P., Valsamma, J., & BrightSingh, I. S. (2011). Anti-lipopolysaccharide factor and crustin-III, the anti-white spot virus peptides in *Penaeus monodon*: Control of viral infection by up-regulation. *Aquaculture*, 319(1-2), 11-17.
- Teshima, S., Rokutan, K., Nikawa, T., & Kishi, K. (1998). Macrophage colony-stimulating factor stimulates synthesis and secretion of a mouse homolog of a human IgE-dependent histamine-releasing factor by macrophages in vitro and in vivo. *J Immunol*, 161(11), 6356-6366.

- Thaw, P., Baxter, N. J., Hounslow, A. M., Price, C., Waltho, J. P., & Craven, C. J. (2001). Structure of TCTP reveals unexpected relationship with guanine nucleotide-free chaperones. *Nat Struct Biol*, 8(8), 701-704. doi:10.1038/90415
- Thiele, H., Berger, M., Skalweit, A., & Thiele, B. J. (2000). Expression of the gene and processed pseudogenes encoding the human and rabbit translationally controlled tumour protein (TCTP). *Eur J Biochem*, 267(17), 5473-5481.
- Thomas, G., Thomas, G., & Luther, H. (1981). Transcriptional and translational control of cytoplasmic proteins after serum stimulation of quiescent Swiss 3T3 cells. *Proc Natl Acad Sci U S A*, 78(9), 5712-5716.
- Tirasophon, W., Roshorm, Y., & Panyim, S. (2005). Silencing of yellow head virus replication in penaeid shrimp cells by dsRNA. *Biochem Biophys Res Commun*, 334(1), 102-107. doi:10.1016/j.bbrc.2005.06.063
- Tonganunt, M., Nupan, B., Saengsakda, M., Suklour, S., Wanna, W., Senapin, S., . . . Phongdara, A. (2008). The role of Pm-fortilin in protecting shrimp from white spot syndrome virus (WSSV) infection. *Fish Shellfish Immunol*, 25(5), 633-637. doi:10.1016/j.fsi.2008.08.006
- Towb, P., Bergmann, A., & Wasserman, S. A. (2001). The protein kinase Pelle mediates feedback regulation in the Drosophila Toll signaling pathway. *Development*, 128(23), 4729-4736.
- Tran, S. E., Meinander, A., & Eriksson, J. E. (2004). Instant decisions: transcription-independent control of death-receptor-mediated apoptosis. *Trends Biochem Sci*, 29(11), 601-608. doi:10.1016/j.tibs.2004.09.009
- Tung, C. W., Wang, C. S., & Chen, S. N. (1999). Histological and electron microscopy study on Macrobrachium muscle virus (MMV) infection in the giant freshwater prawn, *Macrobrachium rosenbergii* (de Man), cultured in Taiwan. *J. Fish Dis.*, 22, 71-75.
- Tuynder, M., Susini, L., Prieur, S., Besse, S., Fiucci, G., Amson, R., & Telerman, A. (2002). Biological models and genes of tumour reversion: Cellular reprogramming through

- tpt1/TCTP and SIAH-1. *Proceedings of the National Academy of Sciences of the United States of America*, 99, 14976–14981.
- Unajak, S., Boonsaeng, V., & Jitrapakdee, S. (2006). Isolation and characterization of cDNA encoding Argonaute, a component of RNA silencing in shrimp (*Penaeus monodon*). *Comp Biochem Physiol B Biochem Mol Biol*, 145(2), 179-187.
doi:10.1016/j.cbpb.2006.07.002
- UniProt, C. (2019). UniProt: a worldwide hub of protein knowledge. *Nucleic Acids Res*, 47(D1), D506-D515. doi:10.1093/nar/gky1049
- van de Braak, C. B., Botterblom, M. H., Liu, W., Taverne, N., van der Knaap, W. P., & Rombout, J. H. (2002). The role of the haematopoietic tissue in haemocyte production and maturation in the black tiger shrimp (*Penaeus monodon*). *Fish Shellfish Immunol*, 12(3), 253-272.
- Vaniksampanna, A., Longyant, S., Charoensapsri, W., Sithigorngul, P., & Chaivisuthangkura, P. (2019). Molecular isolation and characterization of a spatzie gene from *Macrobrachium rosenbergii*. *Fish Shellfish Immunol*, 84, 441-450.
doi:10.1016/j.fsi.2018.10.015
- Wang, B., Li, F., Dong, B., Zhang, X., Zhang, C., & Xiang, J. (2006). Discovery of the genes in response to white spot syndrome virus (WSSV) infection in *Fenneropenaeus chinensis* through cDNA microarray. *Mar Biotechnol (NY)*, 8(5), 491-500.
doi:10.1007/s10126-005-6136-4
- Wang, L., Zhi, B., Wu, W., & Zhang, X. (2008). Requirement for shrimp caspase in apoptosis against virus infection. *Dev Comp Immunol*, 32(6), 706-715.
doi:10.1016/j.dci.2007.10.010
- Wang, P. H., Liang, J. P., Gu, Z. H., Wan, D. H., Weng, S. P., Yu, X. Q., & He, J. G. (2012). Molecular cloning, characterization and expression analysis of two novel Tolls (LvToll2 and LvToll3) and three putative Spatzle-like Toll ligands (LvSpz1-3) from *Litopenaeus vannamei*. *Dev Comp Immunol*, 36(2), 359-371.
doi:10.1016/j.dci.2011.07.007

- Wang, P. H., Wan, D. H., Chen, Y. G., Weng, S. P., Yu, X. Q., & He, J. G. (2013). Characterization of four novel caspases from *Litopenaeus vannamei* (Lvcaspase2-5) and their role in WSSV infection through dsRNA-mediated gene silencing. *PLoS One*, *8*(12), e80418. doi:10.1371/journal.pone.0080418
- Wang, P. H., Wan, D. H., Gu, Z. H., Qiu, W., Chen, Y. G., Weng, S. P., . . . He, J. G. (2013). Analysis of expression, cellular localization, and function of three inhibitors of apoptosis (IAPs) from *Litopenaeus vannamei* during WSSV infection and in regulation of antimicrobial peptide genes (AMPs). *PLoS One*, *8*(8), e72592. doi:10.1371/journal.pone.0072592
- Wang, Q., Fang, D. A., Li, W. W., Wang, J., & Jiang, H. (2011). A novel TCTP gene from the crustacean *Eriocheir sinensis*: possible role involving metallic Cu²⁺ stress. *Biol Bull*, *221*(3), 290-299. doi:10.1086/BBLv221n3p290
- Wang, S., Zhao, X. F., & Wang, J. X. (2009). Molecular cloning and characterization of the translationally controlled tumor protein from *Fenneropenaeus chinensis*. *Mol Biol Rep*, *36*(7), 1683-1693. doi:10.1007/s11033-008-9369-2
- Wang, W., Wu, X., Liu, Z., Zheng, H., & Cheng, Y. (2014). Insights into hepatopancreatic functions for nutrition metabolism and ovarian development in the crab *Portunus trituberculatus*: gene discovery in the comparative transcriptome of different hepatopancreas stages. *PLoS One*, *9*(1), e84921. doi:10.1371/journal.pone.0084921
- Wang, W., Yang, S., Wang, C., Shi, L., Guo, H., & Chan, S. (2017). Gill transcriptomes reveal involvement of cytoskeleton remodeling and immune defense in ammonia stress response in the banana shrimp *Fenneropenaeus merguensis*. *Fish Shellfish Immunol*, *71*, 319-328. doi:10.1016/j.fsi.2017.10.028
- Wang, X. W., & Wang, J. X. (2013). Pattern recognition receptors acting in innate immune system of shrimp against pathogen infections. *Fish Shellfish Immunol*, *34*(4), 981-989. doi:10.1016/j.fsi.2012.08.008
- Watson, F. L., Puttmann-Holgado, R., Thomas, F., Lamar, D. L., Hughes, M., Kondo, M., . . . Schmucker, D. (2005). Extensive diversity of Ig-superfamily proteins in the

- immune system of insects. *Science*, 309(5742), 1874-1878.
doi:10.1126/science.1116887
- Widada, J. S., & Bonami, J. R. (2004). Characteristics of the monocistronic genome of extra small virus, a virus-like particle associated with *Macrobrachium rosenbergii* nodavirus: possible candidate for a new species of satellite virus. *J Gen Virol*, 85(Pt 3), 643-646. doi:10.1099/vir.0.79777-0
- Wiriya, L., Amornrat, P., & Wilaiwan, C. (2007). Cloning and expression of a TCTP homolog from the ovaries of banana prawn. *Marine Biology*, 150(3), 455-462.
- Wu, A. R., Neff, N. F., Kalisky, T., Dalerba, P., Treutlein, B., Rothenberg, M. E., . . . Quake, S. R. (2014). Quantitative assessment of single-cell RNA-sequencing methods. *Nat Methods*, 11(1), 41-46. doi:10.1038/nmeth.2694
- Wu, W., Wu, B., Ye, T., Huang, H., Dai, C., Yuan, J., & Wang, W. (2013). TCTP is a critical factor in shrimp immune response to virus infection. *PLoS One*, 8(9), e74460. doi:10.1371/journal.pone.0074460
- Wu, W., Zong, R., Xu, J., & Zhang, X. (2008). Antiviral phagocytosis is regulated by a novel Rab-dependent complex in shrimp *penaeus japonicus*. *J Proteome Res*, 7(1), 424-431. doi:10.1021/pr700639t
- Xu, A., Bellamy, A. R., & Taylor, J. A. (1999). Expression of translationally controlled tumour protein is regulated by calcium at both the transcriptional and post-transcriptional level. *Biochemical Journal*, 342, 683-689.
- Xu, J., Han, F., & Zhang, X. (2007). Silencing shrimp white spot syndrome virus (WSSV) genes by siRNA. *Antiviral Res*, 73(2), 126-131. doi:10.1016/j.antiviral.2006.08.007
- Yang, C., Zhang, J., Li, F., Ma, H., Zhang, Q., Jose Priya, T. A., . . . Xiang, J. (2008). A Toll receptor from Chinese shrimp *Fenneropenaeus chinensis* is responsive to *Vibrio anguillarum* infection. *Fish Shellfish Immunol*, 24(5), 564-574. doi:10.1016/j.fsi.2007.12.012
- Yang, G., Yang, L., Zhao, Z., Wang, J., & Zhang, X. (2012). Signature miRNAs involved in the innate immunity of invertebrates. *PLoS One*, 7(6), e39015. doi:10.1371/journal.pone.0039015

- Yang, L. S., Yin, Z. X., Liao, J. X., Huang, X. D., Guo, C. J., Weng, S. P., . . . He, J. G. (2007). A Toll receptor in shrimp. *Mol Immunol*, *44*(8), 1999-2008.
doi:10.1016/j.molimm.2006.09.021
- Yang, Y., Yang, F., Xiong, Z., Yan, Y., Wang, X., Nishino, M., . . . Yang, X. (2005). An N-terminal region of translationally controlled tumor protein is required for its antiapoptotic activity. *Oncogene*, *24*(30), 4778-4788.
- Yao, X., Wang, L., Song, L., Zhang, H., Dong, C., Zhang, Y., . . . Bi, Y. (2010). A Dicer-1 gene from white shrimp *Litopenaeus vannamei*: expression pattern in the processes of immune response and larval development. *Fish Shellfish Immunol*, *29*(4), 565-570. doi:10.1016/j.fsi.2010.05.016
- Yarm, F. R. (2002). Plk phosphorylation regulates the microtubule-stabilizing protein TCTP. *Mol Cell Biol*, *22*(17), 6209-6221.
- Yeh, S. P., Liu, K. F., Chiu, S. T., Jian, S. J., Cheng, W., & Liu, C. H. (2009). Identification and cloning of a selenium dependent glutathione peroxidase from giant freshwater prawn, *Macrobrachium rosenbergii*. *Fish Shellfish Immunol*, *27*(2), 181-191.
doi:10.1016/j.fsi.2009.03.022
- Yodmuang, S., Tirasophon, W., Roshorm, Y., Chinnirunvong, W., & Panyim, S. (2006). YHV-protease dsRNA inhibits YHV replication in *Penaeus monodon* and prevents mortality. *Biochem Biophys Res Commun*, *341*(2), 351-356.
doi:10.1016/j.bbrc.2005.12.186
- Yoganandhan, K., Sri Widada, J., Bonami, J. R., & Sahul Hameed, A. S. (2005). Simultaneous detection of *Macrobrachium rosenbergii* nodavirus and extra small virus by a single tube, one-step multiplex RT-PCR assay. *J Fish Dis*, *28*(2), 65-69.
doi:10.1111/j.1365-2761.2004.00606.x
- Youngcharoen, S., Senapin, S., Lertwimol, T., Longyant, S., Sithigorngul, P., Flegel, T. W., & Chaivisuthangkura, P. (2015). Interaction study of a novel *Macrobrachium rosenbergii* effector caspase with B2 and capsid proteins of *M. rosenbergii* nodavirus reveals their roles in apoptosis. *Fish Shellfish Immunol*, *45*(2), 534-542.
doi:10.1016/j.fsi.2015.05.009

- Yount, N. Y., Bayer, A. S., Xiong, Y. Q., & Yeaman, M. R. (2006). Advances in antimicrobial peptide immunobiology. *Biopolymers*, *84*(5), 435-458. doi:10.1002/bip.20543
- Yu, Y., Wei, J., Zhang, X., Liu, J., Liu, C., Li, F., & Xiang, J. (2014). SNP discovery in the transcriptome of white Pacific shrimp *Litopenaeus vannamei* by next generation sequencing. *PLoS One*, *9*(1), e87218. doi:10.1371/journal.pone.0087218
- Zhang, D., Li, F., Weidner, D., Mnjoyan, Z. H., & Fujise, K. (2002). Physical and functional interaction between myeloid cell leukemia 1 protein (MCL1) and Fortilin. The potential role of MCL1 as a fortilin chaperone. *J Biol Chem*, *277*(40), 37430-37438.
- Zhang, H., Wang, J., Yuan, J., Li, L., Zhang, J., Bonami, J. R., & Shi, Z. (2006). Quantitative relationship of two viruses (MrNV and XSV) in white-tail disease of *Macrobrachium rosenbergii*. *Dis Aquat Organ*, *71*(1), 11-17. doi:10.3354/dao071011
- Zhang, M., Ma, J., Lei, K., & Xu, X. (2010). Molecular cloning and characterization of a class II ADP ribosylation factor from the shrimp *Marsupenaeus japonicus*. *Fish Shellfish Immunol*, *28*(1), 128-133. doi:10.1016/j.fsi.2009.10.008
- Zhang, X. W., Wang, X. W., Huang, Y., Hui, K. M., Shi, Y. R., Wang, W., & Ren, Q. (2014). Cloning and characterization of two different ficolins from the giant freshwater prawn *Macrobrachium rosenbergii*. *Dev Comp Immunol*, *44*(2), 359-369. doi:10.1016/j.dci.2014.01.009
- Zhang, Y., Qiu, L., Song, L., Zhang, H., Zhao, J., Wang, L., . . . Huang, B. (2009). Cloning and characterization of a novel C-type lectin gene from shrimp *Litopenaeus vannamei*. *Fish Shellfish Immunol*, *26*(1), 183-192. doi:10.1016/j.fsi.2008.03.008

VITA

NAME Phongthana Pasookhush

DATE OF BIRTH 16 September 1992

PLACE OF BIRTH Bangkok

INSTITUTIONS ATTENDED 2013, BSc (Hons) (Biology), Srinakharinwirot University

HOME ADDRESS 62 Paholyothin54/3
Sai Mai Bangkok, THAILAND
10220

PUBLICATION P. Pasookhush, C. Hindmarch, S. Longyant, P. Sithigorngul, W.G. Bendena, P. Chaivisuthangkura. Transcriptomic analysis of *Macrobrachium rosenbergii* (giant fresh water prawn) postlarvae in response to *M. rosenbergii* nodavirus (MrNV) infection: de novo assembly and functional annotation. *BMC Genomics*. 2019; 20(1): 762.

P. Pasookhush, S. Longyant, P. Sithigorngul, P. Chaivisuthangkura. Development of duplex loop-mediated isothermal amplification (dLAMP) combined with lateral flow dipstick (LFD) for the rapid and specific detection of *Vibrio vulnificus* and *V. parahaemolyticus*. *North American Journal of Aquaculture*. 2016;78(4), 327-336.

P. Chaivisuthangkura, A. Vaniksampanna, P. Pasookhush, S. Longyant, P. Sithigorngul. Taura syndrome virus. In: Dongyou Liu, editor. *Molecular Detection of Animal Viral Pathogens*. CRC Press, Boca Raton, London, New York Washington, D. C., 2016, p. 16-25

